Alma Mater Studiorum – Università di Bologna

DOTTORATO DI RICERCA IN

Biologia Cellulare e Molecolare

Ciclo XXVII

Settore Concorsuale di afferenza: E5/02

Settore Scientifico disciplinare: BIO11

TITOLO TESI

Evaluation of 3D cell culture systems for host-pathogen interaction studies

Presentata da:

Pasquale Marrazzo

Coordinatore Dottorato

Chiar.mo Prof. **Davide Zannoni**

Relatore

Dott**. Alfredo Pezzicoli**

Tutor Dottorato

Chiar.mo Prof. **Vincenzo Scarlato**

Co- relatore

Dott. **Marco Soriani**

Esame finale anno 2015

“Le savant n'est pas l'homme qui fournit de vraies réponses ;
c'est celui qui pose les vraies questions."

“Scienziato non è colui che sa dare le vere risposte, ma colui che sa porre le giuste domande.”

- Claude Lévi-Straus

TABLE OF CONTENTS

LIST OF ABBREVIATIONS

2.5D	two and one-half-dimensional
2D	two-dimensional
3D	three-dimensional
3R	reducement, refinement, replacement
AB	Alcian Blue
Ab	antibodies
Abs	absorbance
AEC1	Alveolar Epithelial Cell type I
AEC2	Alveolar Epithelial Cell type II
ALI	air-liquid interface
AP	Apical
APC	Antigen Presenting Cell
APC	allophycocyanin
AQP3	Aquaporin-3
BALT	Bronchus-Associated Lymphoid Tissue
BC	Basal cell
BE	Bronchial Equivalent
b-FGF	basic-fibroblast growth factor
BL	Basolateral
BMe	Basement membrane
BM-MSC	Bone Marrow mesenchymal stem cell
BSA	Bovine Serum Albumin
C. difficile	Clostridium *difficile*
CBC	Crypt Base Columna
CC	Ciliated Cell
CCSP	Clara Cell Secretory Protein
CD*	Cluster Differentiation
CDI	C. *difficile* disease
CDI, CDAD	(C. difficile associated disease)
CFSE	Carboxyfluorescein succinimidyl ester
ChoP	phosphorylcholine
CK*	Cytokeratin (n°)
Cl-C	Club Cell
COPD	Chronic Obstructive Pulmonary Disease
CRP	C-reactive protein
CZ	conducting zone (of respiratory tract)
DAPI	4',6-diamidino-2-phenylindole
DC	Dendritic Cell
DC-BE	Bronchial Equivalent with Mesenchymal Stem Cells
DPBS	Dulbecco's phosphate-buffered saline
EC	Enterocytes
ECM	Extra Cellular Matrix
EE	Enteroendocrine
EGF	Epithelial Growth Factor
EnO	Enteroids
ENR	EGF, Noggin, R-spondin
ESC	Embryonic Stem Cell

❖ LIST OF ABBREVIATIONS

FABP4	Fatty Acid Binding Protein 4
FITC	fluorescein isothiocyanate
GC	Goblet Cell
G-CSF	Granulocyte-Colony Stimulating Factor
GF	growth factor
GM-CSF	Granulocyte-Macrophage Colony-Stimulating Factor
GTD	glucosyltransferase domain
Hap	Haemophilus adhesion and penetration protein
HBEC	Human Bronchial Epithelial Cell
HE	Hematoxylin and Eosin (staining)
Hib	Haemophilus *influenzae* type B
HLF	Human Lung Fibroblast
HMW	High Molecular Weight (adhesin)
HPV	Human Papillomavirus – 16
HSC	Hematopoietic stem cell
HTS	High throughput screening
HUVEC	Human Umbilical vein endothelial cell
IFN-y	Interferon gamma
IGC	Intestinal Goblet Cell
IHC	Immunohistochemistry
IL-	Interleukin-
IP-10	Interferon gamma-induced protein
iPSC	induced Pluripotent Stem Cells
ISC	Intestinal Stem cell
ISCC	Intestinal Stem Cell Consortium
ISCT	International Society for Cellular Therapies
ITGa6	Integrin alpha chain alpha 6.
LL-37	(Cathelicidin antimicrobial peptide)
LOS	Lipooligosaccharide
Lu-MSC	Lung resident Mesenchymal Stem Cell
Mabs	monoclonal antibodies
MIP-1a	Macrophage Inflammatory Protein
MoDC	Monocytes derived Dendritic Cells
MSC	Mesenchymal stem cells
MSC-BE	Bronchial equivalent with dendritic cells
MUC5AC	Mucin 5 ac
MUC5B	Mucin 5 b
NEB	Neuro-epithelial bodies
NGFR	Nerve growth factor receptor
NHBE	Normal Human Tracheo-)Bronchial Epithelial Cells
NHLF	Normal Human Lung (adult) fibroblast
NTHi	Non-Typeable Haemophilus *influenzae*
O.C.T.	Optimum Cutting Temperature
OD	Optical density
OMP	Haemophilus outer membrane protein
PAS	Periodic acid–Schiff
PBMC	Peripheral Blood Mononuclear Cells
PC	Paneth Cell
p-DC	pulmonary- Dendritic Cell
PDGFR	Platelet-Derived Growth Factor receptors

PF	paraformaldehyde
PI	propidium iodide
PNEC	Pulmonary Neuroendocrine Cells
PS	Penicillin – Streptomycin
PNECs	Pulmonary neuroendocrine cells
RA	Retinoic Acid
RANTES	Regulated on Activation, Normal T cell Expressed and Secreted (protein)
SBA	Serum Bactericidal Activity
SCGB1A1	secretoglobin, family 1A, member 1
SV40	Simian virus 40
T3SS	Type III secretion system
TAC	Transit-Amplifying Cells
TcdA	Clostridium *difficile* Toxin A
TEER	trans epithelial electric resistance
TJ	Tight Junction
TNF a	tumor necrosis factor alpha
ToxA	C. *difficile* TcdA toxin
ToxB	C. *difficile* TcdB toxin
UC-MSC	Umbilical Cord - derived Mesenchymal Stem Cells
VEGF	Vascular Endothelial Growth Factor
ZO1	Zonula Occludens Protein 1

INTRODUCTION

1 Traditional cell culture models: limits and benefits

1.1 Mammalian cell lines and primary cells

Our current knowledge of the molecular basis governing biological processes such as physiology, development and pathology, are based on cellular models. A cellular model would be useful to simplify complex physiological systems (e.g. organs and tissues) or to standardize a whole-living organism to study undiscovered biological mechanisms. The use of *ex vivo* samples, despite the ethical issues, is always linked with the source accessibility of the tissues to be taken out and then kept alive until the desired testing. Also the costs of *ex vivo* testing are a reason to push the demand for more accessible models. To address current medical issues and to recapitulate human being biology, since the beginning of the 20th century, cell-based models offered advantages enabling scientists to observe phenomena inspiring the basis of cellular and molecular biology. Currently, cell culture plays its part not only in basic research but are widely used in the majority of biotechnology applications (Figure 1). Nowadays mammalian cell cultures are well established methods. The traditional 2D cell culture allows to manipulate and to propagate primary cells, tumor-derived or virus-transformed cell lines, even stem cells isolated from the human body. At the same time the possibility to store cells for years by cryopreservation, is a convenient method although a functional impairment may occur after repetitive freeze-thaw cycles. Cell cultures are classified as anchorage independent (they live just suspended in a fluid medium) and dependent (they require a surface to which they can attach to survive and grow)(Table 1).

Continuous cell lines are mainly divided by the immortalization step that characterizes them. Immortalization derives from a spontaneous transformation event or it is induced by viruses or chemicals, otherwise it is mediated by targeted oncogenesis. Inopportunely the immortalization process involves phenotypic alteration in a cell. Sub-culturing of primary cells lead to finite cultures that present Hayflick limit since after limited number of cell divisions, they will senesce irreversibly. Finite cultures maintain several *in vivo* characteristics, but if passaged over time they tend to differentiate and to select for aberrant clones. Until now, thanks to this “flat biology” approach, diverse mechanisms have been characterized under carefully optimized *in vitro* conditions, consisting in favorable artificial environment in which added exogenous factors mirror the tissue pre-isolation growth requirement. In particular, continuous cell lines offered the advantages to

interrogate standardized clonal systems, in comparison with *in vivo* models that have economic and ethical constraints. For example, if the aim of the study is to analyze mitochondria ultrastructure, or to study relatively simple metabolic response, cell lines are likely to be exhaustive. However, the choice to use in an experiment a cell-line or primary cell based model is not a trivial issue. For instance, CaCo2 is a human colon-derived epithelial robust cell-line that can be used for general long-term assays, intestinal absorption studies or as colon cancer model. Even though it is possible to add defined concentrations of soluble growth factors modulating cell functions, the CaCo2 phenotype remains significantly different in terms of protein expression patterns, morphology and absorptive properties. In addition, cell lines compared to primary/finite cells usually display different epigenetic profile, cytokines secretion and plasma membrane markers. On the other hand, primary cell cultures better imitate the parental karyotype and the sensitivity to agents, whereas can reflect the variability existing in a population. Recently, thanks to the ectopic expression (by means of cDNA) of the telomerase activity, responsible to extend telomere lengths and avoid senescence, hTERT-immortalized cells were introduced as alternative to classical primary cell culture. Confident in the fact that they do not present a genomic instability or great phenotypic changes from parental tissue, h-TERT cells offer a good surrogate for biochemical screening, genetic manipulation and *in vitro* HTS. Other advances of using cell lines are represented by the exploitation of viral elements in industrial cell engineering: transfection of SV40 large T-antigen makes a condition by which the immortalization timing is stopped under temperature control, in favor of a quite differentiation; HPV16 E6/E7 gene is able to suppress cell cycle regulators as p53 and RB, inducing a senescent cell replication. Therefore, despite the risk to generate artefacts, cell lines are preferable to avoid a repeated testing of primary cells donors or when primary cells isolation and requested total quantity are technically difficult to obtain, time consuming and costly.
As a matter of fact, after the isolation, any cell loses its interaction with their natural environment. The leading change is morphological and could affect the original physiological functions. Actually many tissues do not require an aligned mesh of ECM. Indeed some primary normal or cancer-derived hemopoietic cells are cultured as a homogenous suspension in surrounding culture medium that does not extremely differ from blood.

Apical, basal and lateral surface are very important elements when cell polarity occurs in tissue. However, this is true for epithelial but not for most of mesenchymal cells. Substrates used for traditional 2D cultures (such as flasks, petri dishes, cell culture plates) are static. Occasionally, plastic or glass surfaces may be partially covered by cells (less than 50%), whereas cells that overly attach and then spread by breaking their reciprocal contacts are often strongly limited to ~5%. Many aspects, varying cellular proliferation and fitness, are controlled by artificial actions that alter the *in*

vivo functions. Here we could do many examples nonetheless it is enough to indicate that just serum addition represents a cause of a stronger adhesion and activation of pathway. Substrate stiffness deeply contributes to cell fate specification: we have learned that MSCs are influenced by different rigidity of the substrate and according to it they follow distinct lineages. In general, in 2D culture stiffness parameters like Young's modulus are considered supra-physiological. Other limitations comprise the accessibility to determined drugs, compounds, microorganisms. In fact the third dimension missing in 2D culture grants the barrier concept existing *in vivo*. Soluble molecules that are added as tester or sustaining factors for the culture easily diffuse in the medium, quickly equilibrate and reach the cells; despite it still needs a strict man-made replacement the contact with the cells is unimpeded. Instead, considering the passage of the delivered molecules through *in vivo* structures, the free space they encounter among ECM, the direction of the movement and the ECM binding capacity itself are all factors contributing to the 2D cell culture imperfection and weakness. Last but not least, in 2D culture it's hard to preserve the cell genotype because the frequent mechanical sub-culturing of cells modify surface receptors and increase senescence, as well a functional impairment that is caused by freezing and thawing. For all these reason there's a tendency to upgrade cell model systems in appropriate combinations of more cell types, mixing cellular and ECM counterpart in the culture, to test more physiological niches.

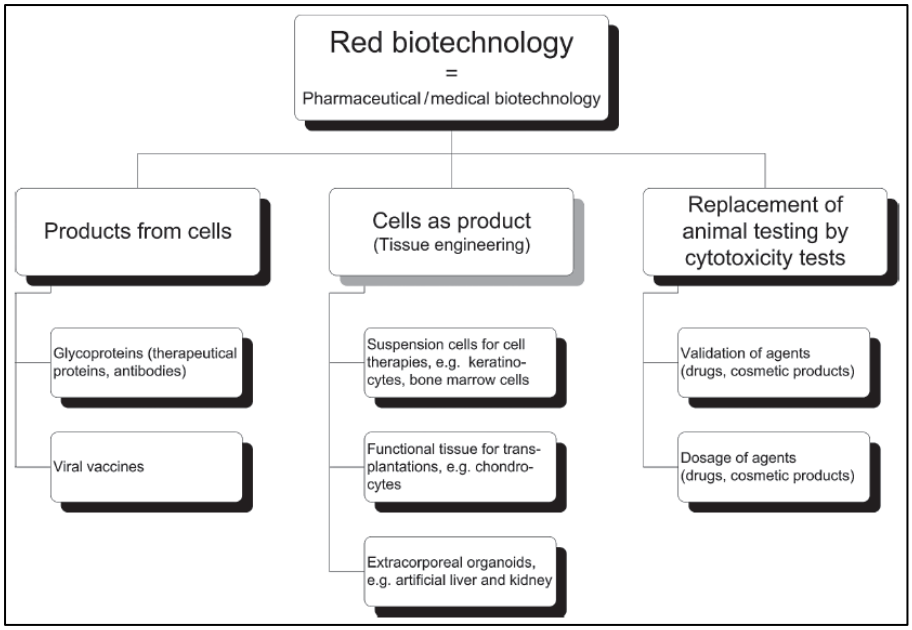

Figure 1 Applications of animal cell cultures. From Eibl et al. 2009 [119]

Type	Origin	Passages
Primary culture	Tissue, isolation	0-1
Finite culture	Primary cells, subculturing	Very limited (adult tissue) 20-60 (fetal tissue)
Continuous cell line	Finite cultures, spontaneous transformation	Unlimited
Transformed cell line	Tumor Tissue, spontaneous or induced transformation	Unlimited
hTERT-immortalized line	Primary cells	Unlimited

Table 1 Cell culture general classification

2 Alternative *in vitro* cell models

2.1 Co-cultures

Monocultures partially reflect the status of multicellular tissues, in particular when the scope of the investigator is to predict the susceptibility of the host during an infection, a process that is characterized in vivo by many cells interacting each other via direct contacts or paracrine signals. More meaningful in vitro models are co-cultures. Basically co-cultures are assembled when at least two cell types reproducing some cellular interactions (paracrine factors, juxtacrine signaling) are simultaneously cultured. Simple co-culture systems contain a mixture of cells in contact with each other (bi-culture), while patterned co-cultures need a physical separation between the cell types. The use of these systems is suitable to study specific cell-cell interaction (i.e. between a NK-Cell and a cancer cell) that can be timely controlled by separating in advance cell type locations. By introducing a compartmentalization, it is possible to study conditioned single cell type responses and recovery them in an easier fashion. This approach would allow a restricted evaluation of joining communication between different cells. According to the needs and the model simplification process, the diverse cell densities may be ideally approximated to the ones of the native tissue. The advantages of using such approaches are schematically showed in Figure 2. It is demonstrated that *in vitro* co-presence has enough influence to enforce regenerative potential of the system components [[1][2][3]. It permits to study rare events happening in nature or check synthetic cell-cell interactions. It permits to study rare events happening in nature or check synthetic cell-cell interactions. It has been proven that co-cultures enhance phenotype markers (e.g., hepatocytes co-cultured with endothelial cells or fibroblast exhibit normal hepatic markers and additional function than the classic albumin production in 2D culture), and allow to analyze activation of the inflammatory state (e.g. co-cultures of monocytes and epithelial cells).

Of importance, the structure of the environment has to be defined and compatible at least with viable and stable cell populations. If co-cultures are intended for longer-term assays (“time-scale problem”), media requirements (including volume) are fundamental to the success of the experiment. In addition, data acquisition must be carefully pre-arranged, especially when co-cultures represent valuable starting points to develop relevant pseudo-tissue models.

2.2 Transwell systems

Very smart devices that facilitate numerous co-cultures set-ups are cell culture inserts (by extension called Transwell). They are historically manufactured to perform migration and invasion assays, although they are frequently employed to mechanically support and compartmentalize the cell

culture. Many companies produce cell culture inserts with different material properties (transparency and toughness) and pore micro-sizing, allowing the user to choose the permeability of the barrier created by the insert according to the aim of the study (drug screening, microbial motility, etc). Technically they are placed in conventional cell culture plates, depending on insert format. For example, in the case of an epithelial cell culture, the use of transwells would allow the isolation of BL and AP layers leading to the possibility to distinguish their phenotypical differences. The characterization of the epithelium produced in trasnwells conditions it is not difficult. TEER measurement is just one method compatible to transwell cell culture systems; it is possible to use instruments such as EVOM or Endhom or Ussing chamber, to assess cell layer integrity and barrier function, considering the formation of cell junctions. Thanks to transwells and ALI-culture the achievement of considerable epidermal and mucosal equivalents is now moving to translational studies. ALI culturing success reflected our capacity to restore physiological parameters, such as free oxygen availability, recapitulating natural stimuli able to lead to the differentiation input within a tissue.

2.3 2.5D cultures

Just the simple addition of native ECM components in the medium is able to produce a tissue-specific commitment and a structured organization by cells. This technique is referred as 2.5 cell culture. Different ECM proteins are recognized by cell surface interactors and as a consequence they assign an orientation that could influence the polarity. The seeding of cells on an organized layer of specific basement membrane proteins (such as MatriGel coating) is usually sufficient to promote sphere-like organization by cells. The choice of the ECM protein/s could also lead to an irregular distribution of the cells. Knowing those features conversely it is possible to exploit the spatial cells arrangement in a way to expose cell compartment in general not easily accessible; for instance, the addition in the medium of antibodies directed versus particular integrins allows the orientation of cell polarity during the culture initiation. These models are indeed a convenient "intermediate" between 2D cell culture and *in vivo* ones, more physiological in terms of parental architecture, leaving the cells open for downstream analysis.

2.4 Fluidics contribution in cell culture

Oxygen, nutrients and other molecules are continuously consumed and produced by cells. Such dynamic distributions are not mimicked in conventional 2D cell culture. Nevertheless, endothelial cells are continuously under shear stress conditions as blood flows over them. This aspect has led to the need of improving cell culture conditions by testing the effect of a precise force exerting on the physiology of cell cultures. These constrains have defined the rationale for applying microfluidics

technology to biological systems. Fluidic devices are tools to incorporate mechanical stress (e.g. pressure) or chemical challenge (e.g. increasing GF concentration) in cells that can recreate this dynamic environment in a small scale. Grouping of valves, channel, tanks and pumps consent to evaluate the response to forces and gradients that usually encounter in nature, like in the vasculature. Microfluidics provide high degree of control over cell culture conditions, especially if robotics is built-in, therefore enlarging mAbs or viral vectors therapeutics production yield in industrial workplace. Fluidic apparatus is suitable also for not-adhering cells. By filtration, gravitational settling and centrifugation, cells and medium containing the therapeutics molecules product of the culture, can be separated. Now, custom-friendly plates and microdevices are more and more offered in the market to the not-expert in the field to analyze particular cell populations (e.g. endothelial, myo-fibroblast) or for single live-cell analysis. However, this approach may encounter optimization problems such as a variable 1) flow rate (laminar or not); 2) consumption rate of nutrients; 3) gas levels (including evaporation problem) and 4) positioning of delicate cells in channels.

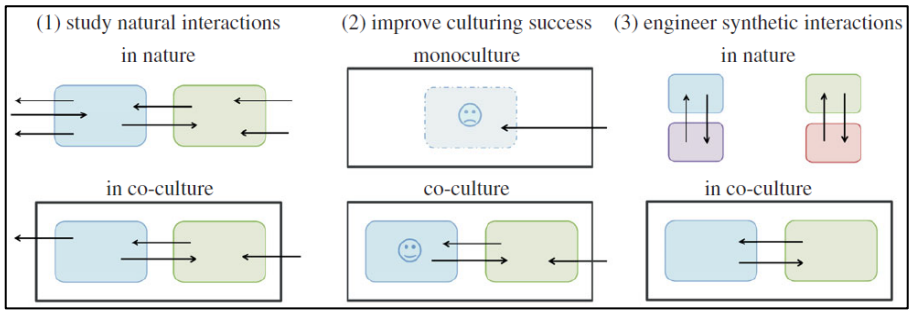

Figure 2 Co-culture definition and motivation. From Goers et al. 2014[120]

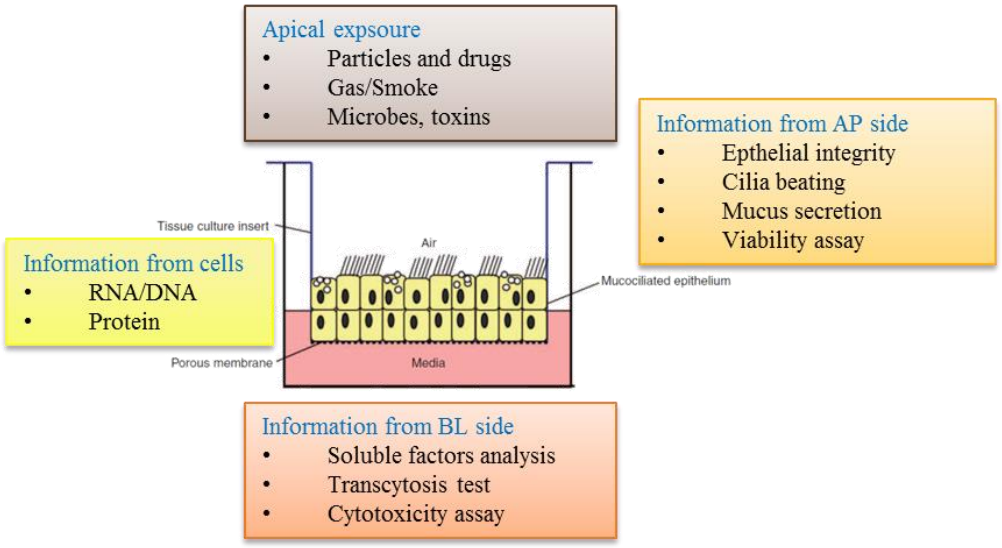

Figure 3 Schematic of experimental output obtainable from a transwell-model of the respiratory epithelium

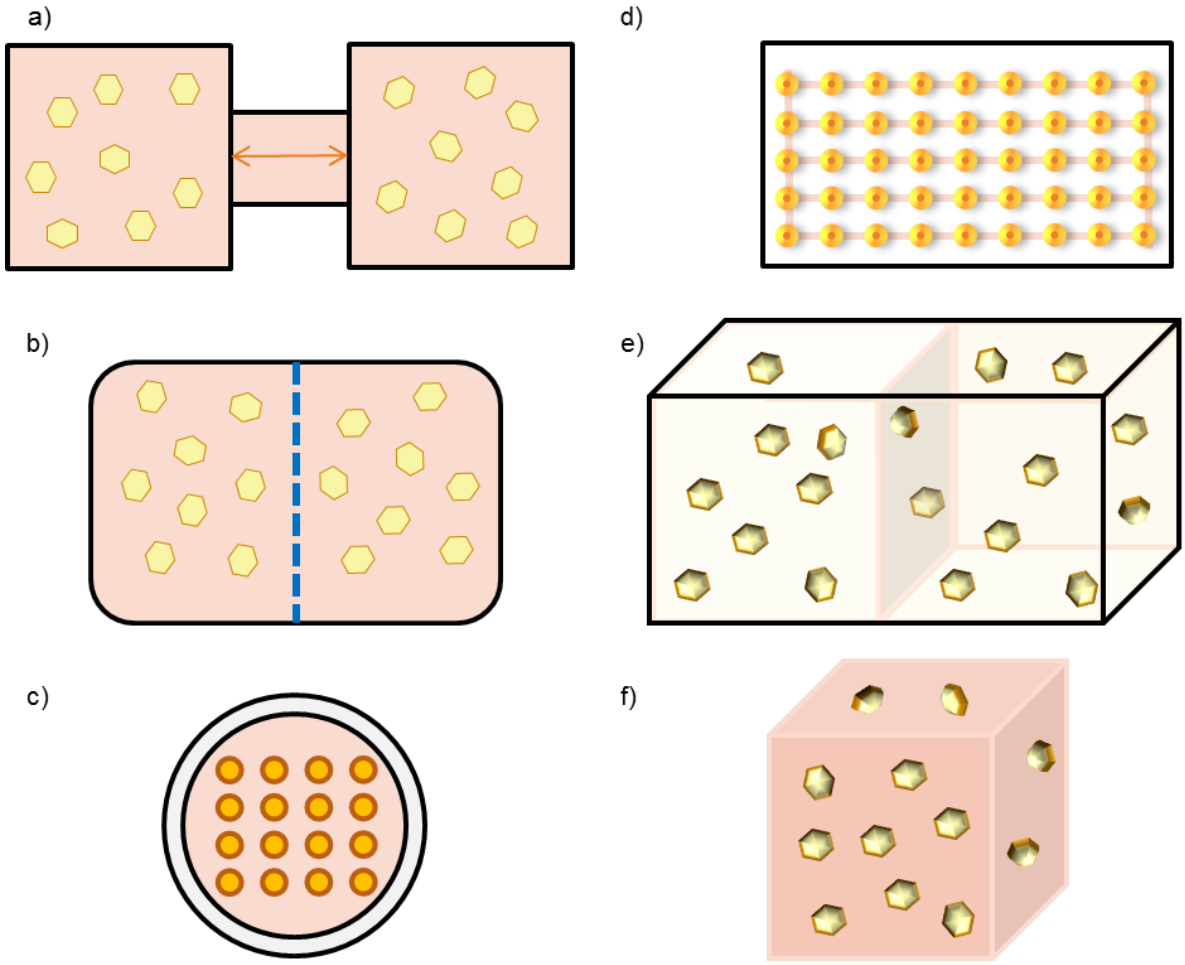

Figure 4 Schematic representation of co-cultures set-up. In 2D culture a channel (a) or a membrane (b) or surface adhesion (c) separate single cells or colonies. Evolution of these approach in 3D conditions comprised microfluidic hanging drop plates (d), bioreactors(e) and hydrogel encapsulation (f).

3 3D cell culture models

A wide variety of engineered cultures to genuinely recreate the molecular circulation of signals in response to external perturbation have been developed so far[4][5], [6].

These models are meant to replace e*x vivo* ones that involve direct culturing of tissue from human or animal sources preserving their dimensions. Indeed, although e*x vivo* models are useful when animal tissue harvesting does not constitute a limitation, such approach is hardly feasibly for host-pathogen interaction studies. Even though the technological advances in engineered model tissues are notably (e.g. in scaffolding or defined synthetic matrix), the mirroring of *in vivo* conditions remains a big challenge, mainly because of the highly heterogeneous and time-variable composition of the extracellular constituents. Indeed, each tissue has differences in their cyto-architecture and the actual determinants of cell differentiation are often not well-elucidated and the mechanical forces vary. The fundamental issue is the extent to which *in vivo* complexity of the tissue/organ is recapitulated in the designed 3D culture. One possibility is to deconstruct the organ/tissue into their smaller units (layers, cells or matrix) and then recombine them selectively in a 3D structure.

Three-dimensional tissue engineered models can be mainly divided in scaffold-based and scaffold-free constructs. Below are described a few of the most popular approaches.

3.1 Scaffold-based constructs

Implanting cells or tissues into a 3D scaffold composed of natural derived ECM or synthetic or semi-synthetic materials (such as hydrogels) is the most common technique that resembles the architecture of various tissue types. Such tissue equivalents are recognized as efficient toxicological study substrates, disease models and as general *in vivo* models surrogate. For instance, fibroblasts added to a collagen frame enable the formation of an underlying realistic dermis and the self-organization of full human skin. Actually de-cellularized tissues, with the ability of retaining native composition and distribution of GFs and ECM, seems to be the most promising scaffolds suitable both to regenerative medicine and *in vitro* modelling tissue engineering, with a demonstrated success also in tracheal transplantation[7]. A lot of techniques are being utilized to fabricate solid scaffolds for 3D cell culture, including lithography, electro-spinning, bio-printing, microarrays.

3.2 Scaffold-free constructs

Spinner flask is the most used technique to generate suspension clustered cultures (spheroids), in a higher quantity than liquid overlay or hanging drop methods. Magnetic spinner prevents the cells to adhere to any surfaces and assists in nutrients and waste transport. However, this approach may

result in 3D aggregates, heterogeneous in size and shape and the physical forces applied can be detrimental on the behavior of cells. As an alternative surface to the traditional well and flask, micro-carrier beads are commercially available with a wide range of physio-chemical parameters, allowing the culture in rotating vessels. They appear advantageous wherever higher cell density is required, moreover for the culture of sensitive cells types (such us endothelial cells) and since their use decreases necrosis problems occurring in spheroids.

Organoid cultures were first described many decades ago, but just recently, caught the advance in stem cell isolation, their utility is increasing especially in translational study. Organoid cultures, in terms of cells explanted and self- rearranging, imitate the physiology of many human and animal tissues very well. Organoids protocols were available for the mammary gland, kidney, prostate, lung, intestine, stomach, liver, and pancreas [8] as well as tools for relevant prognostic and predictive assays. Organoids, expanded from ESCs, from iPSCs or from primary stem cells, are typically cultured into commercial matrices, enabling optical imaging.

3.3 3D bioprinting

3D bioprinting is being applied to regenerative medicine to address the need for tissues and organs suitable for transplantation. Compared with non-biological printing, 3D bioprinting involves additional complexities, such as the choice of materials, cell types, growth and differentiation factors, and technical challenges related to the sensitivities of living cells and the construction of tissues[9]. The integration of technologies from the fields of engineering, biomaterials science, physics, biology and medicine addresses the control of tissue geometry, mechanics and 3D patterning networks.

3.4 Organ-on-a-chip

An organ-on-a-chip is a microfluidic cell culture device. It is created with microchip manufacturing that monitor/control physicochemical cell environment and simulate tissue/organ physiology. By mimicking the multicellular and tissue-tissue interfaces and vascular perfusion of the body, these devices reproduce a superior functionality in vitro than conventional cell culture systems.

3.5 Imaging in 3D cell culture

Disappointingly, the imaging of 3D cultures is still challenging [4]. The main obstacle is the scattering of light in thick specimens. Confocal microscope enables multicolor imaging up to ~100 μm deep within the tissue, while two-photon microscopy avoids this issue. Reduced photobleaching and phototoxicity, high resolution via multiple-view reconstructions, long working distance objectives and higher speed, make instead the LSFM ideal for 3D culture purposes. [6], [10]–[12]

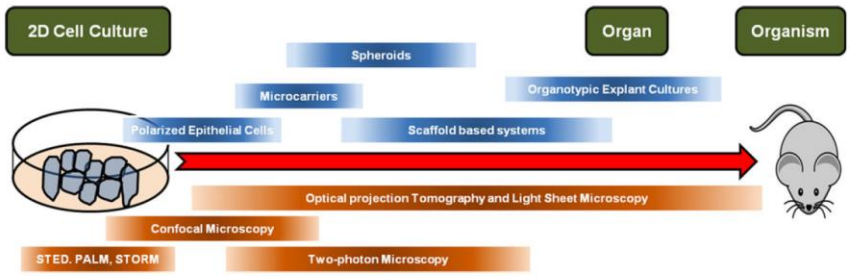

Figure 5 3D optical microscopy techniques in relation to 3D cell cultures methods. Source: Page et al. 2012[4]

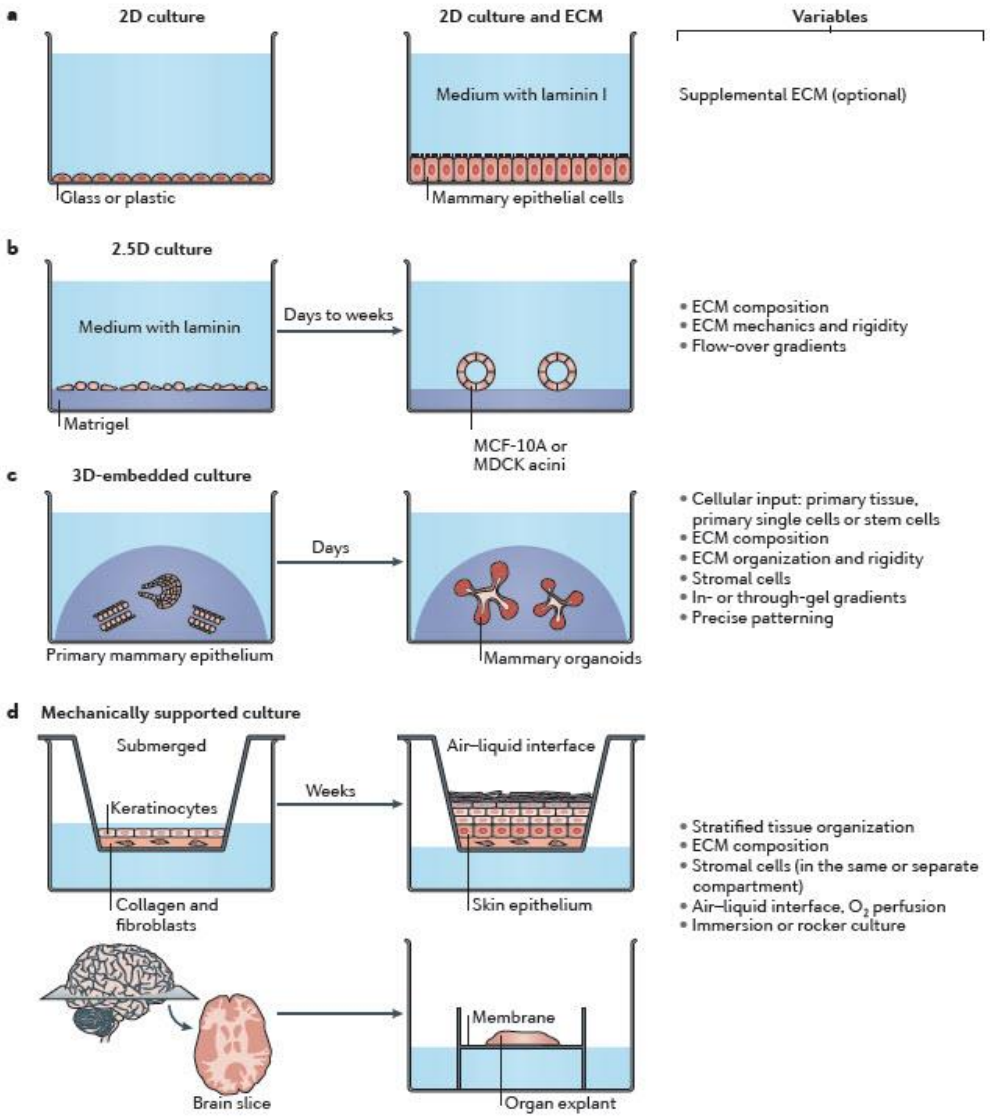

Figure 6 Major aspects of different cell culture environments. Source: Shamir et al. 2014 [121]

4 Cellular systems for host-pathogen interaction

4.1 Current infection models limitations

Human organs incessantly changes microenvironments. The beginning of the infection causes firstly a homeostatic imbalance. Able to attach, internalize and survive inside the cells, bacteria arm their virulence machinery and adapt to this imbalance made of metabolic changes and immune response, thus starting a productive or recurrent infection. In this context, the *in vitro* studies are focused on the single cell types, comprised in the barrier function critical for the initiation of the disease. Epithelial monolayer cultures contributed to our understanding of how microbes use host receptor to establish their virulence, but remain unable to depict a global immune response to pathogens because of the absence of immune cells. Indeed the biological events triggered by the cytokines produced by discrete immune cell types can be missed when these cells are not present in the cell culture. In principle, by missing a single cell type we may alter the signaling events or factors favoring microbial colonization.

Extensive use of monoculture *in vitro* is however often chosen because of the difficulties by *in vivo* models in recognizing host signaling pathways involved during pathogenesis. Even if the *in vivo* output is a general issue, in the field of infection diseases this is considered a non-trivial issue whereas the investigator has to consider the behavior of a specific human pathogen. The value of animal models in vaccine development is indeed part of a large debate in the scientific community. First of all, many bacteria are not widespread pathogenic among the mammalian species, in fact it is not rare that they exhibit a tropism restricted to particular specie to realize the infection. Our effort to recapitulate particular infection disease through an animal *in vivo* are most of the times imprecise for the choice of the model itself; they could be not predictive of the humans because of the difference in metabolism and anatomical infected districts. This topic is very important to be taken into account for intervention strategies and in particular for vaccine discovery, with the opportunity to decrease clinical trials failing. Furthermore, development of methods to replace, reduce and refine animal experiments (the 3Rs approach) is currently one of the major need of research and development of therapeutics.

In contrast to the relative complexity of *in vivo* models, the comparison between monocultures and co-cultures are a controlled way to infer with the signals maintaining the cell-maturation and synergistic response to the microbes. Cell co-cultures are increasingly being used to study the pivotal role of discrete cells in response to microbial products or whole microbes infection. The

experimental design of course is affected by of both cell and microbe viability. Overgrowth of bacteria leads to hide small interesting events beyond a faster death of the cells. The use of UV-radiated bacteria it is an optimal compromise to study microbial components because biochemical features of the whole-organism are preserved and have maintained function.

In the last decade, serum-free condition is tending to be a must, almost for primary cells culture. In alternative, tissue microbiology and intravital techniques are emerging for that need, thanks to recent cutting-edge technology such as multi-photon imaging [13]–[15]

4.2 3D cell cultures as new paradigm in infection biology studies

Currently the most encouraging models able to acquire information about the host response to infections are 3D cell culture, especially for difficult-to-culture pathogens. They are valuable research tools when they are possibly coupled to a careful selection of the *in vivo* model. Usually the localization of TJs and ECM deposition in such 3D model like organoids can impact the process of the *in vitro* infection reconstituting a protecting barrier and preserving host cell integrity against invasion. As reported in the literature, 3D cellular models often generate data in agreement with *in vivo* reports and they have helped scientists to reconsider part of the knowledge derived from 2D cell cultures experiments. In particular, fortunate 3D cell cultures, even of cell lines, allowed the propagation *in vitro* of human specific viruses [16], not possible in the past neither in animal models. Intestinal organoids used to evaluate *in vitro* salmonella pathogenesis have shown that a mutant for *invA* gene (lacking a form of T3SS) is still able to invade the host [17]. This clearly shows that there could be bacterial components, previously considered essential in 2D culture, that are actually dispensable in a more physiological setting. 3D *in vitro* epithelial models also resemble the *in vivo* balance of pro- and anti- inflammatory cytokines following particular infections [14]. Likewise in 3D models, mucus is also patterned in a more physiological manner. Considering that the mucus can have a dual role with regard to pathogens, as innate barrier containing antimicrobials and material protection and as source of nutrients and pleasing ECM ligands, it is likely to influence a lot the output linked to the mechanism investigated. However, a major challenge for the study of host–pathogen mechanisms in three-dimensions is the use of biomaterials that will not affect verisimilar cell exposure to pathogens and exclude a non-physiologically manner interaction [18].

4.3 Opportunistic pathogens emerging

Although we have a good comprehension of the epidemiology and of clinical manifestations of several infectious diseases, sometimes we miss the relevant information to understand how the host colonization process influences the onset of disease. Bacteria living in normal human flora live as commensals until the equilibrium among the bacterial resident species are not disturbed. Our

attempt to treat and prevent particular diseases led in a simultaneous increase in pathogenicity acquirement by commensals bacteria. This switch to the opportunistic behavior is evident for two bacteria taken in exam in our study, NTHi and C.*difficile*, and here below briefly described.

4.3.1 Non-typeable Haemophilus *influenzae*

H. *influenzae* is a gram-negative coccobacillus. Isolates of *Haemophilus influenzae* are divided into encapsulated and nonencapsulated forms, with the last lack serotypical discrimination. Non-typable Haemophilus influenzae (NTHi) is a human-restricted member of the normal airway microbiota in healthy carriers and an opportunistic pathogen in immunocompromised individuals. NTHi is recognized a significant pathogen in children, and also in adults is the main cause of otitis media, community-acquired pneumonia, COPD, exacerbations in cystic fibrosis. Importantly, invasive diseases caused by NTHi infections have been steadily recognized since Hib and pneumococcal vaccination began. [19]

Nonencapulated strains present a huge heterogeneity linked to virulence factors differential pattern, thus varying the interplay with the host and making stronger therapies useless. In NTHi we referred for LOS (and not LPS) because a lipid A moiety and saccharide core but no O side chains are present on the bacterial membrane. LOS and ProteinD are considered major ciliotoxicity effectors. OMPs are implicated in mucus adherence and antigenic variation. More virulent NTHi strains can count in a panel of adhesins: HWM, Hap, Hia (similar to Hsf of Hib). Host immune mechanisms are needed to be evaded and to reach a persistent state at the mucosal airway surfaces. This is the reason why NTHi expresses an IgA1 protease that specifically contributes to counteract local immune response. The phase variation, i.e. the capacity by NTHi of challenge its surface structures to quickly adapt under different host conditions, is mostly associated to LOS modifications, in particular with sialic acid and ChoP decoration [20].

NTHi strains are adherent *in vivo* and to AP of transwell polarized airways cells (like CALU-3) and were confirmed to form biofilm which increases antibiotics resistance. NTHi seems can cross the epithelial barrier, assumed via paracytosis, and survive inside epithelial cells, then trespasses the subepithelial space with the option to infect also non-epithelial cells Figure 7. Whether NTHI resides in the respiratory tract is a question with no clear answer so far. Several bronchial models were used in the past, comprising ALI-transwell based (Baddal *et al*, unpublished) and Epiairway[21], to characterize the effect of long-term co-culture of NTHi with human tissues, but a deeper understanding of microbial virulence factors and live infection studies are required to decipher the best strategy to develop vaccine against NTHi broad spectrum.

4.3.2 Clostridium *difficile*

C. *difficile* is gram-positive bacillus, obligate anaerobic and spore-forming bacterium. CDI is at the present considered to be one of the most important causes of health care-associated infections, with a recent increase in mortality trend. The cause is traceable in the wrong or over-use of antibiotics provoking the intestinal microflora unbalance. C. *difficile* transmission follows fecal–oral route. The incidence of infection is greater in hospitals due to C.*difficile* acquisition through ingestion of spores, the same transmitted from healthcare personnel and other patients as well. An overview of the pathophysiology events is resumed in Figure 8. The formation of a pseudomembrane is a characteristic sign of inflammatory C. *difficile* reaction. Clinical manifestations in adults can range from mild diarrhea to even death (fulminant colitis, toxic megacolon, peritonitis). The most characterized as well important virulence factors are Toxin A (TcdA) and toxin B (TcdB), which are located, along with surrounding regulatory genes; without this equipment such C.*difficile* strain is considered non-pathogenic. Usually an IgG response to ToxA makes the difference between a non-asymptomatically carriage and onset of CDI. The diagnosis is traditionally based on the cytotoxin neutralization assay with high sensibility (but usually detecting only the more potent ToxB) and progressed into high specific immunoassays against both toxins. Antimicrobials administration (vancomycin and metronidazole) unfortunately disrupts the protective microflora, guiding to recurrent CDI symptoms nonetheless. Currently the best therapy appears the fecal transplantion, MAbs development (against the toxins) showed great potential to cure but has to be improved, while a vaccine is still far to be released. [22], [23]

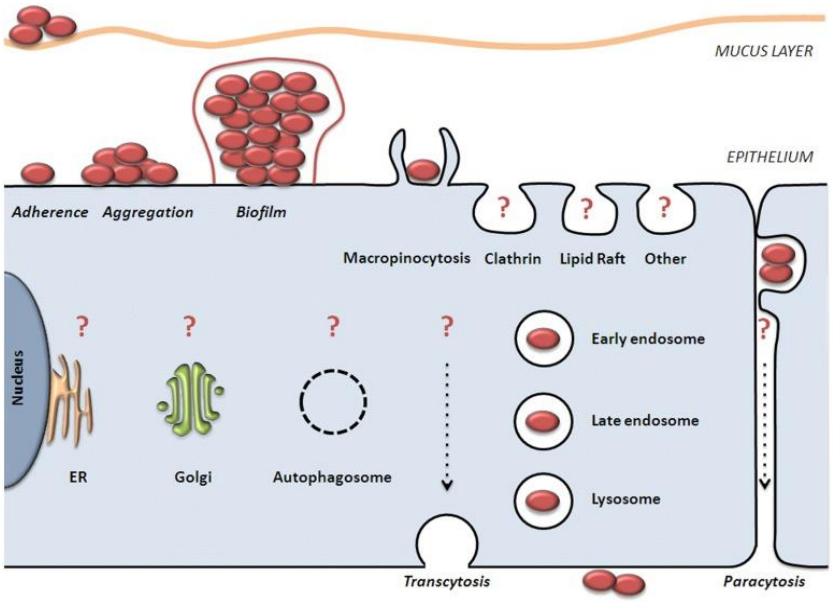

Figure 7 Model of NTHi infection. Source: Clementi et. al 2011[122]

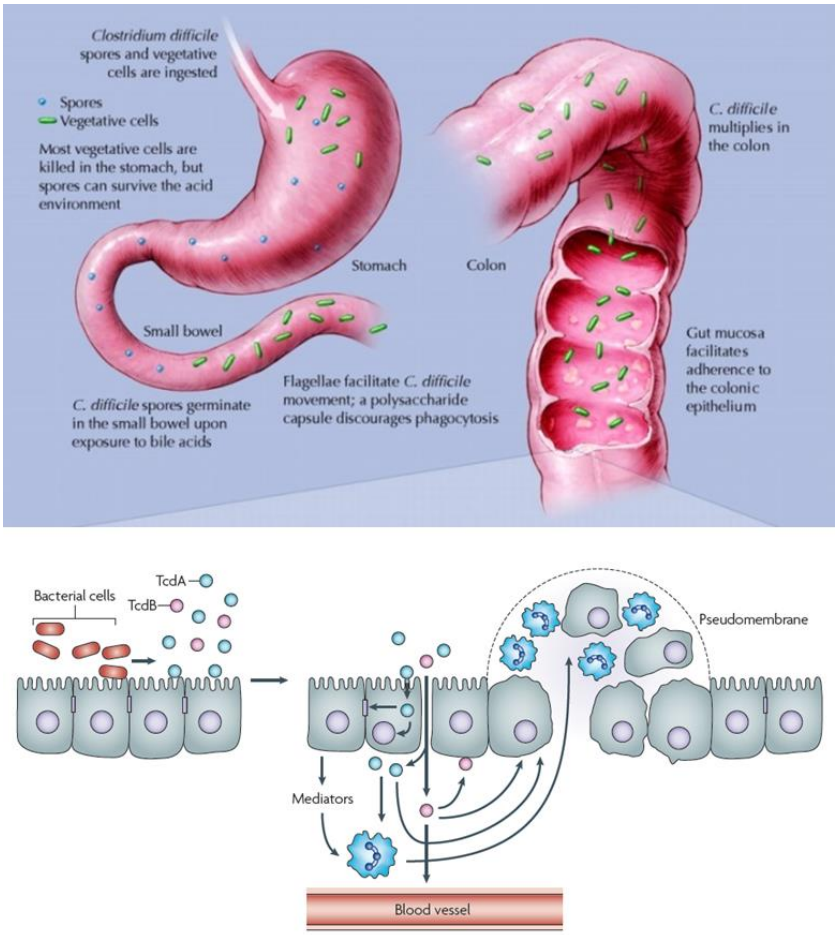

Figure 8 Pathogenesis of C. difficile infection. Sources: a) Poutanen et al 2004, [123] b) Rupnik et.al 2009 [22]

AIM OF THE STUDY

5 Thesis objectives

Standard *in vitro* models are not able to totally capture the physiological complexity typical of body districts, such us the lung or the intestine, and this limits the capacity to develop vaccine based on the understanding of bacterial infection strategies. Recently developed 3D cell culture models can better represent the tissue physiology and can work as valid human *in vitro* tissues equivalents.

In this context my PhD project has been focused on the development and evaluation of primary cell 3D models, with the objective of providing a new tool suitable for antigen discovery with the specific aim of unravelling mechanisms typical of pathogenesis dynamics, microbial cell targets and immune evasion. To achieve these goals we planned to reconstruct *in vitro* distinct host niches representing in particular the mucosa that acts as first innate defense against bacterial colonization.and infection.

The main objective of my study has been to set up reproducible conditions allowing the formation of a human organotypic culture of the conductive zone of the human respiratory tract. In particular the strategy was to setup a mechanical supported co-culture, centered on a two-component cell system reflecting the key features of the epithelial and connective tissue. We also created models based on three cellular components. These systems were planned as alternatives for current cell-lines based studies of binding, uptake, transcytosis, co-localization, toxicity, cellular activation as well as immune cell recruitment. The main characteristics of the 3D model are:

- consistency for a long-term study;
- adequate biomimicry;
- comfortable access to the epithelial face to perform apical infection;
- unnecessary automation, basic equipment sufficient;
- prospect of cellular tracing;
- protein localization;
- proven heterotypic cell interactions;

Our strategy has been based on the chronologic and modular introduction of the following elements:

- a synthetic scaffold, to support the cellular micro-scale environment;

- HLFs, as main constituent of the mesenchyme;
- HBECs, as source of epithelial cells;
- ALI-culture to stimulate differentiation trough air exposure;

  and alternatively:
- innate immune cells or stromal stem cells, as a third cellular component;
- 176 NTHi strain, to perform a suitable infection;
- PBMCs, to study their recruitment to the infection site.

We deeply characterized the 3D model especially by the use of microscopy.

Furthermore, as secondary objective, we planned to use a promising protocol to grow a gut-derived cell model, whit a major focus on the identification of cell components targeted by toxins and on epithelial homeostasis disruption by microbial virulence factors. Indeed we investigated mouse-derived EnOs in terms of growth, selective vulnerability and survival, after exposure of C. *difficile* TcdA.

DEVELOPMENT OF AN ORGANOTYPIC RESPIRATORY MODEL

The human respiratory tract has the crucial role of exchanging gases with the external environment and it is usually sterile in the section that goes from the glottis to the lungs. Somethimes happens that commensal or pathogenic bacteria can exceed the natural barriers and colonize/infect the middle-lower airways. Indeed during the basic function of breathing, airways are exposed to external particles comprising bacteria and viruses. Therefore the air filtering process is a vital function of the respiratory tract in which the innate immune system is involved.

6 Literature review

6.1 Human airways anatomy, cell types and function

The human respiratory tract differs in mammalian species for length and histology of the different tract (see Figure 9), as consequence of different metabolism and oxygen uptake. We will focus on the conducting zone (CZ) comprising nose, pharynx, larynx, trachea, bronchi, divided in 2 main compartments, mucosa and submucosa; taken together, the *macro* structure is formed by consecutive layers, starting from the epithelial one, then the connective tissue, smooth muscle tissue, cartilage in superior part. Proceeding to lower anatomical regions the cartilage and glandular tissue are reduced, while muscles presence depends on the physiological difference in the tract. The significance of the variation in distribution of secreting cells and mucous glands in the different species is uncharacterized. Alternatively, the division of the respiratory system could refer to upper and lower respiratory tract, with larynx working as dividing line.

The respiratory mucosa shares 2 zones, which are the epithelium and the *lamina propria*. *Lamina propria* is formed of connective tissue with inclusion of capillaries, mucous glands and resident immune cells. However, until the end of conducting zone and before the respiratory zone performing gas exchange (respiratory bronchioles, alveolar ducts, and alveoli), the epithelium is pseudostratified and columnar, covered by mucus and motile cilia. Basically, the pseudo-layer consisted of three main types of cells: ciliated epithelial cells, mucus cells and basal cells.[24]

Basement membrane (BMe) is the ECM separating wall between the two parts of the mucosa; it anchors epithelial cells making strong their adhesion, it provides survival signals for the epithelium, it attends to cellular polarization, it works as a physical barrier. The upper layer of the basement membrane is the *basal lamina*, divided in *lamina lucida* and *lamina densa* (mostly collagen IV and

laminin V) secreted by epithelial cells, while the lower is *lamina reticularis* synthesized by subepithelial cells. [25][26]

6.2 Major cell types and components of the conductive airways

Ciliated and mucus cells work together to conduct the so called mucociliary cleareance, in which pathogens are trapped in mucus and then removed by cilia.

Ciliated cells (CCs) represent over 50% of external epithelial layer and are responsible for the mucus transport, ans as consequence for the clearance of external material trapped in. Hundreds of cilia are outstretched from the AP of each ciliated cells, with basal bodies working to anchor them. A lot of mitochondria are necessary to transmit energy to the cilia coordinated beating. Average lenght of cilia is ~6 μm [27]. CCs are defined high-grade differentiated, their maturation is dependent on FoxJ1 expression. The mucous layer acts as a fluid reservoir and maintains constantly humid cilia lengthways. Two major mucins are present in human airways: MUC5AC and MUC5B, produced respectively by Goblet cells (GCs) and submucosal glands. Mucin production was shown to be regulated by inflammatory mediators [25], such as LPS, TNF-a and IL-1, IL-17, IL-13. Mucus-producing goblet cells are sparse in the airways of adult mice but abundant in human airways [28]. GCs, by electron microscopy, have a cytoplasm containing electron-lucent granules, rich in high molecular weight glycoproteins, which are acidic [29]. Different oligosaccharide side chains (with sialic acid or sulfate) can be detected by histochemical techniques, such us AB for acidic mucins and PAS for neutral mucosubstances.

BCs are the most characterized part of the endogenous progenitor cells present in airways[30]. They lie on basement membrane in trachea and main bronchi. New markers for the identification of basal cells based on *in vivo* studies are continuously discussed, however many of them are established for the respiratory epithelium (Figure 13).Among this list it is recognized the prominence of p63, a transcription factor expressed at basal cells of stratified epithelia throughout the body. Mice homozygous for a mutant Trp63 die postnatally [31]. In normal lung, p63 intensely stained nuclei of bronchial reserve cells but did not stain ciliated cells or alveolar epithelial cells, neither non-epithelial cells. p63 is expressed in BCs lining the BMe in bronchial epithelium. AQP-3, protein channel present in epithelia exposed to water loss [32]. Relying on transplantation studies of fetal human respiratory tissues into immunodeficient mice, AQP-3 was shown to mark basal layer of cells and able to regenerate mucociliary phenotype and glandular also [33]. In general, at molecular level Notch signaling is required for the differentiation, but not self-renewal, of BCs. Sustained Notch signaling activation, which promote secretory than the ciliated fate, is required for luminal differentiation [28], [34]–[36].

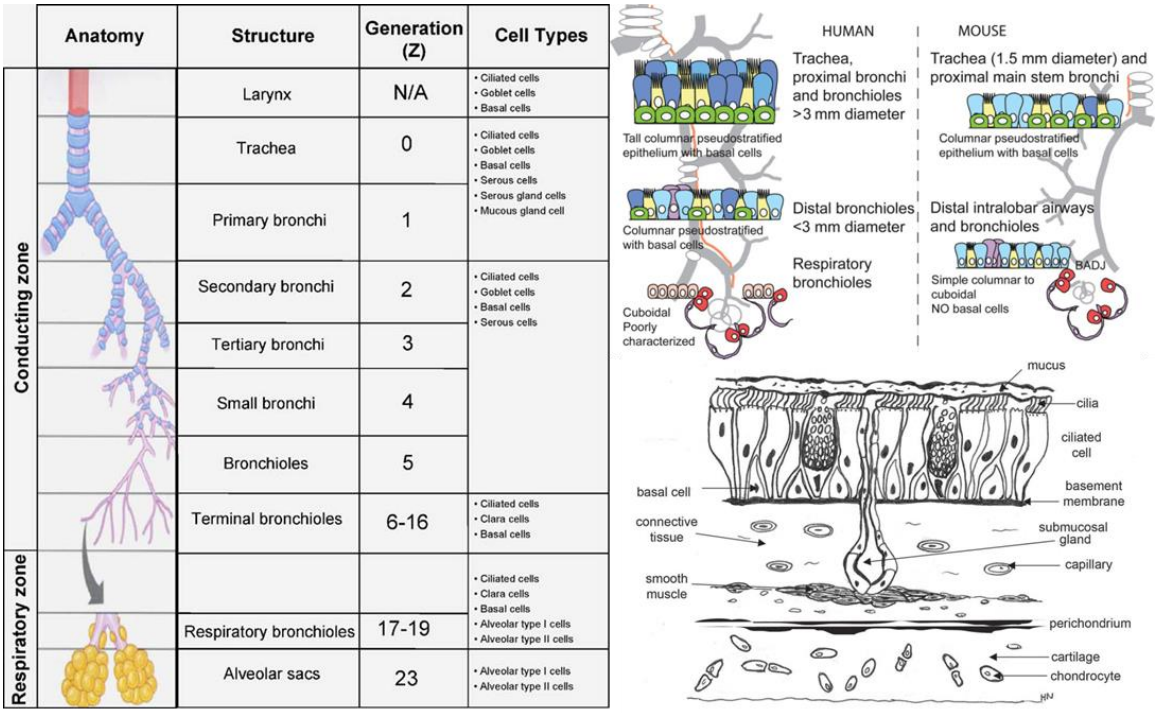

Figure 9 Anatomical and histological structure of human airway wall. Adapted from Berubè et 2010 [124], Roomans et al 2010 [125], Wansleeben et al 2013 [36]

6.3 Minor cell types

Furthermore there are other cells such as brush cells and endocrine cells (PNEC). Brush cells possess a tuft of microvilli at their apical surface and apart from a possible absorption role, their function is still to be characterized, but recent evidences suggested they are chemosensory cells. They also seem to recognize microbial compounds and modulate epithelial response to the infection. PNECs (or Kulchitsky Cells) also occurs individually, with pyramidal morphology, or in small cluster called NEB, they are known to produce many kind of granules, including serotonin and calcitonin, they sense hypoxia and nicotine, are innervated by sensory nerve fibers.

6.4 Host-defense and immunoregulatory cell types

Following airway damage, immune system and proliferation and differentiation of resident progenitor or stem cell pools are necessary in order to maintain a protective barrier.

Moving towards the respiratory zone, the epithelium becomes a simpler columnar/cuboidal monolayer and all the three cell types, described above, gradually reduce in number, in favor of Club cells appearance. Club cells (ClC) are non-ciliated secretory cells, present mainly in bronchioles and with a very heterogeneous morphology among the species. They reverse into the lumen secreted forms of CSSP (also known as uteroglobin, CC-10), mucins, specific antiproteases, p-450 mono oxygenates and antimicrobial peptides. Surprisingly they also act as progenitor cells where BC population is decreasing according to the anatomical changes. Indeed their function

translated from pulmonary host defense hypothesis to a stem cell reservoir population. They have a repairing role, protective against direct external damage than the normal cellular homeostatic replacement. Club cells are ready to exit from a steady state for replicating and substituting high differentiated cells as Ciliated or Goblet (that's possible to talk about "redifferentiation"). In addition, Club cells are able to dedifferentiate in BCs [37] in case of their ablation or either in AECs after lung chemical injury [38]. The pathways controlling differentiation and development of Club cells are poorly characterized and they are conditioned by ongoing i*n vivo* lineage-tracing studies.

In addition, immune cells residing within the mucosa are freely to migrate between the two compartments, because the presence of specialized pores in BMe [26]. These cells include mast cells, intraepithelial lymphocytes, dendritic cells and macrophages; in some cases there are organized lymphoid aggregates called BALT [39]. Many groups searched for the number and localization of the immune cells resident in the airways, but imprecise description was recorded, perhaps resulted by limitations techniques at that time. It is not the intention of the thesis to discuss about all this immune cell types, except a note for dendritic cells. They are powerful APC, involved in the second innate mechanism of defense (see Figure 10)

Residing within the airway mucosa, pulmonary DCs (p-DC) sample the content they caught, migrate and then present these antigens to T-cells. In the lung the migratory patterns of p-DCs are highly dependent upon inflammatory conditions. DCs recruitment to the lung is increased and renewing after injury challenge and inflammation onset. Resident p-DCs are not a homogeneous population, maybe because they reflect different stages of maturation, and for this reason their classification is generally based on anatomical location or surface markers. In 1986 APCs with dendrites were found within the human airway wall, just above the basal lamina, with extending cytoplasmic processes [40]. Their identification in human bronchial tract was confirmed after different tissue digestion protocols and lung sections immunohistochemistry against MHCII (high levels) [41] but also by infrequently positive staining for CD1a [42]. Studies regarding their localization (dissimilar among the species) studies in CZ and phenotypic analyses showed that the human intraepithelial DCs have more endocytic activity (supposing a tolerogenic one), CD1a expression (similar to Langherans cells [41] whereas the subepithelial cells do not [43]. According to this investigation [44] the p-DCs seemed to possess an immature phenotype similar to the *in vitro* DC obtainable with the protocol provided by Sallusto [45].

Last noticeable cell type that should be introduced are Mesenchymal stem cells (MSCs). MSCs represent a heterogeneous subset of multipotent stromal cells, resident in many different adult tissues, that exhibit the potential to give rise to cells of diverse lineages, not only mesodermal. MSCs are widely defined and accepted by ISCT as population with positive simultaneously

expression for CD90, CD105 and CD73, with a concomitant absence of CD45 and CD34 [46][47]. MSCs have potent paracrine trophic, anti-apoptic, angiogenic, but especially immunomodulatory effects. In particular they are poorly immunogenic, immunoprivileged and immunosuppressive [48]. Unlike MSCs isolated from many other tissues, lung resident MSCs (Lu-MSC) still lack of conspicuous characterization and their recognition is recent among the scientific community [49]. Lu-MSCs were isolated probably for the first time by Sabatini [50] in bronchoalveolar lavage fluid from human lung allografts [51] as well as fetal and adult lung digests [52] and tracheal aspirates [53].

The beneficial effects of MSCs after injury are likely linked to indirect support to the epithelium instead of a direct replacement / substitution role of the damaged cells. The idea is that Lu-MSCs, as BM-MSCs, create a supporting environment for HSCs during haematopoiesis. HSCs are an essential element of the epithelial stem/progenitor cell niche in the adult lung. Despite it is still controversial whether Lu-MSCs can undergo mesenchymal-to-epithelial-transition, [54]. A comparison study not only confirmed that Lu-MSCs possess part of the immune regulatory properties broadly described in BM-MSCs, but also showed a partial *in vitro* differentiation toward the epithelial lineage. Recent *in vivo* studies indicate that mesenchymal stem cells (MSCs) can boost the treatment of sepsis induced by bacterial infection in lung and gut animal models [55], [56]. It seems that apart from capacity to interact and recruit immune cells activity [57], [58] also their intrinsic antimicrobial properties [48] are capable to improve survival and enhanced bacterial clearance. They indeed produced antimicrobial peptides such as LL-37 [59]. Unexpectedly the antibacterial role of MSCs is not proven by a consistent medline. *In vitro* MSCs (compared to HLFs) inhibit the growth of Gram– and Gram+ bacteria, and even their conditioned medium [60]. Recently *in vivo* administration of MSCs and of their microvesicles showed reduce acute inflammatory lung injury [61] . This data are maybe the last accompanying the evidence of MSCs beneficial activity in endotoxemia, acute lung injury, or sepsi models. For further information we suggested our references list [62].

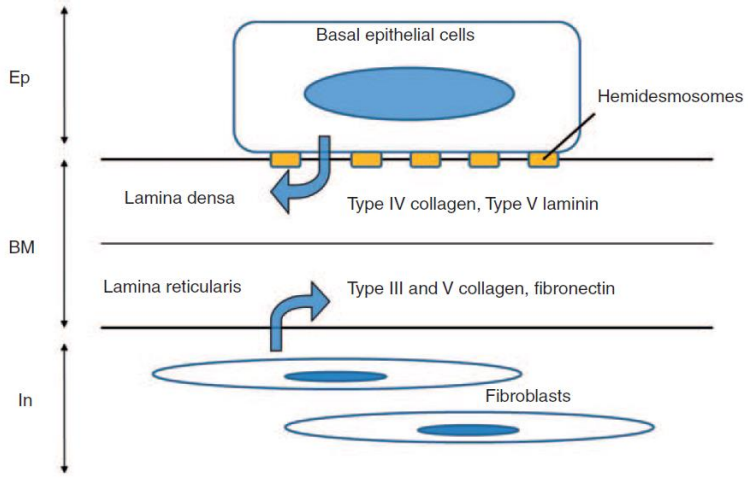

Figure 11 Schematic of basement membrane at the axis between epithelium and *lamina propria*. Source: Tam et al.2011.

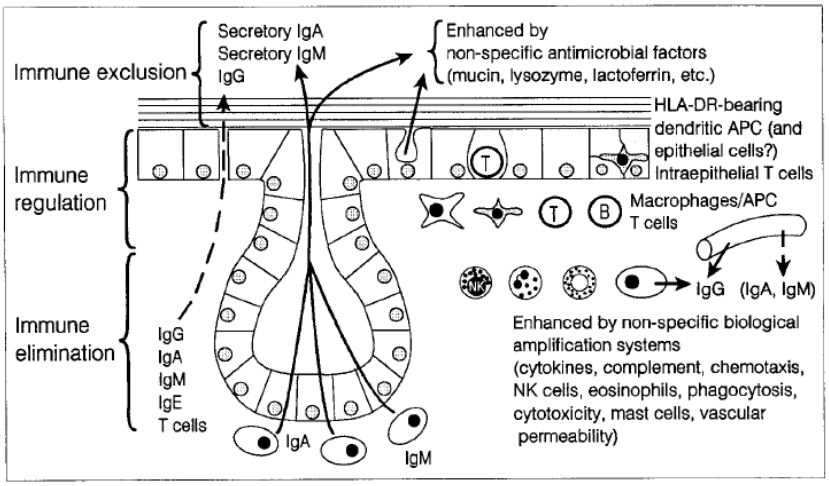

Figure 10 The three immune functions present at the level of the mucosa. Source: Demedts et al.2005.

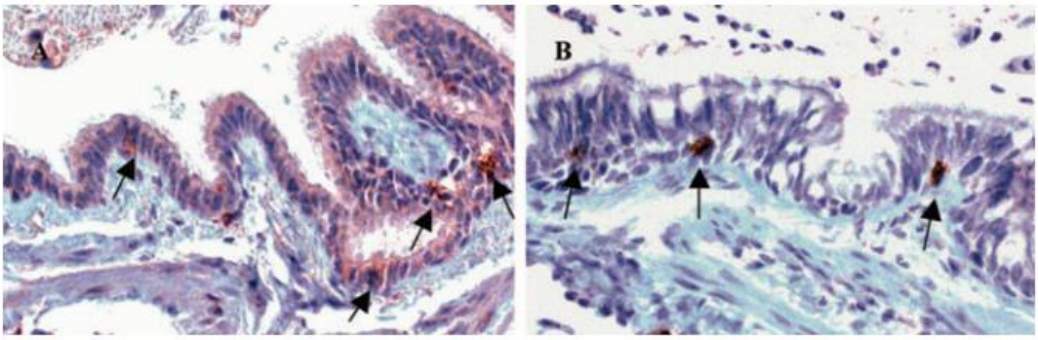

Figure 12 Immunohistochemical analysys for CD1a (A) and Langerin (B) in human lung sections. Source: Brandtzaeg,et al 1995

Gene symbol (protein)	Reference for expression in mouse	Reference for expression in human
Trp63	Rock et al., 2009	Araya et al., 2007
Snai2	Parent et al., 2004; Rock et al., 2009	J.R.R. and B.L.M.H., unpublished data
Ngfr	Rock et al., 2009	Rock et al., 2009
Egfr	Rock et al., 2009	Voynow et al., 2005
Pdpn	Farr et al., 1992; Rawlins et al., 2009	Human Protein Atlas[a]
Krt5	Schoch et al., 2004; Rock et al., 2009	Human Protein Atlas[a]
Krt14	Hong et al., 2004	Nakajima et al., 1998
Aqp3	Rock et al., 2009	Avril-Delplanque et al., 2005
Cdh3 (P-cadherin)	Rock et al., 2009	Human Protein Atlas[a]
Itgb6 (integrin β6)	Rock et al., 2009	Araya et al., 2007

[a]http://www.proteinatlas.org/

Figure 13 Selected markers list for BCs. Source: Rock et al. 2010

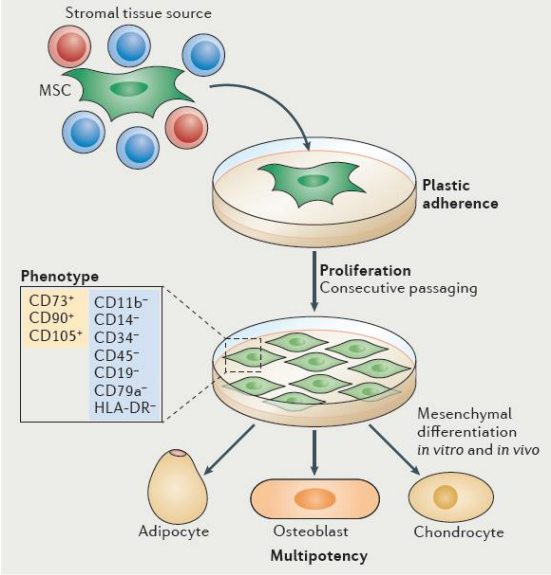

Figure 15 Criteria for the definition of MSCs. Source: Le Blanc.et al 2011

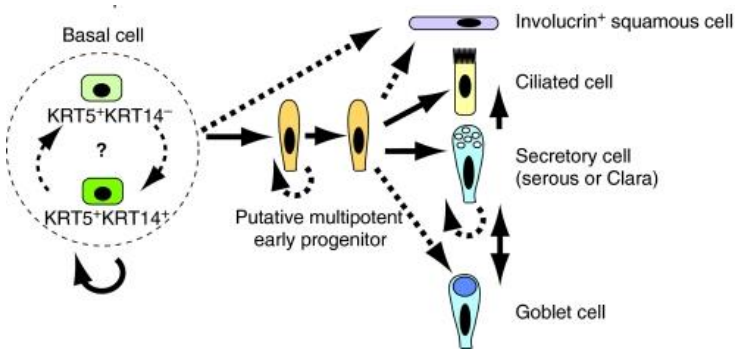

Figure 14 Model for the self-renewal and differentiation of basal stem cells in mouse and human airways Source: Rock et al 2010.

6.5 State of art: cell culture models of the airway

The progress in cellular biology methods and *ex-vivo* models currently allow scientists to examine minute mechanisms such as happening during early embryonic lung, but this possibility, as we already mentioned, is restricted and not feasible to study several host-pathogen interactions because immediately restricted to availability of organs from laboratory animals.

Until last decade the models used to understand microbial interaction with the host, also to study epithelial airway cells, were commonly human cell lines, like alveolar cell line "A549". The latter are continuously used in non-appropriate mode in host-pathogen interaction protocols without curing the fact that is functionally deficient for TJs formation and epithelial integrity. The bronchial epithelium 16HBE14o- or BEAS-2B, cell line are not able alone to display a physiologically close-reconstruction of that tissue, such as a simultaneous cilia formation, mucus secretion, TJs expression, epithelium repair capacity. Indeed BEAS-2 cells resulted instead unsuitable to study airway barrier function, lacking marker of full differentiation capacity (mucins) and showing poor TEER. As confirmation of aberrant cell phenotype and discrepancy among laboratories protocols, the formation of functional 16HBE14o– cell layers requires the presence of submerging condition, in contrast to other airway epithelial cells [63].

The actual more recognized model to study absorption and permeability of airway epithelia is Calu-3, lung adenocarcinoma cell line. Cultured at ALI those cells acquire a great secretory phenotype, a columnar morphology and showed a similar TEER trend in comparison with primary bronchial cells. Unfortunately, unlike primary bronchial cells, Calu-3 polarized on transwells, even after ALI phase, do not differentiate into layers of basal cells or mature cells developing cilia, probably because their parental epigenetic memory is linked to a phenotype similar to gland cells. in this way, ALI conditions for Calu-3 cells are not as critical in promoting cellular differentiation as it is for HBECs. Pronounced polarization occurs either in submerged conditions [64] while mucin secretion, and tight junctions can vary a lot between ALI / submerged conditions. Generally, all the above cell line system still require serum–condition, retain of a spontaneous uncontrolled tumor-derived growth capacity or own a differentiation potential stopped by in vitro transformation.

Recently, scientists strive to get outcome from primary cells or combinations of cell lines in co-culture. HBECs obtained directly from biopsies are available as low passage from several commercial sources. HBECs constitute a multipotent population of cells ($p63^{high+}$) [37], [65] that share markers with the airway basal cell signature. This purified population is capable of self-renewal. Higher cell passage ($>4^{th}$) lose the ability to differentiate in a complete mucociliary

phenotype [66], in contrast to hTERT immortalized BC line (like BCi-NS1)[67] that retains characteristics of the original primary cells for over 40 passages.

Previous history on bronchial primary cells documented the importance of some soluble factors in this kind of culture. Serum-free condition is more functional to obtain multilayers and differentiation of epithelium [68], [69]EGF stimulates the proliferation and influences the cell maturation process. BPE is mitotic agent and it is involved in ciliated differentiation [70]. RA is extremely important precondition to reach tissue differentiation [66].

By the way, ALI phase is preferable in culture primary cells, because is more physiological condition to recapitulate airway epithelium function than submerged conditions [71]; the switch to evolve AP in a "dry" culture certainly affect the thickness (cell height and number of cell layers) of the epithelium in a time-dependent manner [68], [72]. Extensive time in culture in some cases cause the de-differentiation of the forming *in vitro* tissue.

The possibility to resemble the whole respiratory epithelium in 2.5D culture models arose just few years ago [73].Rock et al., starting from fractionated $CK5^+$ murine basal cells, showed the formation of "tracheospheres" within 1 week, immersed in Matrigel plated on transwell membranes and grown under ALI conditions. By day 20^{th} these surviving spheres underwent luminal expansion and contain differentiated CCs and BCs. The same result was obtainable starting from human airway $NGFR^+$ $ITG\alpha6^+$ cells. No secretory cells were detectable in that system. A similar approach was made by Wong and co-workers and their study confirmed the multipotency of (commercially available) HBECs under different culture protocols [74].They obtained glandular acinar structures when HBECs were overlaid on Matrigel and covered with an EGF-enriched medium (protocol similar for mammary acini morphogenesis [75]). Efforts recently published by Danahay et al. reported "bronchosperes", derived from HBECs, that recapitulate the key elements of the conducting pseudostratified epithelium [76] and that enable HTS discarding transwell use. Thanks to a similar report, we know that progenitor cells of the respiratory zone, identified in AEC2s [77], can form self-renewing and differentiated (both mature AEC2s and AEC1s) "alveolospheres" [78] when they are co-cultured combining transwell, matrigel and ALI conditions, with primary $PDGFR\alpha^+$ lung stromal cells (a population that include fibroblasts and lipofibroblast in proximity of alveoli[34]. In parallel, importantly, MRC5s (human fibroblast cell line) were necessary to support isolated $HTII\text{-}280^+$ cells (AEC2s cells) to form human alveolospheres however without retaining the differentiating capacity[77]. Alveolar spheroids obtainable stimulating iPSCs are described in a co-culture with fetal lung fibroblasts [79].

Use of transwells and of natural ECM substitutes enabled more complex co-culture setup.

A sophisticated 3D airway *in vitro* construct has been established with the aim to offer a model to study angiogenesis in asthma, but the work made known the importance of the use of cells co-cultured in 3D conditions to develop an organized capillaries network. HUVECs were coated on dextran beads and suspended in a fibrin gel toghether with a sheet of HLFs and finally HBECs, separately differentiated on transwell inserts, are added to the co-culture. The addition of HLFs in gels to the model was critical to allow HUVECs migrating off the beads, while HBECs promoted an increase in VEGF production thus suggesting a role in directing angiogenesis. Further evidence of the importance of the heterotypic interactions happening in lung and interesting to develop intelligent *in vitro* set-up belonged to a model of airway branching [80]; 3D-culture of VA10 (a BC-like cell line) in presence of HUVEC generated bronchio-alveolar structures that are regulated by stromal soluble factors as FGF. Interestingly, VA10 alone or HUVEC monoculture (in the same Matrigel conditions), or neither A549-HUVEC co-culture, displayed branching, pointing out the importance to respect the tissue origin to arrange as much as possible the proper artificial niche.

The choice of the epithelial cell type should be very careful: co-culture of HBEC/Wi-38 but not of 16HBE14o-/Wi-38 made a both multilayered and differentiated epithelium [72]. Goto et al. had the distinctive idea to use natural biological membrane rich in ECM, like amniotic membrane, as replacement of the BMe to differentiate HBEC and afterwards add tracheal fibroblasts for the last part of the culture [81].

We preannounce that a lot of the existing models are based on collagen matrix populated by stromal cells to mirror the *lamina propria.* Like what happens in dermal equivalent reconstruction [82], many 3D airway model were generated until now by embedding lung fibroblast in a collagen matrix [83]. A very elegant protocol was offered by the group of Swartz to develop a physiological 3D model with primary human epithelial cells and fibroblast embedded in a gel [84]. Such sort of models, like the one achieved by Vaughan et al., cannot exclude the contraction phenomenon by the gel [85].“Bronchial equivalents” proposed by Paquette et al. revealed that optimal peripheral anchorage of the gel prevented collagen contraction by fibroblasts, showing a way to fix this technical complication [69]. Interestingly, Pageau et al. showed how collagen concentration and composition affected the phenotype of bronchial epithelial cells in 3D culture, as well the contribution of tumoral fibroblasts (as soluble factors carrier) can interfere with the epithelial homeostasis[[86]. Indeed different subtypes of fibroblasts can exert different effects on the epithelial cells and viceversa [87].

Relatively simply transwell co-cultures of epithelial cell lines and immune cells demonstrated that there are tissue responses such us particular cytokine production only in presence of inter-cellular communications and paracrine signaling [88]. Previously Chakir et. al compared the interaction between immune cells (T cells) and derived bronchial resident cells (HBECs and HLFs) between normal and asthmatic biopsies [89]. Among the concrete attempts of coupling innate immune cells with a respiratory mucosa equivalent, the list goes to be shorter. Since ten years ago Rothen-rutishauser and colleagues worked to develop immunocompetent lung co-cultures; A549 cells, in the form of transwell monolayer, were surrounded on their polar sides respectively by macrophages and dendritic cells, with the aim to analyze particles interactions in a relevant model [90]. Choe et coworkers adapted their model, mentioned before, to unravel thin mechanisms during airway remodeling; by introducing eosinophils in the epithelial-mesenchymal culture they discovered that the combination of mechanical strain and activation of inflammation (but not by either one alone) induced epithelium thickness [91]. 16HBE14o– epithelial cells and human blood monocyte-derived macrophages and DCs are organized in co-cultures by Lehmann et. al. in 2010 [92]. Later, Svensson group developed a beautiful transwell supported model containing 16HBE14, DCs and MRC-5s. In the last case, the use of cell lines was justified by the advantage of easily tracing transfected fluorescent cells [93]. The dendritic population was confirmed to be a mobile element in the artificial environment set. The same group was able to show that the DCs are responsive external stimulation, like inflammation stimuli given to the organotypic model, finally following DCs fascinating migration within the model. Similar reconstruction was described and published in 2014 [94]. A 3D model comprised of these 3 key cell types present in upper airway epithelium (Calu-3, MRC-5 and DCs) were initially grown on individual scaffolds and then assembled together before probing the model with inflammation mediators [95].

Original investigation was carried on by whom wanted to check the benefits to include interesting stromal population like MSCs in airway *in vitro* systems. Transwell inserts were used as BMe substitute on which adult BM-MSCs were cultured on the lower side and NHBEs on the opposite one [87] . Analysis of apical secretions showed that mucin production increased over time, with peak secretion for NHBEs alone, whereas the secretion by NHBE cells co-cultured with MSCs remained constant for an earlier and longer period. In particular Kobayashi et. al evaluated differential contribution of gingival fibroblasts and A-MSCs to the differentiation of a 3D collagen model suitable to be transplanted [96]. Fibroblast density was correlated with GCs production and comparable to alternatively used tracheal fibroblasts. A-MSCs seemed to give an advantage in epithelial cell proliferation (at the level of BC) but in the absence of fibroblasts, there was no clear cell polarity [96]

Definitely, above described panel of references enhances the role by environmental conditions and of cell type itself to affect the differentiation of cells in 3D culture. Moreover this fact suggested and impacted the development of airway mimicking *in vitro* models too.

Cell model	Derivation	Pros	Cons	Micrographs
Calu-3	Carcinoma of the bronchus	Immortalised Form confluent mono-layers Develop Cilia Express mucin genes	Variation in tight junction (TJ) formation	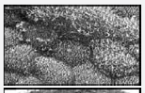
BEAS-2B	Transformed bronchial epithelium	Immortalised Form confluent mono-layers Secrete cytokines Express antioxidants	No mucin secretion Lack TJs	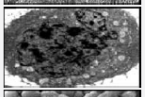
16HBE14o–	Transformed bronchial epithelium	Immortalised Differentiated & multi-layered Develop cilia & microvilli Secrete cytokines	No mucin secretion	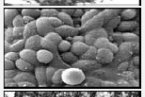
NHBE	Normal human bronchial epithelium (primary cells)	Long lifespan & not transformed Differentiated & multi-layered Form cilia, TJs, secrete mucus Serum-free medium	Not immortal Labour intensive	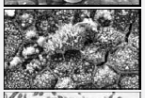
[a]MatTek Epiairway™	Human tracheal/bronchial epithelium (primary cells)	Long lifespan & not transformed Differentiated & multi-layered Form cilia, TJs, secrete mucus Serum-free medium	Not immortal Cost to purchase	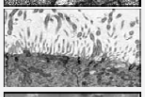
[a]Epithelix MucilAir™	Human respiratory tract (primary cells)	Long lifespan & not transformed Differentiated & multi-layered Form cilia, TJs, secrete mucus Serum-free medium	Not immortal Cost to purchase	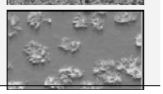

[a] Information was obtained from commercial web-sites.

Figure 18 Overview of epithelial model of the bronchial tract. Source BèruBè et al 2010 [124]

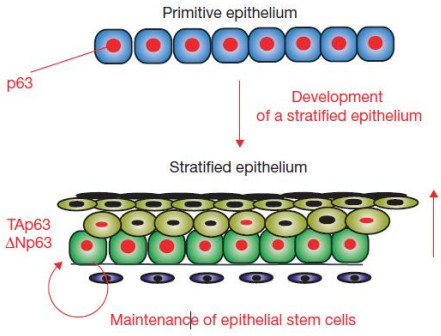

Figure 16 Roles for p63 in the development of a stratified epithelium.Adapted from: Blanpain et al 2007 [127]

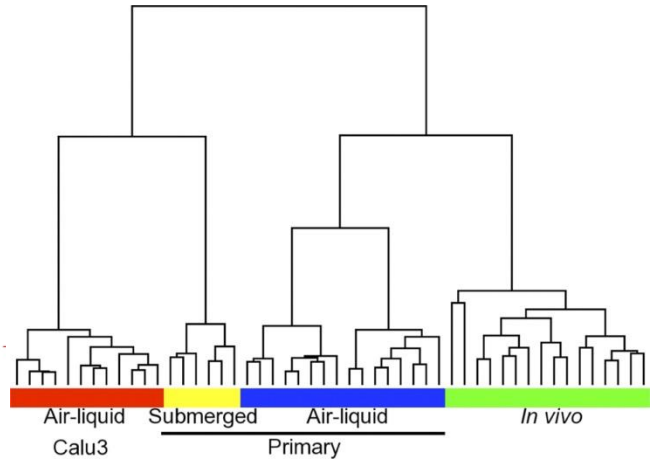

Figure 17 Unsupervised clustering of epithelial respiratory cells. Source: Pezzulo et al 2011[71]

7 Methods

7.1 Lung-derived cell cultures and characterization

Normal human lung fibroblast (NHLF) were purchased from Clonetics™ and cultured in in FGM-2 (Lonza). 3rd P single stocks are expanded in Falcon T75 flasks. For the 3D model co-culture NHLF until passage 8th.

HBEC are obtained from Clonetics™, specifically normal human tracheobronchial epithelial cells (NHBE) are cultured in BEGM (Lonza) and cryopreserved at 2nd P. Medium selection for ALI phase was decided comparing B-ALI(Lonza), that we indicated as m1, and PneumaCult™-ALI (STEMCELL Technologies™), abbreviated as m2.

For the 3D model co-culture NHBEs are expanded in BEGM in Falcon T75 flasks. NHBEs at 3rd P are prepared for the differentiation protocol when the confluence is about 80%. PneumaCult-ALI is the medium used to switch 3D NHBE-culture to the ALI phase. Falcon 12 well-plate Transwells with 0.4 µm, coated with collagen type I solution 0.03 mg/mL for at least 2 h at 37°C, are used to support monolayer differentiation of NHBEs, to check the capability of a HBEC-monoculture to differentiate successfully in parallel to the 3D culture containing them. Cilia beating was assessed by optical microscopy and registered by AxioCam with maximum framing rate and 10X or 20X optical zoom [Zeiss][data not shown].

Accutase solution (Invitrogen) is chosen as dissociation agent for the passaging of lung cells. Usual incubation required to detach cells is 5 min for NHBEs and 3 min for NHLFs.

7.2 Generation of Dendritic Cells

Buffy coats drawn with informed consent from healthy donors are used as source of human PBMCs that are isolated by Ficoll-Paque™ density gradient centrifugation. PBMCs are then processed using Pan Monocyte Isolation Kit MACS® Technology (Miltenyi Biotec™) or RosetteSep™ Human Monocyte Enrichment Cocktail (STEMCELLTechnologies™) to obtain $CD14^+$ $CD16^+$ monocytes by negative selection. Monocytes are seeded in Falcon 12-well plates at density of 500000/mL in advanced RPMI 1640 Medium (Gibco®) supplemented with 10% Fetal Bovine Serum, beta-mercaptoethanol 50 µM, GlutaMAX™ 2mM, and PS solution. To promote *in vitro* differentiation of immature Monocyte-derived Dendritic Cells (MoDC) purified monocytes are cultured for 6 days in presence of 50 ng/mL of human recombinant GM-CSF and IL-4 (Gibco®). Cytokines supplemented medium is refreshed once after 3 days, saving all non-adherent or loosely adherent

cells by centrifuging. On 7th day single MoDC aliquot i harvested, the cells are stained with antibodies cocktails for CD209, CD14 and CD83 (Miltenyi) and surface expression was analyzed by flow cytometry to evaluate their differentiation stage. Different blood donor preparations were preliminary analyzed to check maturation state and donor variability of fresh or thawed cryopreserved MoDCs. Phenotype is compared to a preparation obtained from the same donor using a commercial ready-to-use G4 MoDCs generation kit (Humankine).

7.3 Mesenchymal Stromal Cell culture

Umbilical Cord - derived Mesenchymal Stem Cells (UC-MSCs) screened for specific stem cell surface antigens and derived from human Wharton's Jelly were purchased from ATCC®. They are propagated in MesenPRO RS™ (Gibco®) plus Primocin antimicrobials (Invivogen). Retention of multipotency after expansion period is evaluated checking mesenchymal differentiation towards adipogenic lineage. I*n vitro* adipogenesis induction is performed trough adipogenesis differentiation kit (StemPro®), following the technical sheet indications, culturing MSCs for 2-3 weeks in cell culture plate or even in alvetex scaffold. IL-10 release by MSCs is tested by intracellular immunofluorescent staining and measured by flow cytometry [data not shown]. For 3D cultures MSC are used until passage 7th.

7.4 PBMCs labeling

CFSE 10 μM in PBS is the labelling solution for PBMC, the reaction works at RT. After 2 washes in PBS pelleted cells are resuspended in medium. Correct uptake of the dye is checked under fluorescent microscope. PBMCs aliquot is checked for viability by trypan blue exclusion.

7.5 Stromal 2D-co-cultures

UC-MSCs and NHLFs are seeded sub-confluent and cultured in 6-well plate as monoculture or mixed each other in 1:2 ratio, to select optimal medium conditions for co-culture. Analogous co-cultures, excluding hybrid cell-cell interactions, are set to distinguish the growth of the two inquired cell types; MSCs are cultured in the upper chamber of transparent Transwells 0,4 um pores while NHLFs in the lower chamber. Alternatively Flowell plates (Corning) are prepared separating MSCs and NHLFs populations, seeded with identical density, respectively in 1st and 3rd column of wells and using the middle column well as medium reservoir. FGM2 and MesenPro media combinations are tested. After 1 week culture the cells are fixed and stained with methyl violet 0,5%. mitotic figures and cell number is estimated.

7.6 3D cell culture set-up

7.6.1 Mesenchymal layer production

Alvetex® Scaffold 12-well inserts are pretreated as instructions. PuraMatrix (BD Biosciences) is diluted to 0,8 mg/mL in cold PBS, vortexed and 250 µl added soon on each insert. After 30 min 37°C CO_2 the excess of Puramatrix coating solution is removed by gentle tapping of the insert and a volume of FGM medium, enough to left the insert dish hydrated until next cell seeding, is placed in the lower chamber of cell culture plate. 5* 10^5 NHLF are seeded on the top of the insert in 75 µl of FGM2 medium, then the insert is incubated for 1h at 37°C 5% CO_2 to settle the cells. Afterwards the seeded inserts are flooded with FGM2 and culture medium is refreshed every other day.

7.6.2 Epithelial layer assembly

The day before the epithelialization of the mesenchymal compartment (i.e. the NHLF culture) are coated with a thick gel of rat tail collagen type I. Covering medium is removed from the apical part of the insert and 180 µl of neutralized 2 mg/ml solution in DPBS Ca^{2+} Mg^{2+} are pipetted and left to polymerize for 1h. Coated inserts containing NHLFs are replaced in incubator with submerged conditions. NHBE are harvested from the flask, diluted in trypan blue solution and counted with hemocytometer. Cells with >80% viability are counted and seeded with a density of 11*10^5 cells/cm^2 in 200 µl of BEGM, incubating 1 h at 37°C 5% CO_2,. Subsequently 500 µl of BEGM are pipetted to the top of the insert and the set 3D-culture is moved in incubator for 24h, leaving the medium contacting the above and below of the insert independently. The day after additional medium is added to the well until submerging the insert combined to the cells.

On day 3, each tissue-insert is transferred in the inner chamber of a Falcon inserts 3.0 µm pore size. At that point they are poured in Deep-Well plate (Falcon) and lower chamber of the Falcon insert filled with PneumaCult-ALI maintenance medium, supplemented with Primocin 50 ug/mL. Cultures are maintained with weekly medium replacement. Optionally, from the beginning of the 2^{nd} week, surfaces of the cultures are washed twice with warm DPBS to prevent excessive mucus accumulation. After 3 weeks of ALI-culture, our differentiated BE (Bronchial Equivalent) models are ready-to-use or directly fixed for morphological characterization. In our preliminary studies, we pre-emptively verified viability of the BEs, incubating them in Prestoblue reagent and reading signal after 2 hours of reaction.

7.6.3 Triple co-cultures

For the immunocompetent model (DC-BE), dendritic cells are included during the gel coating of the Alvetex surface, prior to NHBE seeding. MoDCs, resuspended 2*10^6 /mL in their cytokines

supplemented medium, are embedded in the collagen I dilution solution and later seeded $1*10^5$ cells to each Alvetex insert surface. The coating is left hydrated for 24h with basal MoDC medium.

For the stromal hybrid "sustained" model (MSC-BE), a total of 500000 UC-MSCs / NHLFs in ratio 1:3 are seeded in Alvetex insert and cultured in MesenPro until the NHBE addition.

Apart from those modifications, the culture follows the steps above.

The lot number of the lung derived cells are shared during the assembly of 3D cultures when a comparison between dual- and triple-culture is needed.

Figure 19 Cartoon representing tryple cell culture configurations

7.7 Morphological characterization

7.7.1 Histology

The samples are fixed O/N in 4% paraformaldehyde pH 7.6, cut in 2 equal halves along the sagittal plane and processed for paraffin embedding. Then 3/4-µm sections are cut with Leica RM2255 microtome. Deparaffinized and re-hydrated histological sections are stained with Carazzi's Hematoxylin (1min 20 sec) and eosin (13 min), finally dehydrated. Images are acquired by Leica DM5000B microscope. For AB/HE a primary staining step is done for 30 min with Alcian Blue 8GS 1% pH 2.5 and surface of samples are not washed before fixation.

7.7.2 Immunohistochemistry

For immunohistochemistry deparaffinazed slides are pretreated with Cell Conditioning 1 (Roche), .Polyclonal α-laminin is incubated 12h with addition of antibody block (Roche #760-4204). For the detection secondary Ab HRP conjugated is overlaid for 20min and ChromoMap DAB kit is used (Roche #760-159). Immunostainer station is Discovery Ultra (Ventana)..

7.7.3 Frozen section preparation

Samples previously fixed for at least 24 h in PF 4% are soaked (O/N, 4°C) in sucrose 15% and then in a sucrose 30% bath before to include them in O.C.T. compound. The sample is frozen in 10 min in cold isopentane baker and stored at -80 until is processed for cryosectioning. 10 µm or 20 µm sections are made using Leica CM1950 cryomicrotome, fixed on Superfrost slides with ethanol:methanol and are used for immunofluorescence staining.

7.7.4 Whole-sample epifluorescence imaging

Untouched and unwashed fixed samples are stained for qualitative mucus and cilia detection by conventional immunofluorescence. Fixing is in 4% paraformaldehyde for 4 hr. Inserts are rinsed with washing-buffer (PBS, 0.1% bovine serum albumin, 0.2% Triton X-100, and 0.05% Tween- 20), blocked with blocking buffer (washing buffer 10% goat serum) then stained with primary antibodies, diluted in blocking buffer, at 4°C O/N with gentle shaking. Primary antibodies used for this specific assay are anti-MUC5AC (Mouse IgG1, Clone 45M1) and anti-α Tubulin, (Mouse IgG2b, clone 6-11B-1). Fluorescent conjugated secondary antibodies are used 1:200 in blocking buffer. Nuclei as well scaffolds are counterstained with Hoechst 3442 (1:10000). After final washes the samples are stored in PBS protected from the light at 4°C. Overlapping tiled images are acquired through Axiovert-200 microscope (Zeiss) equipped with a motorized stage and Orca-ER-1394 camera (Hamamatsu), in AxioVision suite coupled to MosaiX module.

7.7.5 Immunofluorescence on cut samples and cryosections

ECM deposition by NHLF cultured in 3D culture was assessed with indirect immunofluorescence detection of fibronectin or collagen type I. Alvetex insert containing $1*10^6$ NHLF, were cultured for 5-7 days in FGM2 medium, then fixed in PBS 2 % PF for 15 min. Antibody blocking solution ends with primary Ab 1:400 dilution in PBS 1% BSA is incubated for 1h, RT and gentle shaking. Secondary antibody Alexa-conjugated are used for the detection. Confocal microscopy equipment is a LSM710 system (ZEISS). For immunofluorescence broad analysis washed intact samples are fixed in PF 4% for almost 12 h, while for mucin detection some samples are alternatively fixed in cold Acetone/ Methanol solution for 10 min. Samples are then cut in different parts and washed twice in PBS. PF-fixed samples are also incubated 15 min in permeabilizing solution containing PBS 1% Triton x-100. Non-specific binding is blocked incubating samples for 45 min in cell culture plate wells with PBS 10% goat serum, 3% BSA, 0,1% triton. Antibody dilution buffer is PBS 1% BSA. Primary antibodies are diluted 1:250 and left O/N at 4°C with gentle rocking. The day next species are washed twice for 5 min with gentle agitation. Alexafluor conjugated secondary antibodies such as phalloidin are incubated for 1 h at RT and with rocking. After 5’ of staining with

Hoechst 33342 (1:10000) or DAPI in PBS the samples are washed in copious PBS then visualized under confocal microscope.

For cryosections staining the slides are rehydrated with PBS, following a blocking step of 30 min. After 1 wash in PBS BSA 1%, primary antibodies are diluted in PBS 0,1% Triton and let to cover the slide for 1 h RT. After 3 quick wash, samples are exposed to matching Alexafluor secondary antibodies (or phalloidin) for 30 min prior to 2 wash in PBS and final counterstain with Hoechst - 33342. Finally samples are washed and mounted in Antifade Reagent. Acquisition, depending from the target, is performed through Axiobserver or LSM710 (Zeiss) platforms.

7.7.6 Electron Microscopy

Samples, eventually divided, are fixed in sodium cacodylate buffer 0,1M containing 2,5% glutaraldehyde and 2.5 % paraformaldehyde and stored at 4°C O/N. Samples were washed in the same buffer and then post-fixed in 1% OsO4 in 0.1 M cacodylate buffer pH 7.2 for 1 hour at room temperature and then washed again in the same buffer. Specimens were dehydrated in a graded ethanol series. They were then dried by the critical point method using CO_2 in a Balzers Union CPD 020, sputter-coated with gold in a Balzers MED 010 unit. The observation was made by a JEOL JSM 6010LA electron microscope.

For Transmission Electron Microscopy (TEM), samples were fixed and dehydrated as described above and embedded in LRWhite resin (Multilab Supplies, Surrey, England). The resin was polymerised in tightly capped gelatine capsules for 48 h at 50°C. Thin sections were cut with Reichert Ultracut and LKB Nova ultramicrotomes using a diamond knife, collected on copper grids, stained with uranyl acetate and lead citrate, and observed with a JEOL 1200 EX II electron microscope. Micrographs were acquired by the Olympus SIS VELETA CCD camera equipped the iTEM software.

7.8 Flow cytometry

For IL-10 screening samples are permeabilized antibodies are incubated in BD Cytofix/Cytoperm™ buffer. PE-Mouse α-Human CD1a is used according to the datasheet and diluted in PBS. Flow cytometry reading is performed using Canto II (BD Biosciences). Data analysis was performed with FlowJo software (Tree Star). Cell gate is defined by FSC-SSC parameters to exclude debris or by Live/Dead fixable staining (molecular probe) to exclude not viable cells.

7.9 Cytokines Profiling

To measure cytokine content produced by cells, the co-cultures media before and after ALI period were collected, centrifuged 1 min at 10000 rpm and soon stored at -80°C. Thawed undiluted media from biological triplicates are tested by Bio-Plex Pro™ Human Cytokine 27-plex, based on luminex technology, according to the supplier protocol. BEGM and Pneumacult-ALI reference wells values are used as threshold and also to normalize the different media condition between initial and concluded co-cultures. Media collected by cultures performed in different experimental conditions are considered to weigh good reproducibility of the data [data not shown], but excluded from the comparative analysis dataset. 1:100 and 1:1000 dilutions of media in DPBS are also tested to manage with the detection range. The plate is measured at the Bio-Plex array reader. Bio-Plex Manager software is used for data analysis.

7.10 Infectability test

NTHi 176 strain is cultured on chocolate plates O/N, 37°C, 5% CO2. Single colonies are picked up and bacteria are inoculated in BHI medium supplemented with NAD 2 ug/mL and haemin 10ug/mL. The liquid culture is incubated in rotary shaker, 37°C, until 0.4 OD (Abs 600nm) is reached. Pellected bacteria in exponential phase are resuspended in PneumaCult ALI maintenance medium without antibiotics. BE, starved for 1 day, are moved to a 12-well cell culture plate, with basal chamber only filled. After multiple washes of the BE, dissolved bacteria are pipetted atop BE and let to attach for 2 h, 37°C 5% CO^2. Non-adherent bacteria are collected by several apical washes, before all the treated BE return to the incubator. After 24 h of infection, 1*10labeled PBMC are added in the basal chamber of each BE, suspended in fresh PneumaCult-ALI at the concentration of $0{,}5*10^6$ /mL. After 16h and 32h the samples are fixed in PF 4% for 2 infection time-points. Samples are cryosectioned and analyzed by immunofluorescence. Negative controls of recruitment of PBMCs consist in pairs of BE uninfected, where there could be limited cells migration not induced by bacteria.

7.11 Antibody list

Name	Code	Dilution
α -β tubulin IV	T7941 Sigma	1/250
α-Laminin	T9393 Sigma	1/25
α-collagen I	Ab34710 Abcam	1:400
α- MUC5AC	MAB 2011 Millipore	1:250
α-SCGB1A1	SAB2102083 Sigma	1:1000
α-CK5	MAB3224 Millipore	1:250
α-ZO1	Invitrogen 40-2200	1:125
UltraMap anti rabbit HRP	760-4315 Roche	TDS
α-NGFR	Ab8874 Abcam	1:500
PE- α- CD1a	(clone HI149) (eBioscience)	TDS
FITC- α –IL-10	(clone JES3-9D7) (Invitrogen)	1:20
MODCdifferentiation inspector	130-093-567	TDS
α-p63	ab735 Abcam	1:100
α-ITGα6	ab20142	1:200
α-CD45	clone HI30, Invitrogen	1:50

Table 2 Primary α-human antibodies used in this study. Different clones are cited in paragraphs when used.

7.12 Statistics

Unpaired t-student is used for cytokines levels column comparison. Alternatively, for differentially expression between groups, one-way anova analisys is performed. P-values <0,05 will be considered significative.

8 Results

8.1 Cell culture optimization and characterization

The comparison between m1 and m2 for NHBEs cultured airlift on transwells resulted in a better expression of differentiation markers when using PneumaCult-ALI, evident at morphological level by SEM (not reported here) and immunofluorescence. In 3 weeks both m1- and m2- NHBEs were organized in a tight layer of cells characterized by ZO1 expression, while m2-fed cultures developed longer cilia (average length is 10 μm) and a higher number of GCs ($MUC5AC^+$)(Figure 21).

Adipogenic differentiation of MSCs cultured in 2D or in 3D was confirmed by immunofluorescence staining for fat-producing cells. Neutral lipids vacuoles were not detected in control MesenPro samples. The number of positive vacuolated cells was higher in 3D culture than the 2D. Some of lipid-droplet-filled cells were differentiated along with the adipose lineage since the adypocite specific marker FABP4 was expressed (Figure 20).

MSC/NHLF co-cultures revealed that both media are compatible with NHLFs and MSCs viability *in vitro*. NHLFs growth rate was augmented when they were cultured in FGM2 medium respect to MesenPro medium. FGM2 resulted to be suitable also for MSCs expansion [data not shown]. Since MesenPro is designed to maintain MSC multipotential characteristics and considering the proliferation grade among the different combinations of the co-cultures established, we decided to use MesenPro as culture medium for the MSC-BE, considering that this would not have induced an aberrant phenotype in MSCs profile.

6-days cultured MoDC strongly downregulated the surface expression of the monocyte marker CD14, with only 10% of the cells still expressing this marker. At least 80% of the cells analyzed were positive for CD209, also known as DC-SIGN since it is a specific marker of *in vitro* generated dendritic cells. Cells expressing CD83, costimulatory factor, maturation marker were restricted to nearly 5% of the total attesting the immature dendritic phenotype of MoDC used for the DC-BE. CD1a positivity was detected for about 80% of the cells in accordance with the expected differentiation protocol (resumed results in Figure 22).

Fluorescence labeling of PBMCs was checked before the cells were included within the BE. PMBCs were also screened for viability and were all viable after 24 hour of culture in PneumaCult-ALI.

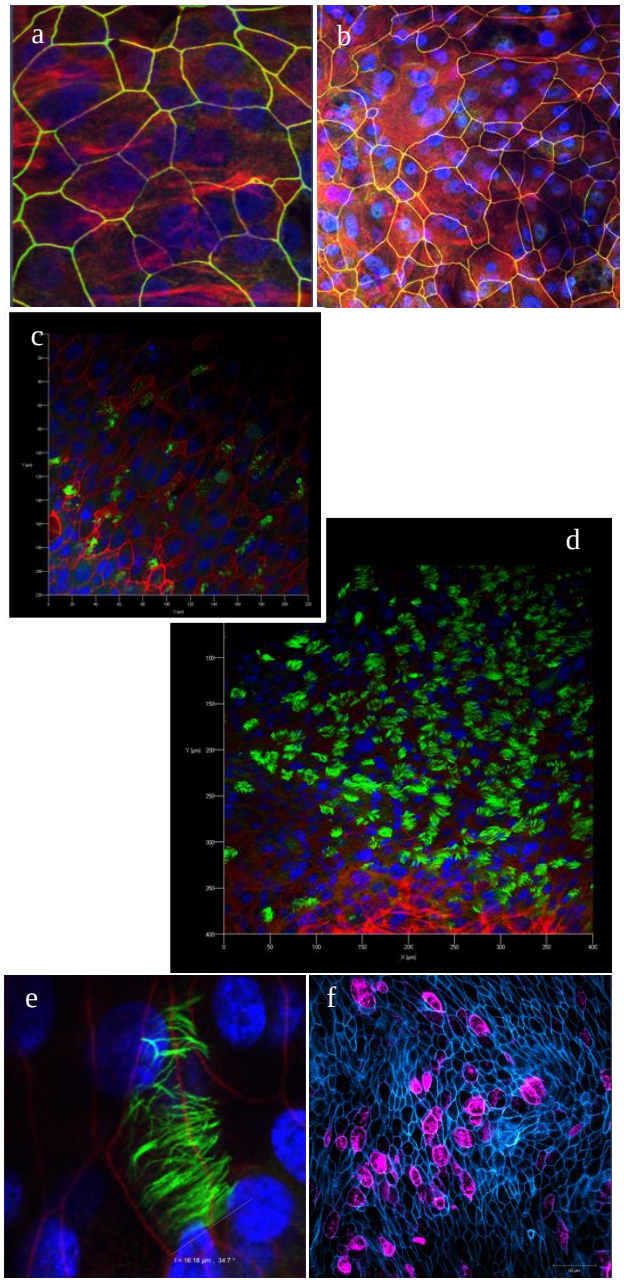

Figure 21 Pneumacult medium is superior for ALI differentiation of NHBEs. Increased ZO1 staining (b) and cilia numbers (d) than in B-ALI medium (a) (c) were obtained.

Cilia length (e) and GCs staining confirmed complete differentiation towards mucociliary phenotype.

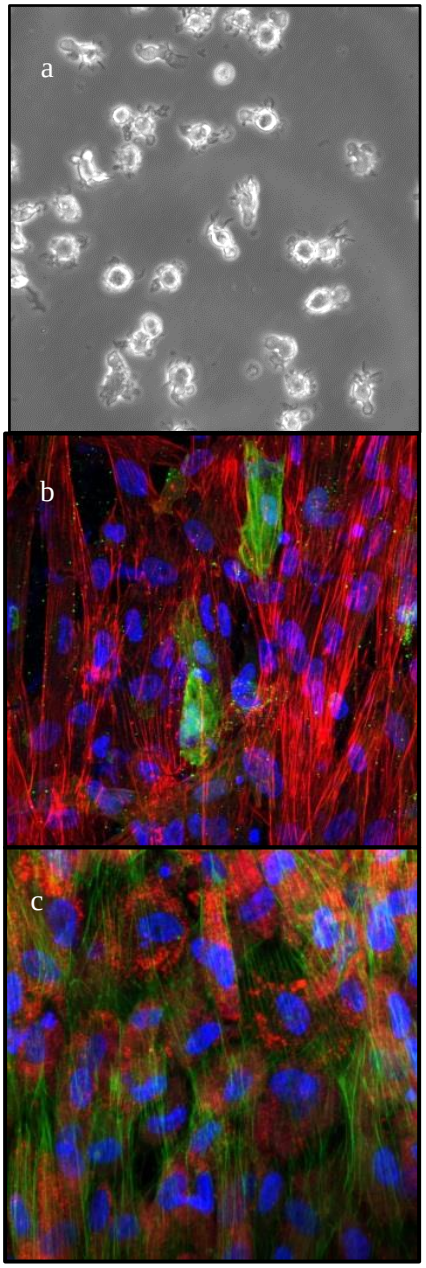

Figure 20 Tryple culture characterization. MoDCs developed classical dendrites after 6 days of culture (a). MSCs retain their multipotency in alvetex scaffold: expression of FABP4 in green (b) and lipid neutral stain in red (C). 40x original magnification.

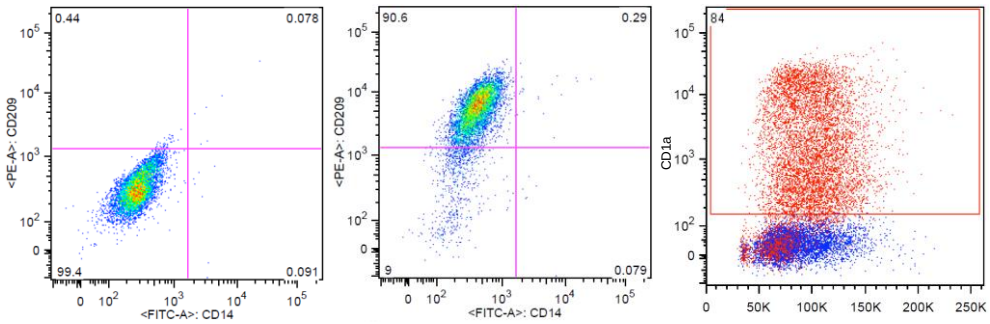

Figure 22 MoDC FACs staining confirms the immature phenotype and CD1a positivity**.** In the third panel blue dots represent an unstained control sample.

8.2 Morphological characterization of the model

8.2.1 Histological appearance

HE single staining or combined with AB, performed on paraffin sections, provided a detailed picture of cell distribution and ideally properly localization within the BE template. Eosin staining highlighted the collagen coating that separates NHBEs from the scaffold. Collagen layer made with lower volumes of coating solution resulted in NHBEs entry into the scaffold [data not shown] and loss of polarity/differentiation. NHBEs grown within the 3D model were in contact with the collagen gel and differentiated into a pseudostratified, sometimes multilayered, epithelium, while the same cells grown on transwells originated a layer of cuboidal and not columnar cells (Figure 23).

AB/HE staining allowed the clear detection of the mucus layer and of mucus-producing cells at the same time in all processed samples (Figure 23). Observations of the basic BE model and derived modifications indicated that the levels of produced mucus was in line with *in vivo* evidences. GCs number and localization were indicative of a good metabolic activity and differentiation grade of the epithelium. Furthermore mucus level was influenced by stromal cells presence (Figure 24). Indeed an increased number of NHLFs in the BE caused the formation of mucus boil reservoirs (data not shown), that disappeared when the stromal cell number was reduced or if the model was periodically washed as in the working protocol. Notably, also MSCs addition resulted in an increased GCs number (Figure 24, Figure 25). Considering the fact that the technical processing of samples affects the stability of the mucus layer, it was difficult to precisely compare different histological preparations even though AB staining clearly indicated that the thickness of the layer was significantly enhanced in 3D conditions respect to standard transwell model (Figure 23). We never detected histological signs of squamous or basal metaplasia.

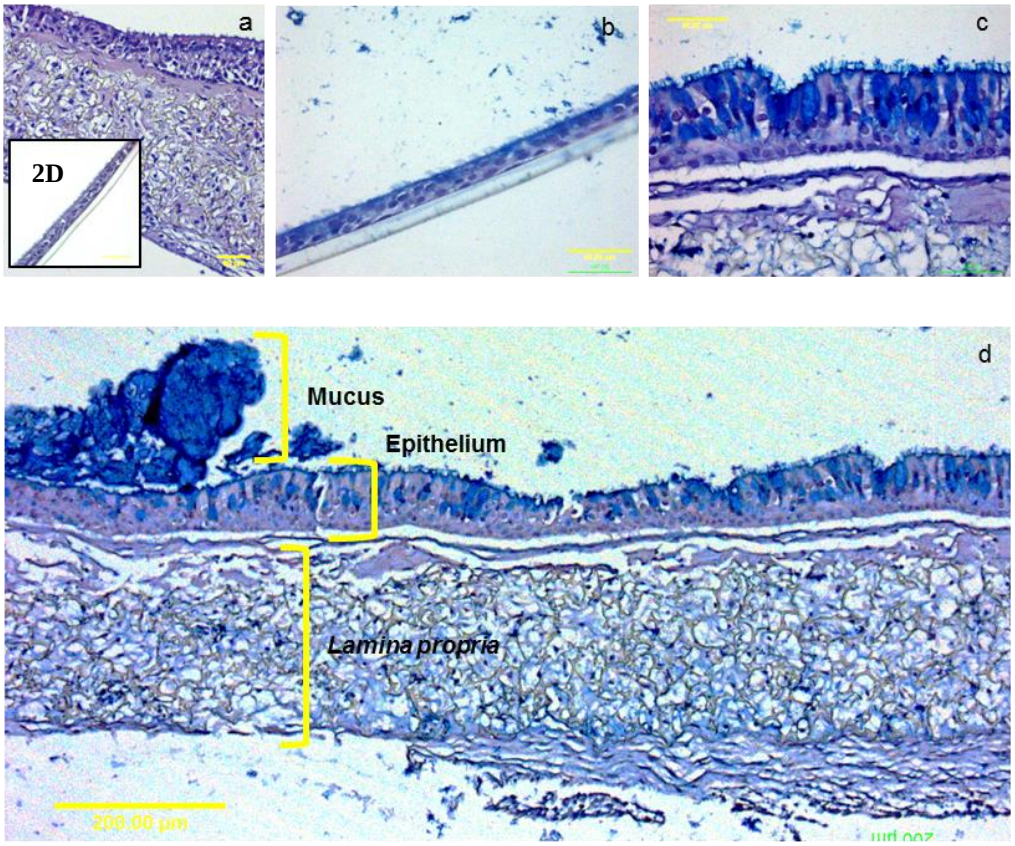

Figure 23 HE staining of BE compared to transwell culture (a). AB-HE (b, c, d) to detect acidic mucins and GCs.

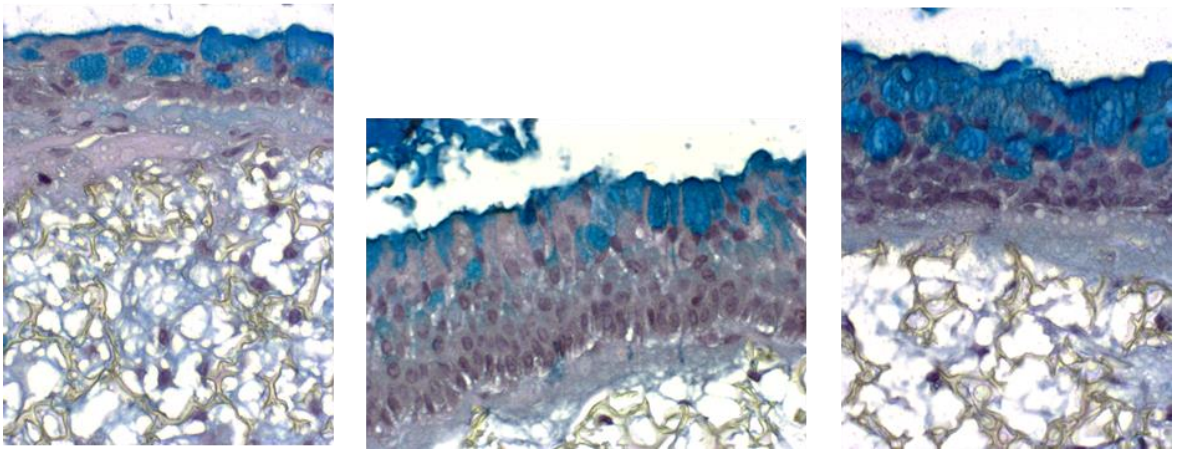

Figure 24 AB-HE staining acidic mucin comparison on DC-BE(a), BE(b), MSC-BE. 40X original magnification.

8.2.2 Mucociliary phenotype *in vitro* mirroring

Confocal microscopy analysis confirmed the morphological phenotype of the epithelium characterized by histology and SEM. Importantly this technique allowed us to distinguish the level of differentiation by staining mature cells trough a specific marker. Ciliated cells stained for acetylated tubulin coupled to a cell membrane marker, phalloidin, allowed the detection of epithelial areas covered with cilia, (Figure 25). We were also able to identify single GCs via MUC5AC staining.

By the use of the MosaiX scanning software we were able to compare CCs and GCs phenotype on the whole insert. The results (Figure 31) showed that the introduction of MSC did not impaired full epithelial differentiation and that there were no differences in the mucus layer between the BE and MSC-BE.

According to SEM analysis NHBEs grown in 3D conditions fully differentiated into a mucociliary epithelium (Figure 27). Indeed the superficial layer of the BE appeared as a thick carpet of cilia somethimes embedded into mucus patches. Depending on mucus distribution on the surface cilia were sometimes stitched together. We rarely detected craters with amount of mucus gushing out the underlying cells (Figure 27, c). We also observed cells without cilia and microvilli. Overall we do not detected appreciable intra- e inter-variability between the different BE models assembled (dual or triple culture).

TEM ultrastructural analysis of the different cells confirmed the nature of CCs and GCs. GCs granules and cilia structure are showed in micro -scale in Figure 28.

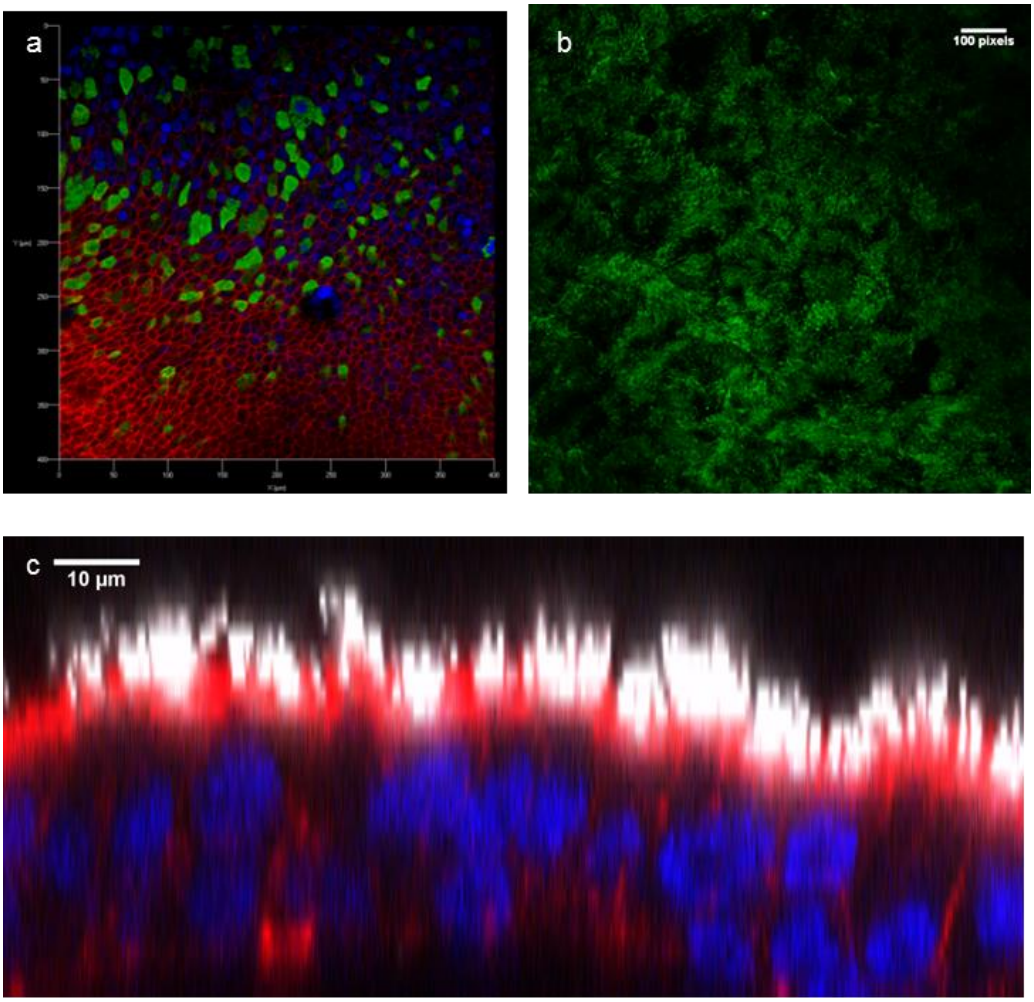

Figure 25 Confocal analysis of BE model: GCs (a) and CCs (b) are showed in green. Cilia distributed along the epithelium are showed in white (c)

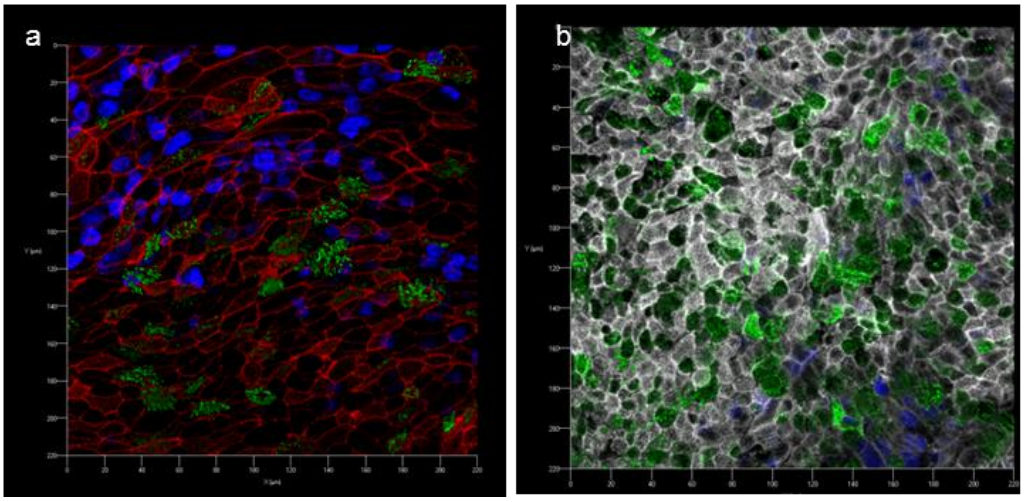

Figure 26 Mucociliary phenotype in triple cultures: DC-BE showed zone poorer in cilia, MSC-BE a small increase in GCs

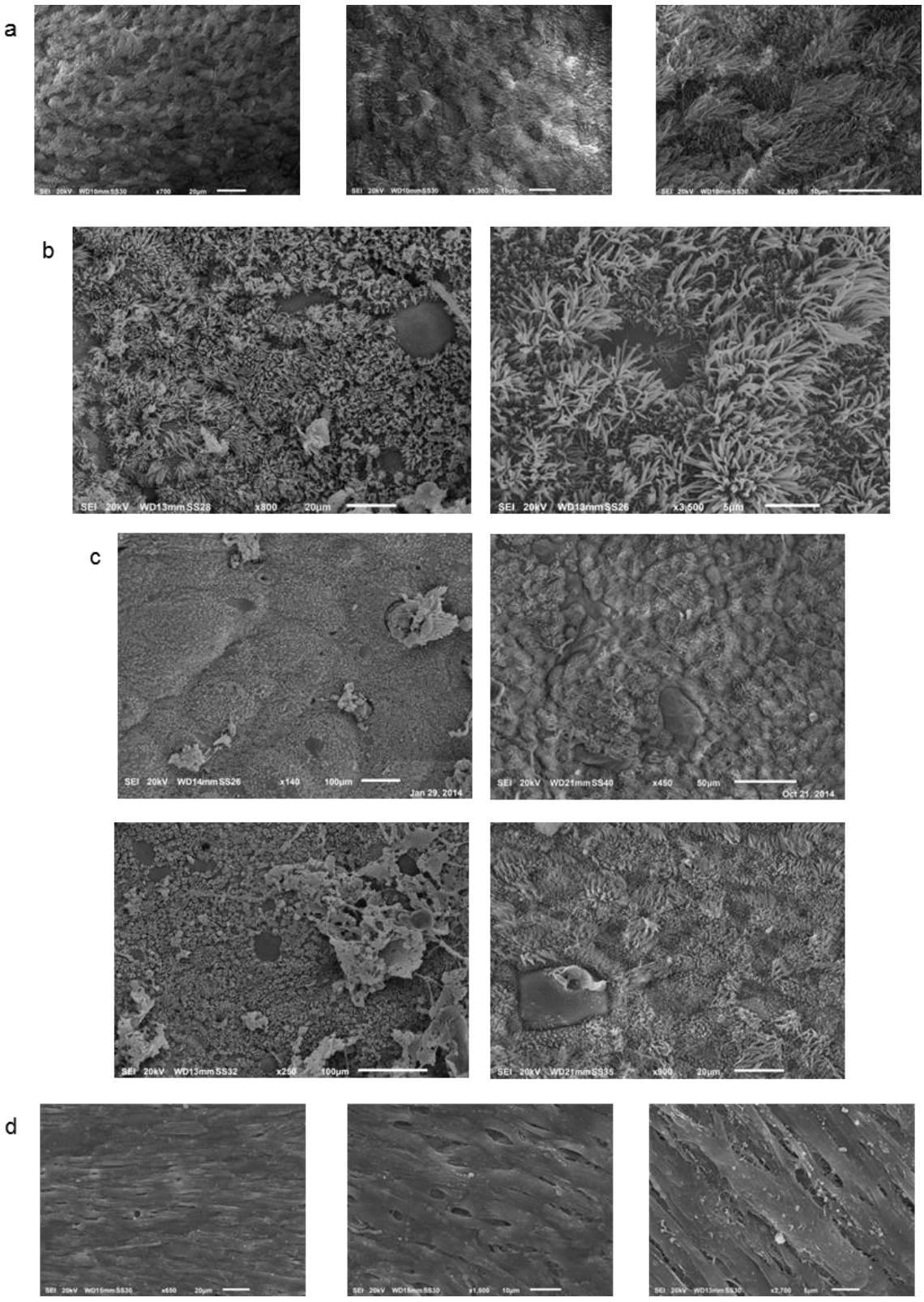

Figure 27 SEM characterization of BEs. General top view of BE (b) and increasing magnifications of CCs rich area (a). Differences in mucus patches (c) between weekly washed (right panels) and not washed BE (left panels). NHLFs and putative culture microvesicles (d).

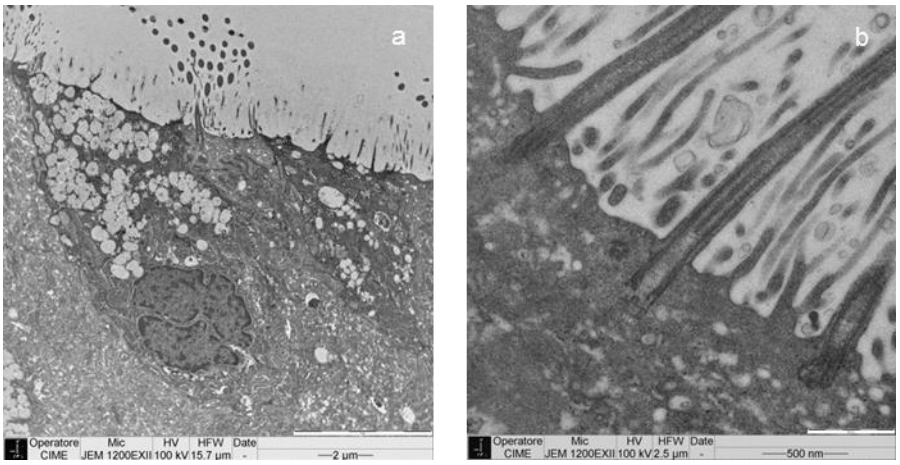

Figure 28 TEM analysis of BE: the nucleus of the GC is at the base of the cell and low-dense granules appear within the cytoplasm (a); basal bodies and microvilli are evident on the apical part of a CC.

8.2.3 Stromal niche formation

To verify that a 3D environment similar to *lamina propria* is formed by the fibroblasts to better accommodate and influence NHBE in the BE construct, we assessed the deposition nearby the cells and the scaffolds of some key components of ECM, such as fibronectin and collagen type I. A dense mesh of fibronectin was formed close to the cells and the fibrillary structures fitted in free space of the scaffold (Figure 31). Collagen I staining is sparsely distributed with a punctate location at the term of fibroblast cells (Figure 30). For laminin staining we cross-refer the results in the next paragraph. From the histological analysis we observed on the bottom of the scaffold a cell sheet made of NHLFs, that reduce its thickness if ALI - BE culture is not supported by transwell membrane. TEM images showed fibroblasts settled in the scaffold close to plastic material.

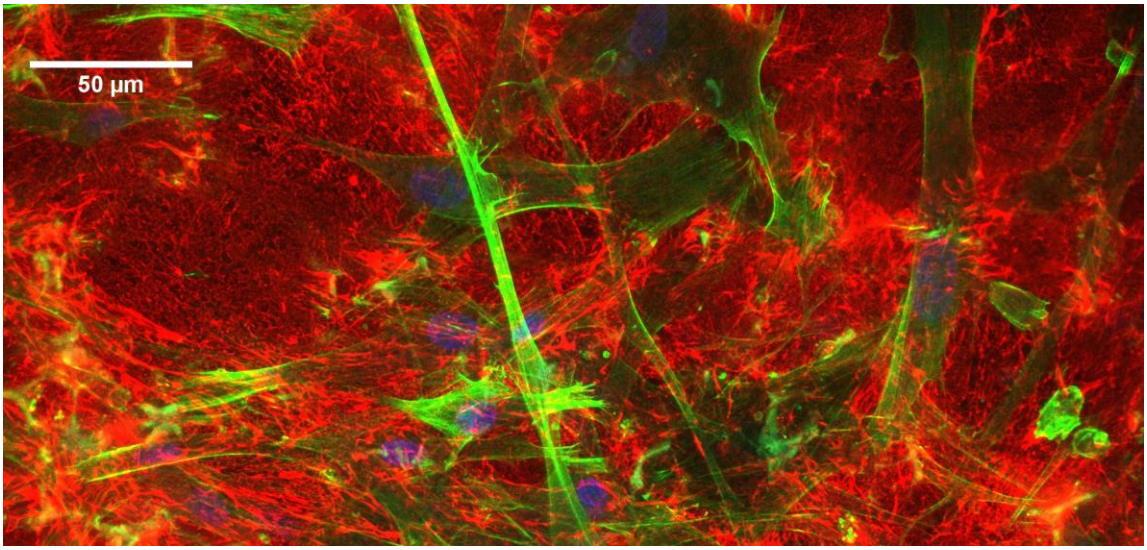

Figure 31 NHLFs cultured in alvetex scaffolds are able to produce ECM as fibronectin (red channel) in a physiological 3D spatial organization. 40x original magnification.

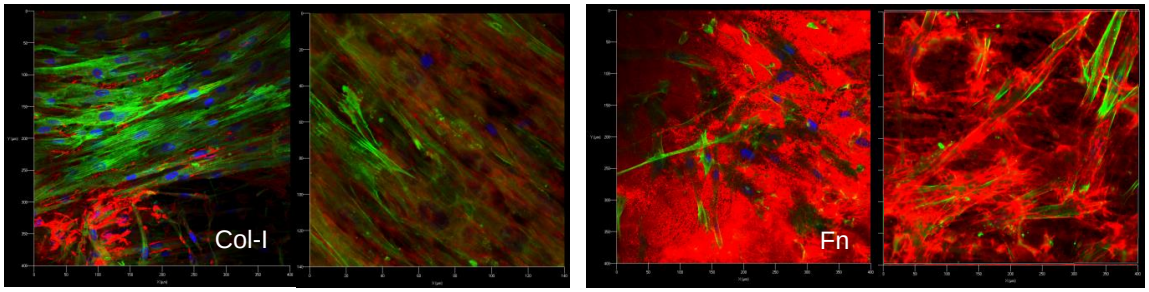

Figure 30 Z-stack 3D rendering of collagen I and fibronectin deposition in NHLFs 3D culture. Top and bottom view. F-actin (green) and DAPI (blue

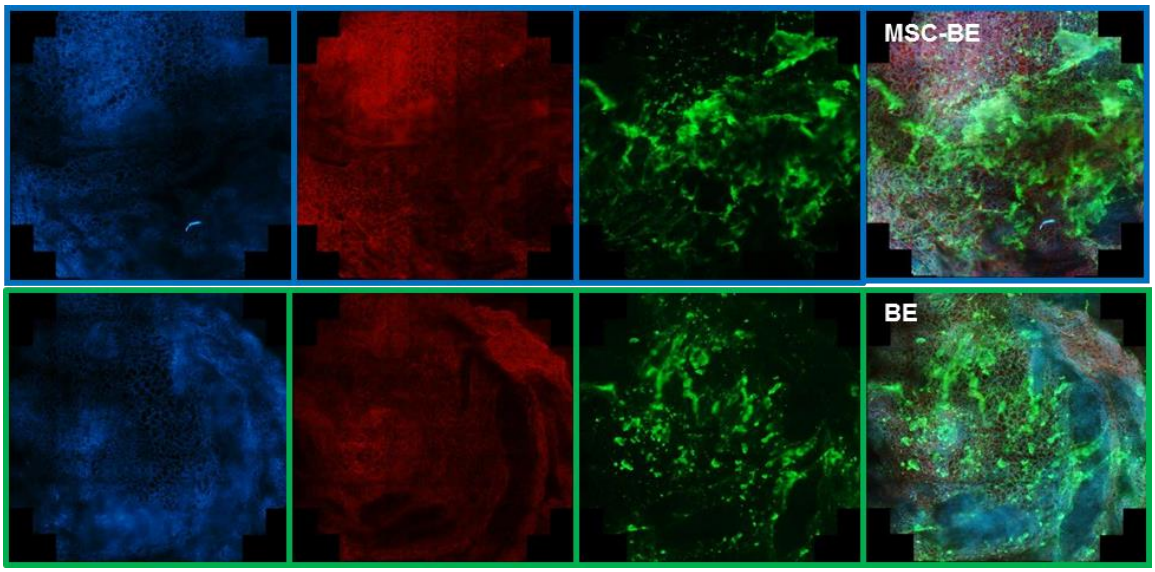

Figure 29 Semi-quantitave analysis by MosaiX reconstruction. Nuclei and scaffold (blue), CCs (red) and mucus (green) staining in BE and MSC-BE. Images are representative results of 3 samples.

8.3 Barrier function

The integrity of the epithelial sheet is indispensable if considering the epithelium a physical barrier against pathogens colonizing the human respiratory tract and typically requires the establishment of tight junctions (TJs) that seal together the epithelial cells forming the barrier. Zonula occludens marker (ZO-1) is generally present when TJs are well formed within a functional epithelial barrier. In the 3D-BEM ZO-1 properly delineated inter-cellular contour at the apical side of the NHBE layer.

To evaluate the formation during the 3D culture of structural key components of the BMe, we searched for the deposition of ECM proteins within the model. In particular, by fluorescent and IHC analysis, we observed a thick and uninterrupted layer of laminin , the major component of BMe *in vivo,* just within the collagen coating between the 2 compartments at the bottom of the epithelium. While immunofluorescence on cryosections clearly showed this line of laminin at the epithelial-mesenchymal interface, the staining was weakly extended to underlying epithelial cells contours and at their BL. In addition a strong laminin deposition close to fibroblasts was visible. The same analysis of NHBEs differentiated on transwell indicated that the laminin signal was scattered throughout the epithelium. Isotype control staining was confined to unspecific signal (probably mucus residues) on some areas of the sections (Figure 33). In addition we detected positive signals for ITGα6, BC marker, receptor for laminin and main component of the hemidesmosomes (Figure 39). Optical microscope observations during the culture period disclosed that most of the MoDCs included in forming D-BEs were lost within the first days of ALI. The presence of the resting MoDCs was assessed by CD45 specific immunostaining.

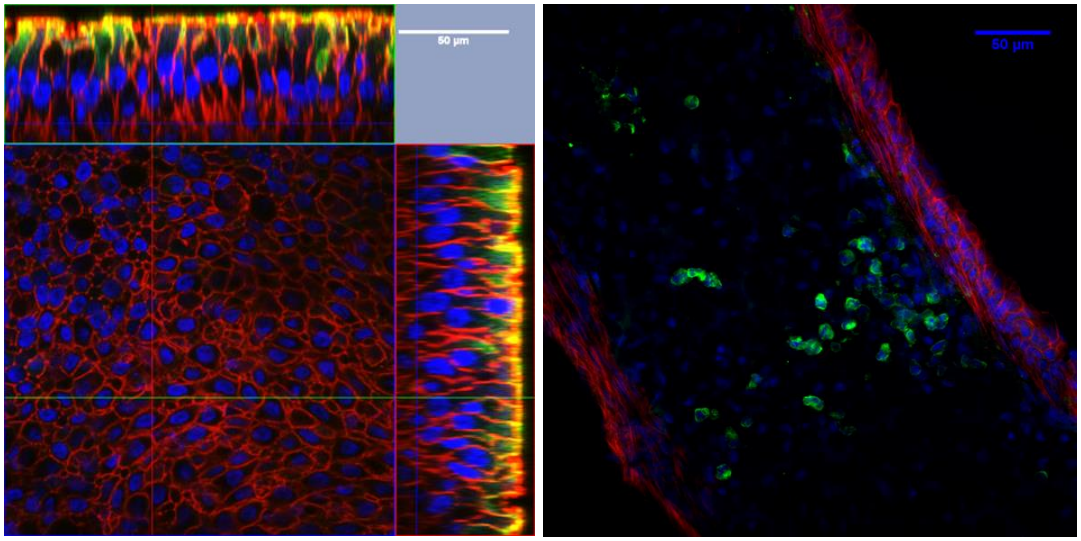

Figure 32 ZO1 (green) located at the AP of NHBEs in BE model indicated TJs formation. F-actin for cellular contours (red). DAPI counterstain nuclei (blue). Z-stack of 30 optical sections. On the right MoDC labeled by CD45 staining in green

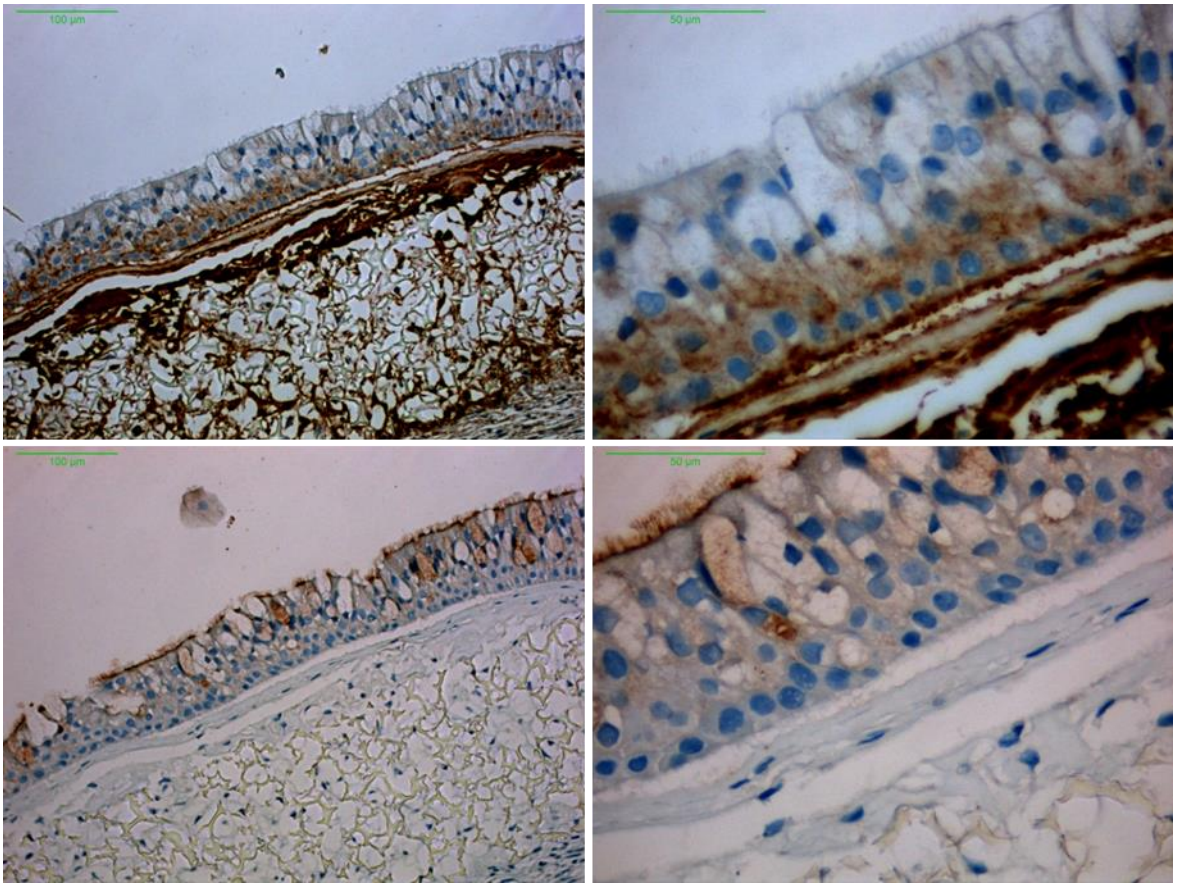

Figure 33 Laminin IHC suggested the formation of a basement membrane co-localized with the collagen coating. Isotype control is shown in the lower panels.

8.4 Tissue renewal

The investigation about the detection of potential homeostasis and repairing mediator cells required to work with cryosections, where all the cells of the epithelium can easily reach the antibodies. Firstly the persistence of progenitor cells in the differentiated epithelium, best candidate as homeostasis driver, was wondered. A cytoplasmic positive staining for CK5 highlighted, in all BE types, the layer of cells attached to the coating (Figure 36). CK5 (type II keratin) data confirmed again the presence of BMe equivalent and the presence of a basal layer of cuboidal cells expressing BCs marker. We investigated also the expression of CK14 (type I keratin), often assembled in pair with CK5, in complex epithelia [97]. The distribution of CK14+ cells did not follow a straight orientation compared to CK5 pattern that was almost parallel to the coating. Furthermore we monitored the nuclear expression of p63, basal cell progenitor marker, in which cells adjacent to collagen coating. Similarly to CK5 distribution we detected only fluorescent nuclei present in the lower part of the epithelium. To verify that BCs exist within this layer, we performed dual immunofluorescence studies. We just found small clusters expressing p63 that co-localized with $CK14^{+(}$ Figure 39). The second transcription factor that we showed is located, resulting with a

strong intensity, in the same considered group of cells $CK5^{+}$, is NGFR, whose expression pattern that decreases until it disappears in the upper layer (Figure 39). We did not see any AQP3 staining in the epithelium produced in 3D *in vitro* conditions.

Since NHBEs were isolated from both human tracheal and bronchial biopsies, we also wanted to check another set of cells able to participate in healing and regeneration, the Club cell. For this reason we used antibodies directed against CC10 protein (murine CCSP), specific protein produced by Club Cells. In cryosections we better verify that CC10 labeled cells are a distinct staining from the one belonged to p63 or CK5 population, and that the staining cover both cytoplasm of these putative Club cells and mucus residues near them. Dual not competitive immunofluorescence for CC10 and MUC5AC on uncut samples revealed that although there is preferential staining of only one marker by the secretory cells there are few double positive cells.

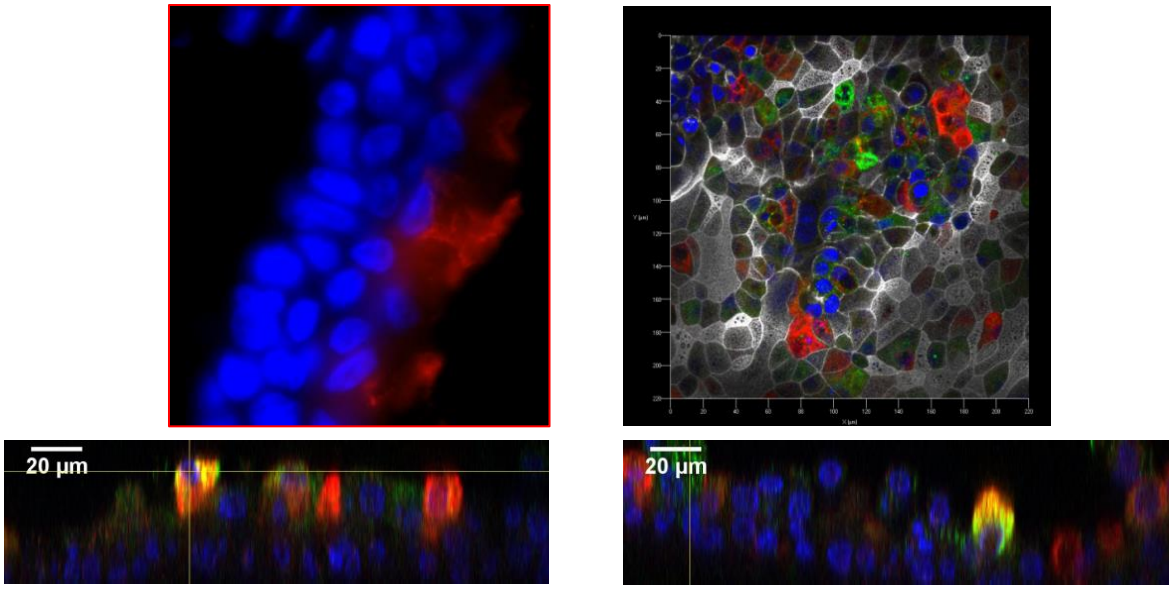

Figure 34 Sequentially in panels: ClCs detection in upper layer of the epithelium (red). GCs(green) (Cl.C (red) and resting cells (gray) triple staining; last panel showed cell double positive for MUC5AC and CC-10 proteins, suggesting linkage between the 2 GCs and ClCs differentiation.

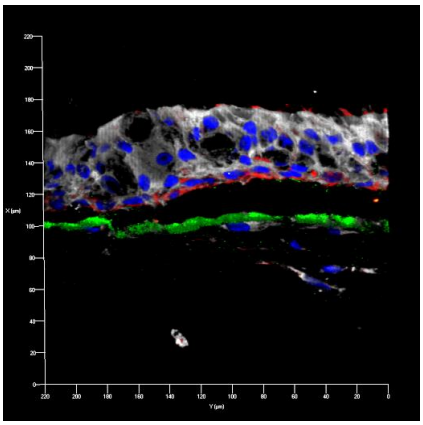

Figure 39 NGFR high-positivity (red) at the bottom epithelial cells and ITGα6 staining (green) lining the coating (detached in this cryosection).

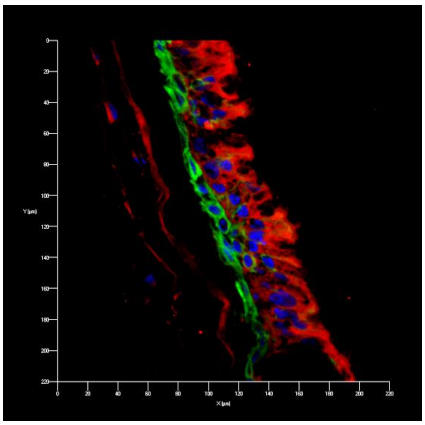

Figure 35 CK5 marked in green the cytoplasm of BCs in a similar section. Hoechst 32442 (blue) for nuclei and trasmitted light signal (red) as counterstain.

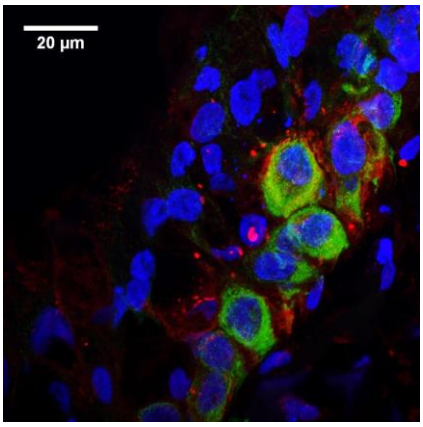

Figure 37 BCs dual staining for NGFR(red) and CK5 (green). DAPI for nuclei in blue.

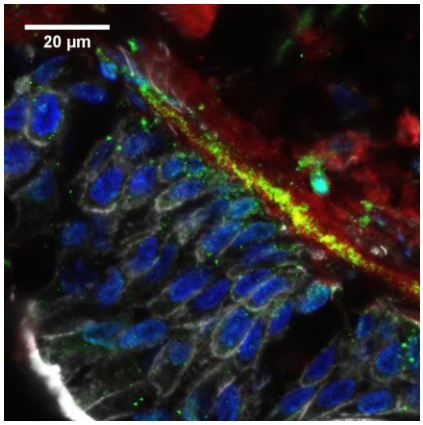

Figure 38 Dual staining for laminin (red) and ITGa6 (green) interacting each other to supply a BMe

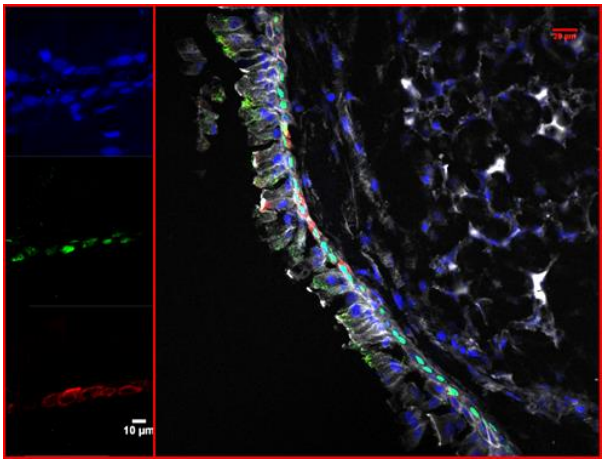

Figure 36 Comparison between p63+ BCs(green signal) and CK14+ cells (red signal). DAPI (blue) and actin staining

8.5 Secretion profile

Quantification of the content of the cytokines released in the medium by three types of BE, showed a marked modification in the cytokines profiling between pre-ALI and final culture levels. Among our panel, IL5 was completely undetected; instead IL17 is not produced by cells. IL9 was discarded by statistics, while GM-CSF data-table was empirically inconsistent considering the relation between its dilution tests. Regarding IL2 only traces were detected in ALI D-BEs. Final plots and comments were derived from undiluted samples analysis, in which we detected all the resting cytokines included in the tester kit.

About the proper GFs production, a related increase is observable during the ALI phase; we noted that all BEs secreted more VEGF and G-CSF and, at the same time, they consumed bFGF. PDGF is slowly produced without fold increase between starting and final cultures.

The chemokines panel is more assorted. IL-4, IL-13, IL-15, MIP-1α and MIP-1β display lowest concentrations in the medium, staying in the pg/mL range. The level of IL-1β is minor of approximately 40X times in contrast to the related anti-inflammatory agonist IL-1ra. In the middle range of the observed concentrations we noted IL-10, TNF-α, IL-7, RANTES, IFN-γ, IL-12p70, with the latter one slightly reaching 1 ng/mL. We attested higher levels in secretion of MCP-1a, eotaxin, IP-10, IL-8, IL-6. Few cytokines are differentially expressed in the final conditions comparing the 3 BEs configurations (Figure 42), while significative differences from the dual culture belonged to the DC-BE model.

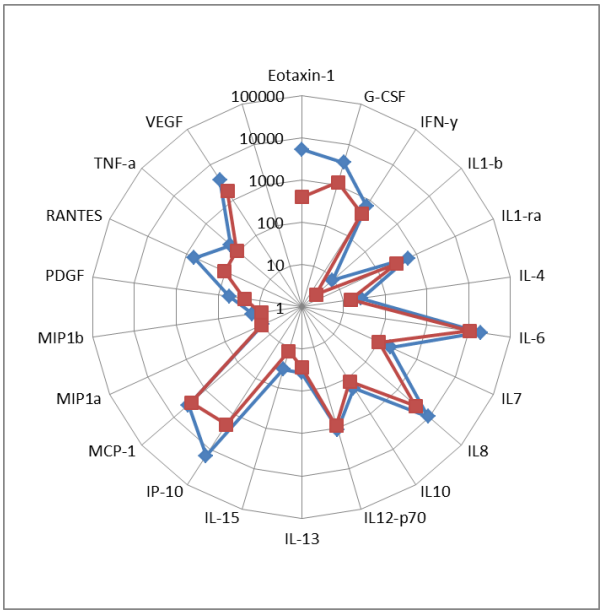

Figure 40 Cytokine production and released levels in culture media by BE before ALI-phase (red line) and at the end (blu line) of the differentiation protocol.

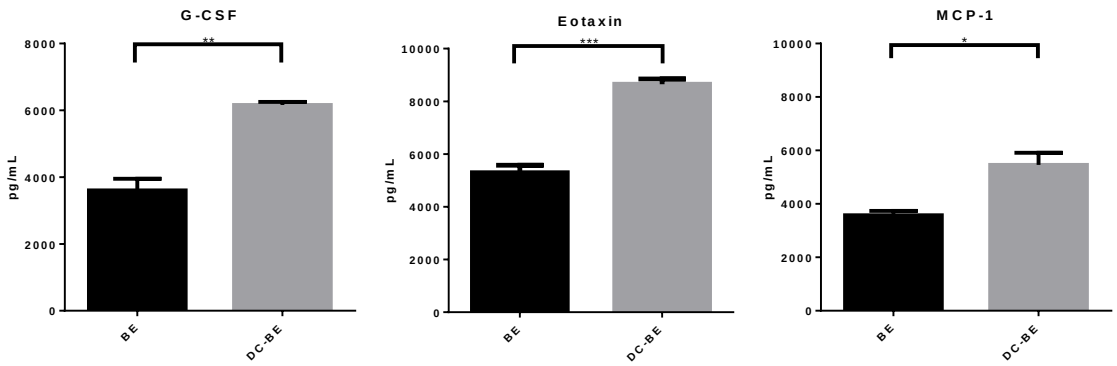

Figure 41 Cytokines differentially secreted because the existence of DCs in the model.

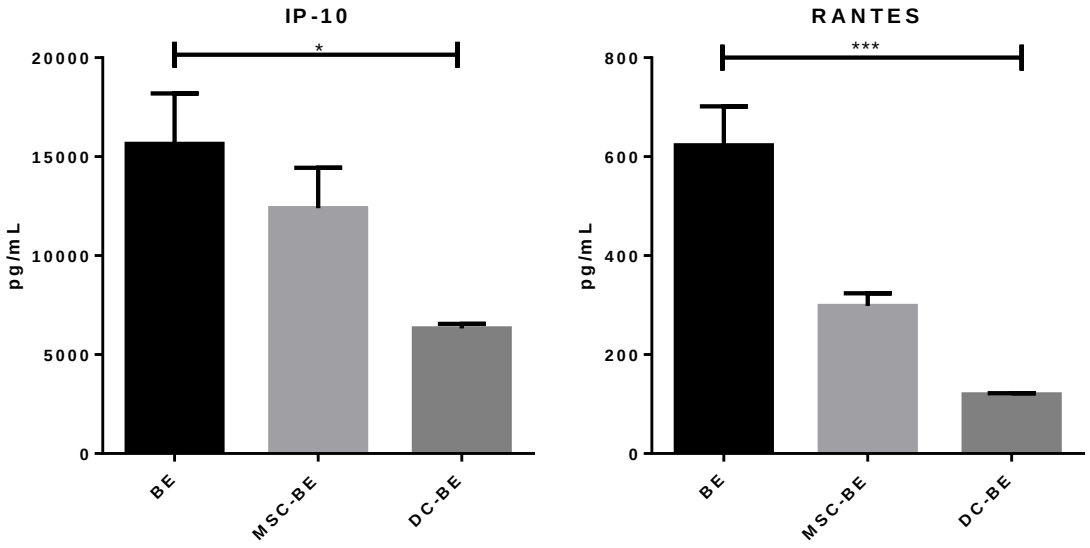

Figure 42 Cytokines differentially secreted between BE and its modified versions

8.6 NTHi infection

For its first adhesion step, NTHi seemed to have a preference for CCs. We found on cryosections diverse cilia not bound to the cell surfaces, but dispersed in the mucus. Isolated bacteria are internalized in some epithelial cells, while more are located paracellular. A lot of bacteria reside in stromal layer, sometimes grouped especially in the bottom of the scaffold, where fibroblasts contacted directly the medium. In the stromal part they are linked to the ECM. Our NTHi-serum recognized also small particles not detectable in uninfected samples. These results are summarized in Figure 43. Finally we did not retrieve fluorescent signal by any PBMC in thick cryosections, neither improving the detection using CD45-FITC antibody.

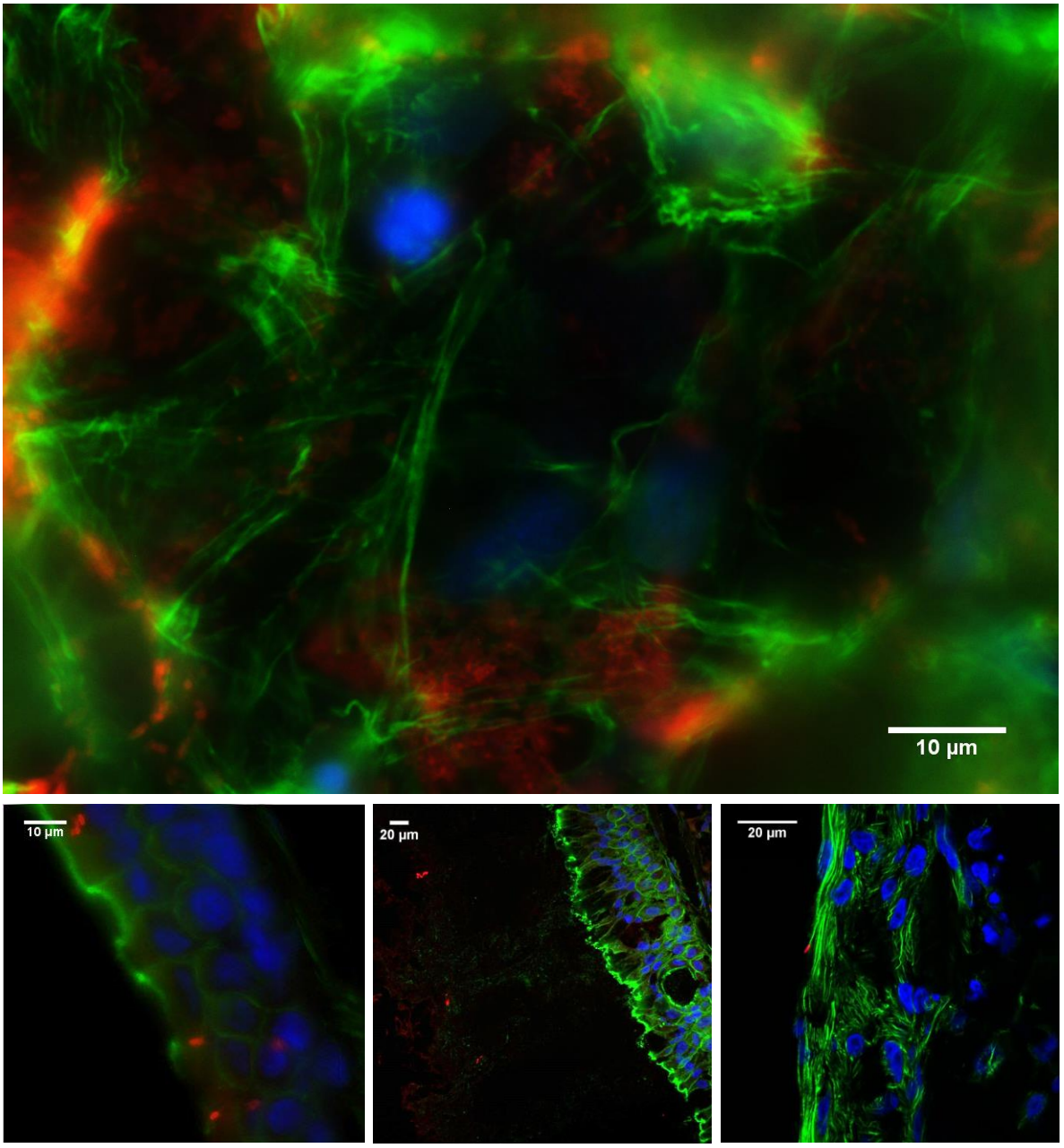

Figure 43 Widefield stack (a,b) and confocal single plane (c,d) fluorescence analysis of BEs infected cryosections at late time-point. NTHi (red) was found in the mucus layer (c), inside epithelium(a), close to stromal niche (b) and able to cross all the thickness of the model (d). F-actin (green) and DAPI (blue) delineates the eukaryotic cells.

9 Discussion

We developed a 3D *in vitro* cell culture aiming at reconstructing the human tracheobronchial tract in which will be feasible to test essential parameters of the response to vaccines. Its physical dimensions and organization made them similar in handling to already *in vitro* tools (like transwell) conventionally used for the same goal. Although it is laborsome, is also a relatively inexpensive approach.

The ultimate goal would be the realization of a system able to answer specific scientific questions by selecting its components (i.e. the addition of a specific cell subset), thanks to the modular setting of the system. Previous references showed that MRC5 fibroblastoid cell line did not adequately recapitulated the niche favoring the alveolar differentiation [77], instead VE10 epithelial cells branched in co-culture with endothelial cells because most probably they derived and mimic the features of the native BCs. Here the choice of using in our model only primary cells derived from normal lung, the native tissue we want to reproduce *in vitro*.

The 3D model owns a stromal compartment consisted of fibroblastic cells. While a porous polystyrene sponge provided just a physical requirement allowing the cells to assemble in a more relevant spatial distribution, we left the lung cells themselves free to reconstruct their acellular niche. Indeed puramatrix coating is just non-protein film and the fibroblasts synthetized ECM such us fibronectin, the "master assembler", and collagen type I, the most abundant matrix in the lung. Abundant fibronectin supposes the formation of bridges between cell surface receptor like integrins and other ECM component as collagen type I. In one of the triple culture we set up we wanted to enrich that niche adding UC-MSCs. The choice of UC-MSCs [98]–[100] derived from a further characterization and dependability in comparison to commercially available Lu-MSCs. In addition it is reported a superior cell biological properties such as improved proliferative capacity and greater differentiation potential of MSC from birth-associated tissues over BM-MSC[101]. Extraembryonic MSCs senesced later and they are biologically closer to ESCs[98]. We bring the possibility that this cell type could confer a supplementary protective role in the context of infection and intoxication, sustaining *in vivo* evidences (listed in the introduction chapter) in which MSCs improved survival or enhanced bacterial clearance. MSCs also can function as fibroblast in the reconstruction of engineered skin [102].

The BE we "grew" *in vitro* is voluntary based on ALI traditional protocol to induce physiological and proven differentiation of lung epithelial cells. Certainly ALI means direct oxygen availability

for an epithelium naturally in contact with fresh air. In addition the medium we used in ALI phase is BPE-free, so the air exposure is more important condition for ciliogenesis [68]. SEM and confocal microscopy were used as favored techniques in order to improve the result and delete counterproductive conditions during the progress of the model development. From this couple of methods we gained a top view of a carpet of motile cilia covering one side of the BEs, as well the preeminent evidence of our success to differentiate NHBEs. Not the entire surface results planar, firstly because there is a different height of the stratified layers, secondly the discrepancy is due to the collagen coating that histology confirmed to have small differences in thickness over the sample. The histological sections staining revealed the content of secretory cells and mucus thickness, while specific immunofluorescence and HE/AB staining confirmed the presence of GCs producing MUC5AC. Occasionally mucus cysts accumulated in the epithelium, without affecting differentiation of surrounding cells, as effect of fibroblast density and mucus accretion. Since there is a not natural removal of mucus from the model those cysts probably appear inside the epithelial layer because the collagen coating prevents the access to the lower part, however obstructed by the scaffold presence. Although daily washes of the pseudotissues were performed to mimic normal mucociliary clearance, establishing a more physiological removal for the mucins produced in these tissues would be more desirable. MSC-BEs seemed to push the NHBEs toward a more secretory phenotype, with more GCs[96], with mucus production almost equal to BEs (by Mosaix data) or either superior (by AB/HE). Additional experiments should clarify this correlation.

The barrier function is crucial against unwanted substances in breathing air *in vivo* and it is not only fulfilled by the epithelial cells but also by the basement membrane *in vivo.* Laminin is a non-collagen protein mostly found in *basal lamina*, working to define this barrier. NHBEs are known to produce lamininV, the isoform responsible for the binding to integrin α6β4, important event during the in *vivo* formation of the basement membrane. In our model we use collagen I gel as coating to provide a low-stiffness and continuous surface to the adhesive NHBEs. As IHC and IF confirmed, under the bottom series of NHBEs, laminin protein is deposited drenching the coating. We could state that the NHBEs in our model, together with NHLFs, synergistically secreted the laminin, supporting the Kobayashi's idea that cocultured fibroblasts sustain the assembling of an *in vitro* substitute for the natural basement membrane. At the same time the merge with ITGα6, signal found close to basal cells - coating area, suggests the formation of hemidesmosome.

Our analysis demonstrated our model can hold potential regenerative mechanisms. Cell homeostasis, tissue repair, and cell turnover vary according the different organs. For example, CCS of the trachea and bronchi have half-lives of 6 months and 17 months, respectively [28]. Unperturbed adult lung is

almost quiescent, but is considered having a facultative regenerative capacity. The respiratory system could respond to injury and insults to repopulate lost cells by inducing proliferation, activating stem cells or progenitor populations, promoting differentiation, or by re-entering the cell cycle. Here we demonstrated the cellular system we developed contains cells in theory able to remodel the airway epithelium, BCs and Club cells. p63 is a p53-homologous nuclear protein that plays a critical role in regulation of stem cell commitment in several epithelia. CK5 is specifically expressed in cells usually undergo transient proliferation and showing multipotent differentiation after injury. $p63^+$ $CK5^+$ are BCs present in the pseudostratified airway *in vivo* and are *bona fide* progenitor cells that exist in our model. Also we detected $CK14^+$ cells, a subset of BCs that increase transiently during repair[34]. One human surface marker is NGFR, whose labeling intensity gradually decreases towards the surface in large superficial cells. Fairly we did not observe on cryosections $AQP3^+$ cells, while we hardly detected few of them by immunofluorescence in not well differentiated transwell samples [data not shown].

We wanted to verify with explorative study the expression levels of cytokines produced by the BEs and their variants, as prior knowledge before undertaking a novel use of our model. We can just compared these levels with the ones measured in supernatants or apical washes of similar *in vitro* models containing HBEC, in particular in models used by Ren [21],Baddal (unpublished), Parker [103]. Values collected did not showed a content very dissimilar than the reference ranges, that, anyway, are very different each other according the culture conditions used. We confirmed previous reports that HBECs produce IL-6 and IL-8 [104]. The airway epithelium precisely produce IL-8 on a constitutive basis [21] and upregulates this cytokine in response to bacterial exposure. IL-8 amount in basal media of BEs is second only to IL-6, the most abundant cytokine we detected in BEs that presented a level higher than all other reference values we considered from literature. We speculated this increase is due to NHLFs co-presence in culture. A lot of other chemoattractive molecules, such as IP-10, MCP-1a, RANTES, IL12-p70, G-CSF, IFNγ, IL1-ra are present in great valuable concentrations; some of them like are differentially expressed by BEs when MSCs or MoDCs are added. IL-1β, IL-9 and in particular IL-13 secretion correlated to a response to damaging stimuli [76]. IL-17A treatment was shown to biases *in vitro* BCs differentiation toward GCs. Just traces of these proinflammatory chemokines are listed in our chemokine output list, if they are detected. What we found in media is also an indication of which cytokines the co-culture consumed during the maturation of the model; bFGF is subtracted increasing the time of culture, very probably because the nutritional need by NHLFs. Regarding VEGF, in theory produced by fibroblasts and specifically by NHLFs [105],we did not infer a firm production by stromal cells, if it is considered that BEs levels were similar to NHBE reference

levels[106]. Anyway all the quantitative data generated are susceptible of discussion. First of all cytokines concentrations are dependent of cell number and culture conditions (2D vs 3D), thus they slightly differ from any reference sample to be compared. Thirdly we could not separate, neither experimentally, the quantitative contributions of the single cell types, because they are not simply cumulative each other. Furthermore, AP and BL of epithelial cells have directional responses in cytokine secretion implying that polarized HBECs can selectively or differentially secrete many cytokines in AP, e.g. in the case of an intrusive pathogen. Since we did not treat the apical surface of the models, we collected only basal media to avoid technical problem related to the density of apical washes, as well we are interested also in the stromal trophic function.

Human lung DC characterization showed a phenotype and an endocytic capacity close to *in vitro* immature DCs. D-BEs indeed are prepared including immature MoDC. DC consisted in a very motile populations, their trafficking to the lymph node and the recruitment to the different anatomical tracts of lung are influenced in nature by inflammation condition. We concluded with the verification that MoDCs faintly persist until the end of the 3 airlift weeks in D-BEs. No one of the immunocompetent model we cited admitted DCs entered the co-culture early and stay for 3 weeks later. The migration to the lower part (and the final partial loss) is very likely an effect happened and already shown in similar 3D organotypic model [93].

Infecting BEs with NTHi we noticed specific signs of ciliotoxicity, paracellular and transcellular transit, use of the host ECM niche. This agree with a putative model of NTHi pathogenesis. In our experimental set-up we did not observe a migration of PBMCs to the infected model. Among plausible explanations of the missing recruitment there are antigravity impediments, obstruction by the bottom NHLFs -sheet, without leaving out the possibility that granulocyte fraction could be involved in place of PBMCs.

APPLICATION OF AN EPITHELIAL INTESTINAL MODEL

10 Literature review

10.1 C.*difficile* Toxins

TcdA and TcdB (also, Tox A and ToxB) are homologous AB toxins, with 49% identity and 63% similarity. The proteins share a common large multi-domain structure, basically composed in a N-terminal glucosyltransferase domain (GTD), a central translocation domain and a C-terminal region mediating receptor binding. TcdA (as TcdB) enter the cell by clathrin-mediated endocytosis. Once the toxins have been internalized, endosomal acidification induces structural changes in the translocation domain exposing hydrophobic segments. Based on an auto-proteolytic step, just the catalytic domain is delivered across the endosomal membrane towards the cytosol. The enzymatic function of the toxins is carried out by a 63-kDa catalytic centre that acts on small GTPases involved in regulation of the cytoskeleton. Historically, cell-rounding and cell death are referred as the cytopathic effect and cytotoxic effect, respectively. Both toxins, also, may account for C. *difficile* opportunistic ability of colonizing the mucosa. Indeed Kasendra et al. showed that in particular ToxA-mediated subversion of cell polarity facilitates the exposure of preferential sites of bacterial binding to the mucosa [107]. Glucosylation of the GTPases prevents their interactions with multiple effectors and regulatory molecules and thereby prevents multiple Rho and Ras pathway signaling involved in cell cycle progression, cell-cell adhesion and maintenance of the cytoskeleton. ToxA and ToxB have been reported to cause death through a number of different mechanisms including apoptosis as well as necrosis. Inactivation of Rho GTPases by ToxA and ToxB results in the disruption of cell-cell junctions, contributing to an increased epithelial permeability.

ToxA is comparable with ToxB in its modification of Rho family substrates, but TcdA only is capable of modifying Rap family GTPases [108]. The mechanisms by which ToxA and ToxB mediate inflammation involving activation of MAP kinase, NFκB and AP-1, and stimulation of IL-8, occurred via two different Rho-dependent and -independent pathways [23] [109][108], [110] .

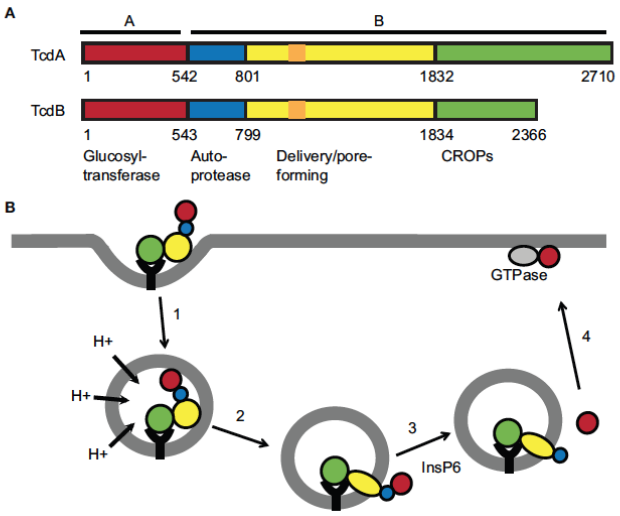

Figure 44 Protein structure and mechanism of action inside the cell by C.*difficile* binary toxins. Source : Pruitt et al. 2012 [110]

10.2 The intestinal epithelium

The intestinal tract consists of two anatomically distinct organs: the small intestine (SI) and the colon. SI epithelial organization reflects its absorptive function, by the presence of finger-like structures called villi. The villi are surrounded by multiple invaginations, the crypts of Lieberkuhn. Luminal epithelial cells are exposed to physical, chemical, and biological insult and up to 10^{11} epithelial cells can be lost in humans daily. New cells must be generated in order to compensate for high rate of cell death on the villi. Stem cell niche resides at the bottom of crypts and produce progenitors called transit-amplifying cells (TAC) that migrate upward toward the crypt/villus border and finally differentiate. Four types of mature cells present in the SI epithelium: enterocytes (EC), absorbing water and nutrients, Goblet cells (IGC), enteroendocrine cells (EE) and Paneth cells (PC) that secrete antibacterial substances (such as cryptdin). In contrast to SI, the colon has an epithelium with multiple crypts associated with a flat luminal surface, a high density of GCs and the absence of PCs. A specific niche enables the constant sustaining of the high cell turnover in the SI. A group of Intestinal stem (ISC) are located closely to PCs and it is surrounded by mesenchymal cells. PCs subset has a low-rate of renewal. They differentiate from secretory cell progenitors, located at the base of the TACs, which follow a downward migration to the crypt [111].

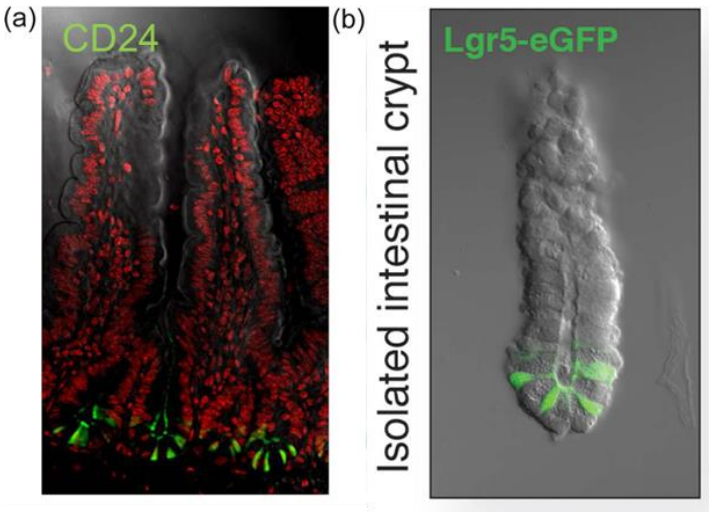

Figure 45 CD24 and Lgr5+ distribution at the bottom of the crypts. Sources: Leushacke M, et al. 2014 [128]Sato et al. 2011[111]

10.3 Intestinal Stem Cells

Two models of ISCs identity historically competed each other: the "+4 position" and the "stem cell zone" model. Leblond's Crypt Base Columnar (CBC) cells are the ISC candidate in the stem cell zone model. Lgr5 is a the receptor for the Wnt-agonistic R-spondins and its expression in restricted in crypts. By lineage-tracing experiments, Baker et al. revealed exclusive expression of Lgr5 in cycling CBCs in SI, that were able to generate all epithelial lineages [112]. $Lgr5^+$ is considered marker of ISC. PCs are an important constituent of the ISC niche; the self-renewal of ISCs are dependent on direct cell contact between ISC and Paneth cells [113]. The second category of ISCs is named "+4 cells" because of their average position (above PCs compartment) in the crypt. They were originally identified by Potten et al. as DNA label-retaining cells. There are not unique marker for +4 cells but a signature of 4 main putative antigens are reported. Bmi1 a member of Polycomb family with an essential role in maintaining chromatin silencing, is a not-selective marker predominantly expressed at +4 position in SI and are not seen elsewhere in the intestinal tract. Isolated $Bmi1^+$ cells are Wnt-independent and minimally overlapping CBCs. Currently the theory that more than one ISC type may coexist is emerging and supported [114]. This assumes a specialized niche environment in which SI use both the distinct ISC populations. In a cooperative model, the cycling CBCs are responsible for daily homeostasis, whereas more quiescent +4 cells can be activated during epithelial repair following injury. Although their separate roles, independent studies showed the +4 markers are expressed by $Lgr5^+$ CBCs. In addition *Bmi1*+ cells contribute to the repopulation of the LGR5- *in vitro* e and *in vivo* bring evidence a complex interplay between the two cell-lineage. Are $Bmi1^+$ and $Lgr5^+$ truly independent ISC pools?

10.4 Gut organoid model

Confident of $Lgr5^+$ cells potency, Clevers's group revealed murine crypts cultured *in vitro* in 3D environment form "organoids" which mimic the histological hierarchy recapitulating *in vivo* SI epithelium. Even though the ISCC [115] classified this epithelial cell culture as "enteroids", we will like to name them with the term that the discovering authors continue to use. The organoids produce all mature cells with physiological localization and frequency patterns. They are composed of a central cyst structure, lined by villus-like epithelium and several surrounding budding structures. The basal side of the polarized cells is oriented toward the Matrigel, whereas secretion by PCs and GCs occurs toward the lumen formed by EC borders. ISCs and PCs reside at the bottom of the budding crypt-like domains. As cells divide and differentiate, they are conveyed along the walls of the crypt. Apoptotic cells are progressively shed into the lumen. The "ENR" combination of growth factors (EGF, noggin and R-spondin 1), simulating the pathway present at the level of the niche, is essential to maintain ISCs *in vitro*. Indeed crypt growth requires EGF and R-spondin, while it is the organoids passaging to require Noggin actually. It was demonstrated that, provided necessary instructory signals, also single $Lgr5^+$ cells are sufficient to generate organoids in the absence of a mesenchymal niche[116]. Similarly $Bmi1^+$ ISCs can generate clonally derived intestinal spheroids containing also $Lgr5^+$ cells[117].

The ENR cocktail is not adequate to sustain efficient *in vitro* propagation of a pure population of ISCs when they lose contact with PCs, actually an important source of various niche factors (Figure 46). The combination of CHIR and VPA, by activating Wnt pathways and suppressing secretory cell specification, maintains ISCs in an undifferentiated state and promote their self-renewal [113].

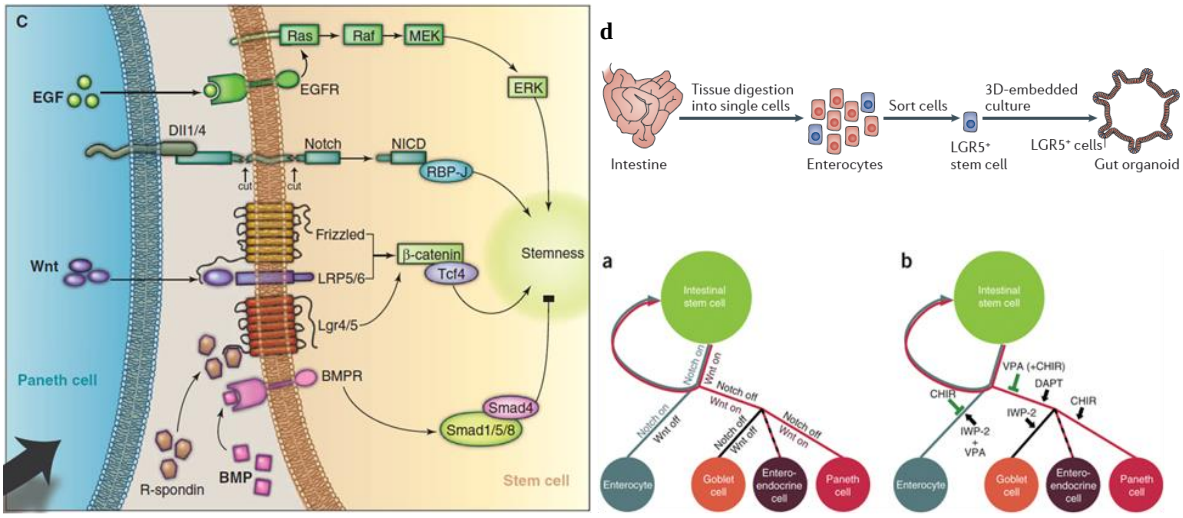

Figure 46 Organoid culture rationale (d) and signaling(a) and GFs/compounds(b) involved in the maintenance in culture (a) of organoids and selecting pathways inducing different lineages. Source: Sato and Clevers, 2013,[129] Yin et al. 2013[113]

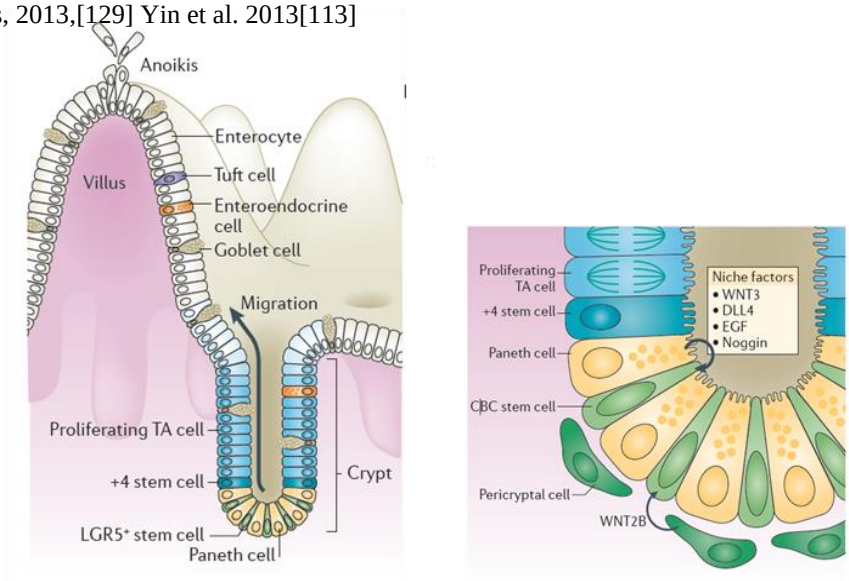

Figure 47 Organization of stem cell niche and effectors in the epithelial hoemostasis. Source: Barker 2013, **[114][112]**

11 Methods

11.1 Organoid culture

The protocol is already described and adapted from Sato et al. 2013. The enteroid culture method was modified from Sato et al. Mouse proximal small intestine (~10 cm) was excised, opened longitudinally, and washed with ice-cold PBS. The intestine was cut into small pieces (~4- to 5-mm diameter) villi are removed by scraping and pieces are incubated in ice-cold PBS containing 2 mM EDTA for 30 min at 4°C. After being rinsed once with ice-cold PBS to remove EDTA, the intestinal fragments were resuspended four times in ice-cold DPBS 0,5 % BSA by repeated, vigorous pipetting, using a 10-ml pipette. Different fractions are collected in BSA coated tubes. The supernatant from selected fractions enriched in crypts is collected and passes through a 70-µm cell strainer to remove tissue fragments. Crypts in the strained solution are separated from suspended single cells by centrifugation (600 rpm, 1 min). The crypts pellet is resuspended with cold PBS, crypts number is counted at the optical microscope. ToxA is eventually diluted and incubated with crypts at this step, allowing the exposure of the toxin to the luminal part of the developing organoids. 500 crypts are mixed with 50 µl of Matrigel (BD Bioscience) for plating in single well 24-well cell culture plates. After polymerization of the Matrigel, culture medium composed of Advanced DMEM/ F12 (Gibco), supplemented with N2 and B27 supplements, containing, PS solution, hepes buffer, 500 ng/ml Rspondin1, 100 ng/ml noggin, and 50 ng/ml epidermal growth factor (EGF) was added and changed every 2–4 days.

11.2 Optical microscopy

Images acquisition of the samples was done using Olympus inverted microscope equipped with cooled color CCD and cellSense software.

11.3 Crypts Viability Assay

Crypts from wt or Lgr5-GFP^{+} mice are isolated as described for organoids culture. Freshly isolated crypts are incubated with ToxA/TcdA 1X or 50X sublytic amounts in medium for 30 min, at 37°C. Samples are incubated on ice, mechanically dissociated trough thin tip pipetting, then stained with L/D working solution or PI. Additionally α-CD24 staining is performed for 20 min. Fixed cells (by PF) are resuspended in tubes and analyzed.

11.4 Organoids viability

Organoids treated with ToxA at the culture iniziation, are scraped from plates and harvested from the matrix by cell recovery solution incubation (BD). Dissociation is performed in a solution HBSS w/o Ca^{+2} and Mg^{2+} supplemented with 0.3 U/ml Dispase (Corning), 0.8 U/ml DNase (Sigma), and 10 µM Y-27632 (Sigma) for 30 min at 37°C. Live/dead staining is performed before prepare cell resuspension for flow cytometry analysis.

11.5 Binding assay

ToxA different preparation (called here "TcdA") is conjugated with AlexaFluor-647 (Invitrogen Kit). TcdA-647 are maintained at 4°C (on ice also). Dissociated crypts are incubated as above. The reaction is stopped fixing 4% PF. Samples are washed twice in cold PBS. To do not affect viability and check the inactivation of the toxin by temperature we measure at the same time viability also of wt type ToxA treated cells. We incubate 50X [C] of ToxA for 20 min on ice, after they are washed and stained with L/D (or PI.). Eventually, cells were washed with 1% PBS/BSA and stained with CD24-APC antibody (clone M1/69 BioLegend). As negative control of specific binding we conjugated and used 647 conjugated BSA. Bound cells are considered in the cell gate and APC^{+}.

11.6 Statistics

The descriptive statistical analysis was performed on Graphpad Prism version 5. Results are expressed as fold change of mean values. Each bar displaying SEM represents a duplicate or a triplicate samples. Data are analyzed with unpaired t-test or Mann-Whitney U test. Values were considered statistically significant if $p<0.05$.

12 Results

12.1 Viability state of the intestinal epithelial cells

Preliminary experiment showed ToxA treated organoids do not affect the growth of organoids, but cellular debris poured out from the epithelium compared to the control organoids. The toxin affect viability of organoids as assessed by flow cytometry live/dead staining. A higher concentrations (10X) did not increase significantly death in organoids (Figure 49). When the toxin is incubated in the same manner but in contact with a crypts not destined to organoids formation, we saw a similar fold change difference in death in 10X [C] of toxin. The discrepancy between treated and untreated samples is persistent also in increasing toxin dose conditions (50X)(Figure 50). A similar comparable trend is led by different ToxA preparation that we called "TcdA". A specific staining for CD24 designed a panel of cell specific death by this population as confirmed by loss of events in flow cytometer counting for the selected marker (Figure 51). In a different binding experiment (Figure 52) we wanted to incubate labeled fluorescent ToxA and TcdA at 4°C to look at the specific binding of some cell set (preliminary no loss of cells in this condition was checked by live/dead assay). This specificity was confirmed consisting in an average 15% of crypts preparations.

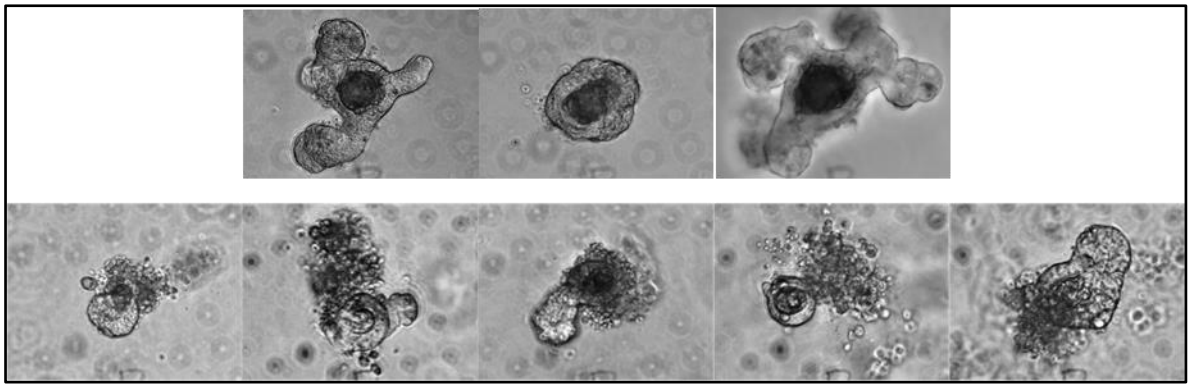

Figure 48 Untreated 4-days cultured organoids (above) and toxin treated organoids (below). Optical microscopy 20X orginal magnification

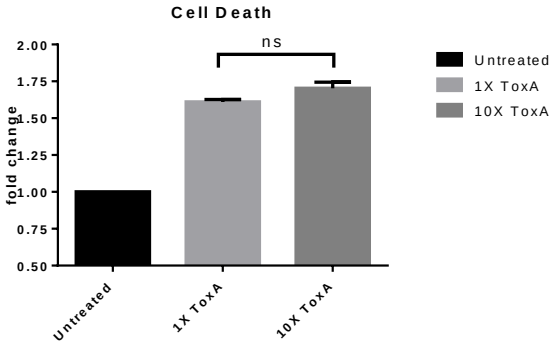

Figure 49 Organoids cells death caused by 37°C intoxication reaction.

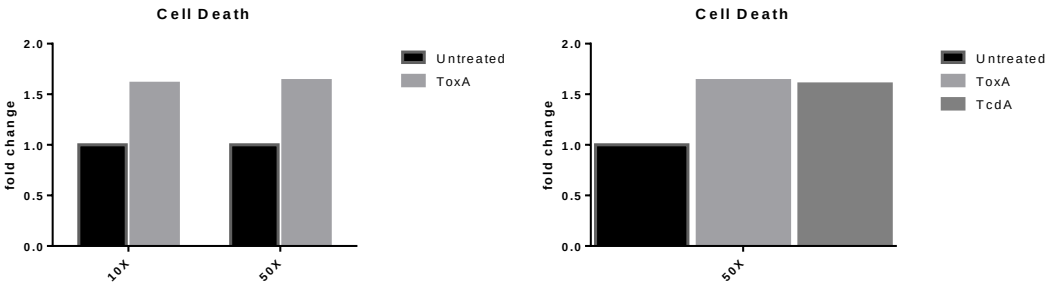

Figure 50 Crypts cells death caused by 37°C intoxication reaction.

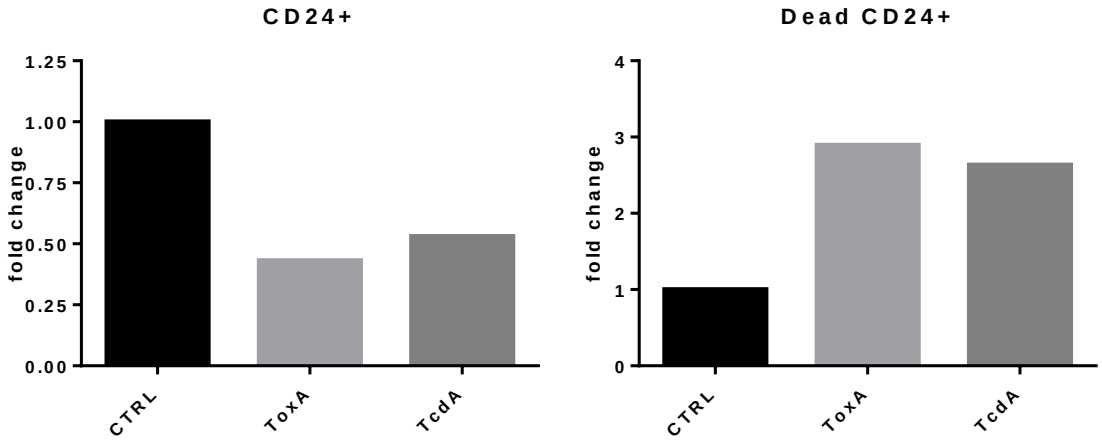

Figure 51 Loss and dead cell subset after 37°C toxin exposure

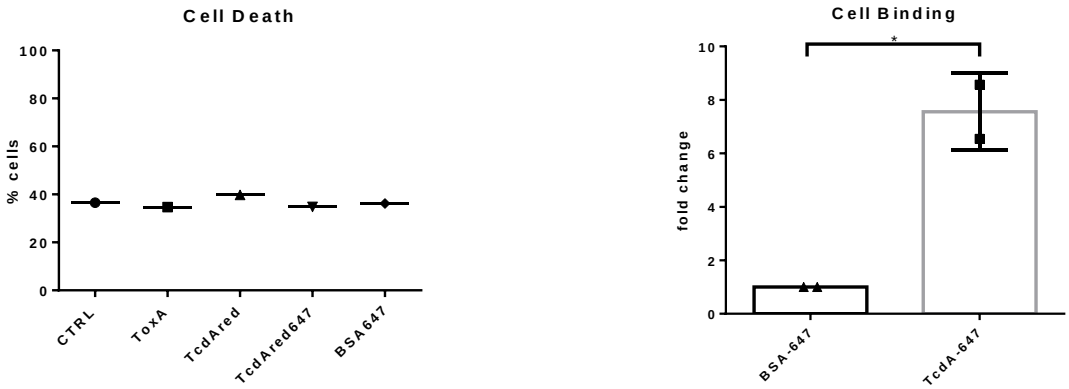

Figure 52 Toxin induced death is inactivated at 4°C (left graph). TcdA-647 selectively bound a cell group in crypts preparation (right graph).

13 Discussion

Using Clevers's method to set up *in vitro* mini-guts, the investigation of C.*difficile* ToxA / TcdA on SI mucosa was proven to affect barrier function, confirming the classical role as well as recent discoveries about this toxin and it suggested role to facilitate bacterial colonization [107]. We also observed toxin-dependent cell death within the organoid model. The same toxicity was soon detectable after shorter incubation with a higher sub-lethal dose of the toxin. In our preliminary experiments on whole crypts preparations, the cytotoxic effect seemed to be associated with a decrease in a subset of cells expressing CD24, a marker highly associated to crypts resident cells.

The organoid model develops all the major intestinal cell types, ISCs included, so during its culture has the possibility to repair acute damages. However an eventual protective or repairing mechanism is difficult to follow over-time. Alternative approach to organoids use could consist in the isolation of the different epithelial populations by FACS that should require a lot of starting material and a long protocol make it inconvenient to get viable intestinal cells for downstream experiments. In conclusion, precise milestones, such as selective cell binding studies, seemed necessary to be achieved prior to validate hypothesis on organoids.

Moving towards a different framework in which ISC and PCs are enriched will be useful to detect early events of the cytotoxicity as specific cell binding and subsequent impairing epithelial regeneration. In this context, the direct use of crypts containing Lgr5-GFP^{+} will enable to identify the ISCs subset, otherwise rare. CD24 staining on crypts is well characterized [118] and Lgr5-GFP+ signal is stronger as well the one observable *in vivo* than in long-lived organoids. In addition tracking the toxin by specific antibodies or fluorescent conjugation may add the opportunity to study spatial modifications in tissue architecture and drive attention on cell-toxin contact significance. By validating specific cell type marker and tracing the toxin trough such methods we are intending to decipher the cellular target of a chief virulence factor of a re-emerging pathogen. Further optimized experiments might support the idea that this toxin is able to interfere in the epithelial gut homeostatic balance, suggesting a correlation with the early phase of the chronic pathogenicity.

CONCLUSION

Scientists routinely work within the 3R's principles of 'Reduction, Refinement and Replacement' of animal experiments. Stressing on this approach, biomimetic *in vitro* tissue models of preclinical studies are highly desirable.

Our knowledge of microbial pathogenesis is historically linked to aberrant in vitro models base on traditional cell culture. At the same time in vivo models derived results, however, can be transferred only partially to humans. We proposed a method to reconstruct a human respiratory mucosa in vitro. Despite of the need of a further characterization, the model that can be obtained provides a functional tool to be suitable in host-pathogen interactions studies. Similar to emerging commercially available ready to use products (Epiairway, MucilAIR) our protocol invite to establish an in-house platform to be superior in term of customizability, competitive ease of use and reduced costs.

Aspects of vaccinology that might be impacted by our 3D airway model are:

a) Measurement of immune-mediated bacterial clearance by antigen-specific antibodies. This application would be fundamental to identify bacterial targets that are really effective as vaccine candidates.

b) Monitoring pathogens behavior at mucosal interfaces to determine the most efficacious strategies to hinder colonization. For example the evaluation of the capacity of specific antibodies to impair bacterial adhesion/biofilm formation would be an added value to vaccine candidate selection.

c) Determination of the best vaccination strategy in order to obtain an effective response at the mucosal barrier. Indeed the plasticity of the model permits the addition of specific cellular subsets as tools to evaluate vaccination efficacy.

d) Evaluation of the inflammatory response to vaccine components, including reactogenicity to LPS/LOS.

In vitro relevant models would also be requested in alternative to complex *in vivo* derived data and because the lack of genetic tools to manipulate C. *difficile*. The intestine constitutes an excellent system for studying regeneration. The cell architecture of the SI draws attention because crypts and villi represent a repetitive multitasking unit to study tissue homeostasis. The intestinal niche is a critical component in governing stem cell behavior and crypts plasticity. Recent progress

in the isolation of ISCs led to the creation *of* 3D cell models that include the entire villus-crypt axis. SI murine organoid culture allows studying early phase of the infection at cellular levels, with a quick recover of the cell targets. This cell culture method could drastically improve the efficiency of GI translational medicine. We used organoids as well-performing tools to elucidate the overall effect of toxins on the homeostasis of gut epithelium. Unraveling ToxA cellular target among stem cell niche may represent a challenge to develop new treatment and prevention strategies for CDI, since the incidence and costs associated are making *it* a significant public health alarm.

REFERENCES

[1] D. J. Maltman and S. A. Przyborski, “Developments in three-dimensional cell culture technology aimed at improving the accuracy of in vitro analyses,” vol. 38, pp. 1072–1075, 2010.

[2] C. A. Nickerson, E. G. Richter, and C. M. Ott, “Studying host-pathogen interactions in 3-D: organotypic models for infectious disease and drug development.,” *J. Neuroimmune Pharmacol.*, vol. 2, no. 1, pp. 26–31, Mar. 2007.

[3] B. M. Baker and C. S. Chen, “Deconstructing the third dimension - how 3D culture microenvironments alter cellular cues,” *J. Cell Sci.*, vol. 125, no. July, pp. 3015–3024, 2012.

[4] H. Page, P. Flood, and E. G. Reynaud, “Three-dimensional tissue cultures: current trends and beyond.,” *Cell Tissue Res.*, vol. 352, no. 1, pp. 123–31, Apr. 2013.

[5] B. Tonnarelli, M. Centola, A. Barbero, R. Zeller, and I. Martin, *Re-engineering development to instruct tissue regeneration.*, 1st ed., vol. 108. Elsevier Inc., 2014, pp. 319–38.

[6] K. L. Schmeichel and M. J. Bissell, “Modeling tissue-specific signaling and organ function in three dimensions.,” *J. Cell Sci.*, vol. 116, no. Pt 12, pp. 2377–88, Jun. 2003.

[7] P. Jungebluth, G. Moll, S. Baiguera, and P. Macchiarini, “Tissue-engineered airway: a regenerative solution.,” *Clin. Pharmacol. Ther.*, vol. 91, no. 1, pp. 81–93, Jan. 2012.

[8] R. E. Hynds and A. Giangreco, “Concise review: the relevance of human stem cell-derived organoid models for epithelial translational medicine.,” *Stem Cells*, vol. 31, no. 3, pp. 417–22, Mar. 2013.

[9] S. V Murphy and A. Atala, “3D bioprinting of tissues and organs,” *Nat. Biotechnol.*, vol. 32, no. 8, pp. 773–785, Aug. 2014.

[10] M. P. Lutolf, “Integration column: artificial ECM: expanding the cell biology toolbox in 3D.,” *Integr. Biol. (Camb).*, vol. 1, no. 3, pp. 235–41, Mar. 2009.

[11] K. M. Yamada and E. Cukierman, “Modeling tissue morphogenesis and cancer in 3D.,” *Cell*, vol. 130, no. 4, pp. 601–10, Aug. 2007.

[12] L. a Kunz-Schughart, J. P. Freyer, F. Hofstaedter, and R. Ebner, “The use of 3-D cultures for high-throughput screening: the multicellular spheroid model.,” *J. Biomol. Screen.*, vol. 9, no. 4, pp. 273–85, Jun. 2004.

[13] B. L. Duell, A. W. Cripps, M. A. Schembri, and G. C. Ulett, “Epithelial cell coculture models for studying infectious diseases: benefits and limitations.,” *J. Biomed. Biotechnol.*, vol. 2011, p. 852419, Jan. 2011.

[14] J. Barrila, A. L. Radtke, A. Crabbé, S. F. Sarker, M. M. Herbst-Kralovetz, C. M. Ott, and C. a Nickerson, “Organotypic 3D cell culture models: using the rotating wall vessel to study host-pathogen interactions.,” *Nat. Rev. Microbiol.*, vol. 8, no. 11, pp. 791–801, Nov. 2010.

[15] A. Richter-Dahlfors and G. Duménil, “Tissue microbiology emerging.,” *Curr. Opin. Microbiol.*, vol. 15, no. 1, pp. 1–2, Feb. 2012.

❖ REFERENCES

[16] T. M. Straub, K. Höner zu Bentrup, P. Orosz-Coghlan, A. Dohnalkova, B. K. Mayer, R. A. Bartholomew, C. O. Valdez, C. J. Bruckner-Lea, C. P. Gerba, M. Abbaszadegan, and C. A. Nickerson, "In vitro cell culture infectivity assay for human noroviruses.," *Emerg. Infect. Dis.*, vol. 13, no. 3, pp. 396–403, Mar. 2007.

[17] K. Höner zu Bentrup, R. Ramamurthy, C. M. Ott, K. Emami, M. Nelman-Gonzalez, J. W. Wilson, E. G. Richter, T. J. Goodwin, J. S. Alexander, D. L. Pierson, N. Pellis, K. L. Buchanan, and C. A. Nickerson, "Three-dimensional organotypic models of human colonic epithelium to study the early stages of enteric salmonellosis.," *Microbes Infect.*, vol. 8, no. 7, pp. 1813–25, Jun. 2006.

[18] C. A. Nickerson, E. G. Richter, and C. M. Ott, "Studying host-pathogen interactions in 3-D: organotypic models for infectious disease and drug development.," *J. Neuroimmune Pharmacol.*, vol. 2, no. 1, pp. 26–31, 2007.

[19] T. F. Murphy, H. Faden, L. O. Bakaletz, J. M. Kyd, A. Forsgren, J. Campos, M. Virji, and S. I. Pelton, "Nontypeable Haemophilus influenzae as a pathogen in children.," *Pediatr. Infect. Dis. J.*, vol. 28, no. 1, pp. 43–8, Jan. 2009.

[20] H. H. Tong, L. E. Blue, M. A. James, Y. P. Chen, and T. F. D. E. Maria, "Evaluation of Phase Variation of Nontypeable Haemophilus influenzae Lipooligosaccharide during Nasopharyngeal Colonization and Development of Otitis Media in the Chinchilla Model," vol. 68, no. 8, pp. 4593–4597, 2000.

[21] D. Ren, K. L. Nelson, P. N. Uchakin, A. L. Smith, X.-X. Gu, and D. a Daines, "Characterization of extended co-culture of non-typeable Haemophilus influenzae with primary human respiratory tissues.," *Exp. Biol. Med. (Maywood).*, vol. 237, no. 5, pp. 540–7, May 2012.

[22] M. Rupnik, M. H. Wilcox, and D. N. Gerding, "Clostridium difficile infection: new developments in epidemiology and pathogenesis.," *Nat. Rev. Microbiol.*, vol. 7, no. 7, pp. 526–36, Jul. 2009.

[23] J. Bien, V. Palagani, and P. Bozko, "The intestinal microbiota dysbiosis and Clostridium difficile infection: is there a relationship with inflammatory bowel disease?," *Therap. Adv. Gastroenterol.*, vol. 6, no. 1, pp. 53–68, Jan. 2013.

[24] R. Breeze and M. Turk, "Cellular Structure , Function and Organization in the Lower Respiratory Tract," vol. 55, pp. 3–24, 1984.

[25] A. Tam, S. Wadsworth, D. Dorscheid, S. F. P. Man, and D. D. Sin, "The airway epithelium: more than just a structural barrier.," *Ther. Adv. Respir. Dis.*, vol. 5, no. 4, pp. 255–73, Aug. 2011.

[26] D. A. Knight and S. T. Holgate, "INVITED REVIEW SERIES : CELLS OF THE LUNG The airway epithelium : Structural and functional properties in health and disease," pp. 432–446, 2003.

[27] S. Ganesan, A. T. Comstock, and U. S. Sajjan, "Barrier function of airway tract epithelium," no. December, pp. 1–9, 2013.

[28] J. R. Rock and B. L. M. Hogan, "Epithelial progenitor cells in lung development, maintenance, repair, and disease.," *Annu. Rev. Cell Dev. Biol.*, vol. 27, pp. 493–512, Jan. 2011.

[29] P. K. Jeffery and D. Li, "Airway mucosa: secretory cells, mucus and mucin genes," *Eur. Respir. J.*, vol. 10, no. 7, pp. 1655–1662, Jul. 1997.

❖ REFERENCES

[30] D. N. Kotton and E. E. Morrisey, "Lung regeneration: mechanisms, applications and emerging stem cell populations.," *Nat. Med.*, vol. 20, no. 8, pp. 822–32, Aug. 2014.

[31] Y. Daniely, G. Liao, D. Dixon, R. I. Linnoila, A. Lori, S. H. Randell, M. Oren, and A. M. Jetten, "Critical role of p63 in the development of a normal esophageal and tracheobronchial epithelium.," *Am. J. Physiol. Cell Physiol.*, vol. 287, no. 1, pp. C171–81, Jul. 2004.

[32] T. Matsuzaki, T. Suzuki, H. Koyama, S. Tanaka, and K. Takata, "Water Channel Protein AQP3 Is Present in Epithelia Exposed to the Environment of Possible Water Loss," *J. Histochem. Cytochem.*, vol. 47, no. 10, pp. 1275–1286, Oct. 1999.

[33] A. Avril-Delplanque, I. Casal, N. Castillon, J. Hinnrasky, E. Puchelle, and B. Péault, "Aquaporin-3 expression in human fetal airway epithelial progenitor cells.," *Stem Cells*, vol. 23, no. 7, pp. 992–1001, Aug. 2005.

[34] B. L. M. Hogan, C. E. Barkauskas, H. a Chapman, J. a Epstein, R. Jain, C. C. W. Hsia, L. Niklason, E. Calle, A. Le, S. H. Randell, J. Rock, M. Snitow, M. Krummel, B. R. Stripp, T. Vu, E. S. White, J. a Whitsett, and E. E. Morrisey, "Repair and regeneration of the respiratory system: complexity, plasticity, and mechanisms of lung stem cell function.," *Cell Stem Cell*, vol. 15, no. 2, pp. 123–38, Aug. 2014.

[35] M. Herriges and E. E. Morrisey, "Lung development: orchestrating the generation and regeneration of a complex organ.," *Development*, vol. 141, no. 3, pp. 502–13, Feb. 2014.

[36] C. Wansleeben, C. E. Barkauskas, J. R. Rock, and B. L. M. Hogan, "Stem cells of the adult lung: their development and role in homeostasis, regeneration, and disease.," *Wiley Interdiscip. Rev. Dev. Biol.*, vol. 2, no. 1, pp. 131–48, 2013.

[37] P. R. Tata, H. Mou, A. Pardo-Saganta, R. Zhao, M. Prabhu, B. M. Law, V. Vinarsky, J. L. Cho, S. Breton, A. Sahay, B. D. Medoff, and J. Rajagopal, "Dedifferentiation of committed epithelial cells into stem cells in vivo.," *Nature*, vol. 503, no. 7475, pp. 218–23, Nov. 2013.

[38] D. Zheng, G. V Limmon, L. Yin, N. H. N. Leung, H. Yu, V. T. K. Chow, and J. Chen, "Regeneration of alveolar type I and II cells from Scgb1a1-expressing cells following severe pulmonary damage induced by bleomycin and influenza.," *PLoS One*, vol. 7, no. 10, p. e48451, Jan. 2012.

[39] S. Y. Foo and S. Phipps, "Regulation of inducible BALT formation and contribution to immunity and pathology," *Mucosal Immunol.*, vol. 3, no. 6, pp. 537–544, 2010.

[40] V. J. Ferrans, M. A. Kaliner, and E. M. Shevach, "dendritic in lung studio vecchio," vol. i, no. February, pp. 436–451, 1986.

[41] J. Maarten, V. Haarst, H. J. De Wit, H. A. Drexhage, and H. C. Hoogsteden, "Distribution and Immunophenotype of Mononuclear Phagocytes and Dendritic Cells in the Human Lung."

[42] I. K. Demedts, G. G. Brusselle, K. Y. Vermaelen, and R. a Pauwels, "Identification and characterization of human pulmonary dendritic cells.," *Am. J. Respir. Cell Mol. Biol.*, vol. 32, no. 3, pp. 177–84, Mar. 2005.

[43] D. N. Cook and K. Bottomly, "Innate immune control of pulmonary dendritic cell trafficking.," *Proc. Am. Thorac. Soc.*, vol. 4, no. 3, pp. 234–9, Jul. 2007.

❖ REFERENCES

[44] L. Cochand, P. Isler, F. Songeon, L. P. Nicod, J. R. Cell, and M. Biol, "Rapid Communication Human Lung Dendritic Cells Have an Immature Phenotype with Efficient Mannose Receptors," 1994.

[45] B. F. Sallusto and A. Lanzavecchia, "From the "Basel Institute for Immunology, CH-4005, Basel, Switzerland; and the *Department of Immunology, Istituto Superiore di SanitY, 1-00161, Rome, Italy," vol. 179, no. April, 1994.

[46] M. Dominici, K. Le Blanc, I. Mueller, I. Slaper-Cortenbach, F. Marini, D. Krause, R. Deans, A. Keating, D. Prockop, and E. Horwitz, "Minimal criteria for defining multipotent mesenchymal stromal cells. The International Society for Cellular Therapy position statement.," *Cytotherapy*, vol. 8, no. 4, pp. 315–7, Jan. 2006.

[47] A. Keating, "Mesenchymal stromal cells: new directions.," *Cell Stem Cell*, vol. 10, no. 6, pp. 709–16, Jun. 2012.

[48] K. Le Blanc and D. Mougiakakos, "Multipotent mesenchymal stromal cells and the innate immune system.," *Nat. Rev. Immunol.*, vol. 12, no. 5, pp. 383–96, May 2012.

[49] K. Sinclair, S. T. Yerkovich, and D. C. Chambers, "Mesenchymal stem cells and the lung.," *Respirology*, vol. 18, no. 3, pp. 397–411, Apr. 2013.

[50] F. Sabatini, L. Petecchia, M. Tavian, V. Jodon de Villeroché, G. a Rossi, and D. Brouty-Boyé, "Human bronchial fibroblasts exhibit a mesenchymal stem cell phenotype and multilineage differentiating potentialities.," *Lab. Invest.*, vol. 85, no. 8, pp. 962–71, Aug. 2005.

[51] L. Jarvinen, L. Badri, S. Wettlaufer, T. Ohtsuka, T. J. Standiford, G. B. Toews, D. J. Pinsky, M. Peters-Golden, and V. N. Lama, "Lung Resident Mesenchymal Stem Cells Isolated from Human Lung Allografts Inhibit T Cell Proliferation via a Soluble Mediator," *J. Immunol.*, vol. 181, no. 6, pp. 4389–4396, Sep. 2008.

[52] J. Hua, H. Yu, W. Dong, C. Yang, Z. Gao, A. Lei, Y. Sun, S. Pan, Y. Wu, and Z. Dou, "Characterization of mesenchymal stem cells (MSCs) from human fetal lung: potential differentiation of germ cells.," *Tissue Cell*, vol. 41, no. 6, pp. 448–55, Dec. 2009.

[53] P. D. Bozyk, A. P. Popova, J. K. Bentley, A. M. Goldsmith, M. J. Linn, D. J. Weiss, and M. B. Hershenson, "Mesenchymal stromal cells from neonatal tracheal aspirates demonstrate a pattern of lung-specific gene expression.," *Stem Cells Dev.*, vol. 20, no. 11, pp. 1995–2007, Nov. 2011.

[54] M. Ricciardi, G. Malpeli, F. Bifari, G. Bassi, L. Pacelli, A. H. Nwabo Kamdje, M. Chilosi, and M. Krampera, "Comparison of epithelial differentiation and immune regulatory properties of mesenchymal stromal cells derived from human lung and bone marrow.," *PLoS One*, vol. 7, no. 5, p. e35639, Jan. 2012.

[55] N. Gupta, A. Krasnodembskaya, M. Kapetanaki, M. Mouded, X. Tan, V. Serikov, and M. a Matthay, "Mesenchymal stem cells enhance survival and bacterial clearance in murine Escherichia coli pneumonia.," *Thorax*, vol. 67, no. 6, pp. 533–9, Jun. 2012.

[56] E. Gonzalez-rey, P. Anderson, M. A. González, L. Rico, and D. Büscher, "Human adult stem cells derived from adipose tissue protect against experimental colitis and sepsis," 2009.

[57] S. H. J. Mei, J. J. Haitsma, C. C. Dos Santos, Y. Deng, P. F. H. Lai, A. S. Slutsky, W. C. Liles, and D. J. Stewart, "Mesenchymal stem cells reduce inflammation while enhancing bacterial clearance and

improving survival in sepsis.," *Am. J. Respir. Crit. Care Med.*, vol. 182, no. 8, pp. 1047–57, Oct. 2010.

[58] S. R. R. Hall, K. Tsoyi, B. Ith, R. F. Padera, J. A. Lederer, Z. Wang, X. Liu, and M. A. Perrella, "Mesenchymal stromal cells improve survival during sepsis in the absence of heme oxygenase-1: the importance of neutrophils.," *Stem Cells*, vol. 31, no. 2, pp. 397–407, Feb. 2013.

[59] A. Krasnodembskaya, G. Samarani, Y. Song, H. Zhuo, X. Su, J.-W. Lee, N. Gupta, M. Petrini, and M. a Matthay, "Human mesenchymal stem cells reduce mortality and bacteremia in gram-negative sepsis in mice in part by enhancing the phagocytic activity of blood monocytes.," *Am. J. Physiol. Lung Cell. Mol. Physiol.*, vol. 302, no. 10, pp. L1003–13, May 2012.

[60] A. Krasnodembskaya, Y. Song, X. Fang, N. Gupta, V. Serikov, J.-W. Lee, and M. a Matthay, "Antibacterial effect of human mesenchymal stem cells is mediated in part from secretion of the antimicrobial peptide LL-37.," *Stem Cells*, vol. 28, no. 12, pp. 2229–38, Dec. 2010.

[61] H. Hospital, S. Jiaotong, and C. S. Francisco, "T RANSLATIONAL AND C LINICAL Human Mesenchymal Stem Cell Microvesicles for Treatment of Escherichia coli Endotoxin-Induced Acute Lung Injury in Mice," pp. 116–125, 2014.

[62] T. J. Wannemuehler, M. C. Manukyan, B. D. Brewster, J. Rouch, J. a Poynter, Y. Wang, and D. R. Meldrum, "Advances in mesenchymal stem cell research in sepsis.," *J. Surg. Res.*, vol. 173, no. 1, pp. 113–26, Mar. 2012.

[63] C. I. Grainger, L. L. Greenwell, D. J. Lockley, G. P. Martin, and B. Forbes, "Culture of Calu-3 cells at the air interface provides a representative model of the airway epithelial barrier.," *Pharm. Res.*, vol. 23, no. 7, pp. 1482–90, Jul. 2006.

[64] J. L. Harcourt and L. M. Haynes, "Establishing a liquid-covered culture of polarized human airway epithelial Calu-3 cells to study host cell response to respiratory pathogens in vitro.," *J. Vis. Exp.*, no. 72, pp. 4–10, Jan. 2013.

[65] J. R. Rock, S. H. Randell, and B. L. M. Hogan, "Airway basal stem cells : a perspective on their roles in epithelial homeostasis and remodeling," *Perspective*, vol. 556, pp. 545–556, 2010.

[66] T. E. Gray, K. Guzman, C. W. Davis, L. H. Abdullah, and P. Nettesheim, "Mucociliary Differentiation of Serially Passaged Normal Human Tracheobronchial Epithelial Cells," *Environ. Heal.*, no. 1.

[67] M. S. Walters, K. Gomi, B. Ashbridge, M. A. S. Moore, V. Arbelaez, J. Heldrich, B.-S. Ding, S. Rafii, M. R. Staudt, and R. G. Crystal, "Generation of a human airway epithelium derived basal cell line with multipotent differentiation capacity.," *Respir. Res.*, vol. 14, no. 1, p. 135, Jan. 2013.

[68] P. M. De Jong, M. A. J. A. Van Sterkenburg, S. C. Hesseling, J. A. Kempenaar, A. A. Mulder, A. M. Mommaas, J. H. Dijkman, and M. Ponec, "Ciliogenesis in Human Bronchial Epithelial Cells Cultured at the Air-Liquid Interface," 1993.

[69] J. Paquette, P. Tremblay, and V. Bernier, "Production of tissue-engineered three-dimensional human bronchial models," *Vitr. Cell. ...*, no. June, pp. 213–220, 2003.

[70] A. B. Clark, S. H. Randell, P. Nettesheim, T. E. Gray, B. Bagnell, and L. E. Ostrowski, "Regulation of ciliated cell differentiation in cultures of rat tracheal epithelial cells.," *Am. J. Respir. Cell Mol. Biol.*, vol. 12, no. 3, pp. 329–38, Mar. 1995.

❖ REFERENCES

[71] A. A. Pezzulo, T. D. Starner, T. E. Scheetz, G. L. Traver, A. E. Tilley, B. Harvey, R. G. Crystal, P. B. Mccray, J. Zabner, P. Aa, S. Td, S. Te, T. Gl, and T. Ae, "The air-liquid interface and use of primary cell cultures are important to recapitulate the transcriptional profile of in vivo airway epithelia," no. 13, pp. 25–31, 2011.

[72] C. Pohl, M. I. Hermanns, C. Uboldi, M. Bock, S. Fuchs, J. Dei-Anang, E. Mayer, K. Kehe, W. Kummer, and C. J. Kirkpatrick, "Barrier functions and paracellular integrity in human cell culture models of the proximal respiratory unit.," *Eur. J. Pharm. Biopharm.*, vol. 72, no. 2, pp. 339–49, Jun. 2009.

[73] J. R. Rock, M. W. Onaitis, E. L. Rawlins, Y. Lu, C. P. Clark, Y. Xue, S. H. Randell, and B. L. M. Hogan, "Basal cells as stem cells of the mouse trachea and human airway epithelium," 2009.

[74] X. Wu, J. R. Peters-Hall, S. Bose, M. T. Peña, and M. C. Rose, "Human bronchial epithelial cells differentiate to 3D glandular acini on basement membrane matrix.," *Am. J. Respir. Cell Mol. Biol.*, vol. 44, no. 6, pp. 914–21, Jun. 2011.

[75] J. Debnath, S. K. Muthuswamy, and J. S. Brugge, "Morphogenesis and oncogenesis of MCF-10A mammary epithelial acini grown in three-dimensional basement membrane cultures.," *Methods*, vol. 30, no. 3, pp. 256–68, Jul. 2003.

[76] H. Danahay, A. D. Pessotti, J. Coote, B. E. Montgomery, D. Xia, A. Wilson, H. Yang, Z. Wang, L. Bevan, C. Thomas, S. Petit, A. London, P. LeMotte, A. Doelemeyer, G. L. Vélez-Reyes, P. Bernasconi, C. J. Fryer, M. Edwards, P. Capodieci, A. Chen, M. Hild, and A. B. Jaffe, "Notch2 Is Required for Inflammatory Cytokine-Driven Goblet Cell Metaplasia in the Lung.," *Cell Rep.*, pp. 239–252, Dec. 2014.

[77] C. E. Barkauskas, M. J. Cronce, C. R. Rackley, E. J. Bowie, D. R. Keene, B. R. Stripp, S. H. Randell, P. W. Noble, and B. L. M. Hogan, "Type 2 alveolar cells are stem cells in adult lung.," *J. Clin. Invest.*, vol. 123, no. 7, pp. 3025–36, Jul. 2013.

[78] W. Yu, X. Fang, A. Ewald, K. Wong, C. A. Hunt, Z. Werb, M. A. Matthay, and K. Mostov, "Formation of Cysts by Alveolar Type II Cells in Three-dimensional Culture Reveals a Novel Mechanism for Epithelial Morphogenesis □," vol. 18, no. May, pp. 1693–1700, 2007.

[79] S. Gotoh, I. Ito, T. Nagasaki, Y. Yamamoto, S. Konishi, Y. Korogi, H. Matsumoto, S. Muro, T. Hirai, M. Funato, S.-I. Mae, T. Toyoda, A. Sato-Otsubo, S. Ogawa, K. Osafune, and M. Mishima, "Generation of alveolar epithelial spheroids via isolated progenitor cells from human pluripotent stem cells.," *Stem cell reports*, vol. 3, no. 3, pp. 394–403, Sep. 2014.

[80] S. R. Franzdóttir, I. T. Axelsson, A. J. Arason, O. Baldursson, T. Gudjonsson, and M. K. Magnusson, "Airway branching morphogenesis in three dimensional culture.," *Respir. Res.*, vol. 11, no. 1, p. 162, Jan. 2010.

[81] Y. Goto and Y. Noguchi, "In vitro reconstitution of the tracheal epithelium," *Am. J. ...*, no. 32, 1999.

[82] C. Brohem, "Artificial skin in perspective: concepts and applications," *Pigment cell ...*, vol. 24, no. 1, pp. 35–50, 2011.

[83] S. Bouhout, J. Pereira, F. Simon, and S. Chabaud, "Production of Tissue-Engineered Human 3D Bronchi In Vitro," 2014.

[84] M. M. Choe, A. A. Tomei, and M. A. Swartz, "Physiological 3D tissue model of the airway wall and mucosa," *Mind*, vol. 1, no. 1, pp. 357–362, 2006.

[85] F. Grinnell, "Fibroblast biology in three-dimensional collagen matrices," *Trends Cell Biol.*, vol. 13, no. 5, pp. 264–269, May 2003.

[86] S. C. Pageau, O. V Sazonova, J. Y. Wong, A. M. Soto, and C. Sonnenschein, "The effect of stromal components on the modulation of the phenotype of human bronchial epithelial cells in 3D culture," *Biomaterials*, vol. 32, no. 29, pp. 7169–7180, 2011.

[87] C. Le Visage and B. Dunham, "Coculture of mesenchymal stem cells and respiratory epithelial cells to engineer a human composite respiratory mucosa," *Tissue …*, vol. 10, no. 9, pp. 1426–1435, 2004.

[88] J. Adamson, L. E. Haswell, G. Phillips, and M. D. Gaça, "In Vitro Models of Chronic Obstructive Pulmonary Disease (COPD)," 2009.

[89] J. Chakir, N. Pagé, Q. Hamid, M. Laviolette, L. P. Boulet, and M. Rouabhia, "Bronchial mucosa produced by tissue engineering: a new tool to study cellular interactions in asthma.," *J. Allergy Clin. Immunol.*, vol. 107, no. 1, pp. 36–40, Jan. 2001.

[90] B. M. Rothen-Rutishauser, S. G. Kiama, and P. Gehr, "A three-dimensional cellular model of the human respiratory tract to study the interaction with particles.," *Am. J. Respir. Cell Mol. Biol.*, vol. 32, no. 4, pp. 281–9, Apr. 2005.

[91] M. M. Choe, P. H. S. Sporn, and M. A. Swartz, "An in vitro airway wall model of remodeling.," *Am. J. Physiol. Lung Cell. Mol. Physiol.*, vol. 285, no. 2, pp. L427–33, Aug. 2003.

[92] A. D. Lehmann, N. Daum, M. Bur, C.-M. Lehr, P. Gehr, and B. M. Rothen-Rutishauser, "An in vitro triple cell co-culture model with primary cells mimicking the human alveolar epithelial barrier.," *Eur. J. Pharm. Biopharm.*, vol. 77, no. 3, pp. 398–406, Apr. 2011.

[93] A. T. Nguyen Hoang, P. Chen, J. Juarez, P. Sachamitr, B. Billing, L. Bosnjak, B. Dahlén, M. Coles, and M. Svensson, "Dendritic cell functional properties in a three-dimensional tissue model of human lung mucosa.," *Am. J. Physiol. Lung Cell. Mol. Physiol.*, vol. 302, no. 2, pp. L226–37, Jan. 2012.

[94] A. T. Nguyen Hoang, P. Chen, S. Björnfot, K. Högstrand, J. G. Lock, A. Grandien, M. Coles, and M. Svensson, "Technical advance: live-imaging analysis of human dendritic cell migrating behavior under the influence of immune-stimulating reagents in an organotypic model of lung.," *J. Leukoc. Biol.*, vol. 96, no. 3, pp. 481–9, Sep. 2014.

[95] H. Harrington and P. Cato, "Immunocompetent 3D Model of Human Upper Airway for Disease Modeling and In Vitro Drug Evaluation," *Mol. …*, 2014.

[96] K. Kobayashi, T. Suzuki, Y. Nomoto, Y. Tada, M. Miyake, A. Hazama, I. Wada, T. Nakamura, and K. Omori, "A tissue-engineered trachea derived from a framed collagen scaffold, gingival fibroblasts and adipose-derived stem cells.," *Biomaterials*, vol. 31, no. 18, pp. 4855–63, Jun. 2010.

[97] B. B. Cole, R. W. Smith, K. M. Jenkins, B. B. Graham, P. R. Reynolds, and S. D. Reynolds, "Tracheal Basal cells: a facultative progenitor cell pool.," *Am. J. Pathol.*, vol. 177, no. 1, pp. 362–76, Jul. 2010.

❖ REFERENCES

[98] P. V Guillot, C. Gotherstrom, J. Chan, H. Kurata, and N. M. Fisk, "Human first-trimester fetal MSC express pluripotency markers and grow faster and have longer telomeres than adult MSC.," *Stem Cells*, vol. 25, no. 3, pp. 646–54, Mar. 2007.

[99] H.-S. Wang, S.-C. Hung, S.-T. Peng, C.-C. Huang, H.-M. Wei, Y.-J. Guo, Y.-S. Fu, M.-C. Lai, and C.-C. Chen, "Mesenchymal stem cells in the Wharton's jelly of the human umbilical cord.," *Stem Cells*, vol. 22, no. 7, pp. 1330–7, Jan. 2004.

[100] D.-W. Kim, M. Staples, K. Shinozuka, P. Pantcheva, S.-D. Kang, and C. V Borlongan, "Wharton's Jelly-Derived Mesenchymal Stem Cells: Phenotypic Characterization and Optimizing Their Therapeutic Potential for Clinical Applications.," *Int. J. Mol. Sci.*, vol. 14, no. 6, pp. 11692–712, Jan. 2013.

[101] R. Hass, C. Kasper, S. Böhm, and R. Jacobs, "Different populations and sources of human mesenchymal stem cells (MSC): A comparison of adult and neonatal tissue-derived MSC.," *Cell Commun. Signal.*, vol. 9, no. 1, p. 12, Jan. 2011.

[102] S. Böttcher-Haberzeth, T. Biedermann, A. S. Klar, L. Pontiggia, J. Rac, D. Nadal, C. Schiestl, E. Reichmann, and M. Meuli, "Tissue engineering of skin: human tonsil-derived mesenchymal cells can function as dermal fibroblasts.," *Pediatr. Surg. Int.*, vol. 30, no. 2, pp. 213–22, Feb. 2014.

[103] J. Parker, S. Sarlang, and S. Thavagnanam, "A 3-D well-differentiated model of pediatric bronchial epithelium demonstrates unstimulated morphological differences between asthmatic and nonasthmatic cells," *Pediatr. …*, vol. 67, no. 1, 2010.

[104] Q. Ge, L. M. Moir, J. L. Black, B. G. Oliver, and J. K. Burgess, "TGFβ1 induces IL-6 and inhibits IL-8 release in human bronchial epithelial cells: the role of Smad2/3.," *J. Cell. Physiol.*, vol. 225, no. 3, pp. 846–54, Nov. 2010.

[105] S. M. Fitzgerald, S. a Lee, H. K. Hall, D. S. Chi, and G. Krishnaswamy, "Human lung fibroblasts express interleukin-6 in response to signaling after mast cell contact.," *Am. J. Respir. Cell Mol. Biol.*, vol. 30, no. 4, pp. 585–93, Apr. 2004.

[106] J. V Thaikoottathil, R. J. Martin, J. Zdunek, A. Weinberger, J. G. Rino, and H. W. Chu, "Cigarette smoke extract reduces VEGF in primary human airway epithelial cells.," *Eur. Respir. J.*, vol. 33, no. 4, pp. 835–43, Apr. 2009.

[107] M. Kasendra, R. Barrile, R. Leuzzi, and M. Soriani, "Clostridium difficile toxins facilitate bacterial colonization by modulating the fence and gate function of colonic epithelium.," *J. Infect. Dis.*, vol. 209, no. 7, pp. 1095–104, Apr. 2014.

[108] R. N. Pruitt, N. M. Chumbler, S. A. Rutherford, M. A. Farrow, D. B. Friedman, B. Spiller, and D. B. Lacy, "Structural determinants of Clostridium difficile toxin A glucosyltransferase activity.," *J. Biol. Chem.*, vol. 287, no. 11, pp. 8013–20, Mar. 2012.

[109] T. Giesemann, M. Egerer, T. Jank, and K. Aktories, "Processing of Clostridium difficile toxins.," *J. Med. Microbiol.*, vol. 57, no. Pt 6, pp. 690–6, Jun. 2008.

[110] R. N. Pruitt and D. B. Lacy, "Toward a structural understanding of Clostridium difficile toxins A and B.," *Front. Cell. Infect. Microbiol.*, vol. 2, no. March, p. 28, Jan. 2012.

❖ REFERENCES

[111] T. Sato, J. H. van Es, H. J. Snippert, D. E. Stange, R. G. Vries, M. van den Born, N. Barker, N. F. Shroyer, M. van de Wetering, and H. Clevers, "Paneth cells constitute the niche for Lgr5 stem cells in intestinal crypts.," *Nature*, vol. 469, no. 7330, pp. 415–8, Jan. 2011.

[112] N. Barker, A. van Oudenaarden, and H. Clevers, "Identifying the stem cell of the intestinal crypt: strategies and pitfalls.," *Cell Stem Cell*, vol. 11, no. 4, pp. 452–60, Oct. 2012.

[113] X. Yin, H. F. Farin, J. H. van Es, H. Clevers, R. Langer, and J. M. Karp, "Niche-independent high-purity cultures of Lgr5+ intestinal stem cells and their progeny.," *Nat. Methods*, vol. 11, no. 1, pp. 106–12, Jan. 2014.

[114] N. Barker, "Adult intestinal stem cells: critical drivers of epithelial homeostasis and regeneration.," *Nat. Rev. Mol. Cell Biol.*, vol. 15, no. 1, pp. 19–33, Jan. 2014.

[115] M. Stelzner, M. Helmrath, J. C. Y. Dunn, S. J. Henning, C. W. Houchen, C. Kuo, J. Lynch, L. Li, S. T. Magness, M. G. Martin, M. H. Wong, and J. Yu, "A nomenclature for intestinal in vitro cultures.," *Am. J. Physiol. Gastrointest. Liver Physiol.*, vol. 302, no. 12, pp. G1359–63, Jun. 2012.

[116] T. Sato, R. G. Vries, H. J. Snippert, M. van de Wetering, N. Barker, D. E. Stange, J. H. van Es, A. Abo, P. Kujala, P. J. Peters, and H. Clevers, "Single Lgr5 stem cells build crypt-villus structures in vitro without a mesenchymal niche.," *Nature*, vol. 459, no. 7244, pp. 262–5, May 2009.

[117] K. S. Yan, L. A. Chia, X. Li, A. Ootani, J. Su, J. Y. Lee, N. Su, Y. Luo, S. C. Heilshorn, M. R. Amieva, E. Sangiorgi, M. R. Capecchi, and C. J. Kuo, "The intestinal stem cell markers Bmi1 and Lgr5 identify two functionally distinct populations," pp. 1–6, 2011.

[118] R. J. Von Furstenberg, A. S. Gulati, A. Baxi, J. M. Doherty, T. S. Stappenbeck, A. D. Gracz, S. T. Magness, and S. J. Henning, "Sorting mouse jejunal epithelial cells with CD24 yields a population with characteristics of intestinal stem cells," pp. 409–417, 2011.

[119] R. Eibl, D. Eibl, R. Pörtner, G. Catapano, and P. Czermak, *Cell and Tissue Reaction Engineering*. Springer Science & Business Media, 2008, p. 363.

[120] L. Goers, P. Freemont, and K. M. Polizzi, "Co-culture systems and technologies: taking synthetic biology to the next level.," *J. R. Soc. Interface*, vol. 11, no. 96, Jul. 2014.

[121] E. R. Shamir and A. J. Ewald, "Three-dimensional organotypic culture: experimental models of mammalian biology and disease," *Nat. Rev. Mol. Cell Biol.*, vol. 15, no. 10, pp. 647–664, Sep. 2014.

[122] C. F. Clementi and T. F. Murphy, "Non-typeable Haemophilus influenzae invasion and persistence in the human respiratory tract.," *Front. Cell. Infect. Microbiol.*, vol. 1, no. November, p. 1, Jan. 2011.

[123] S. M. Poutanen and A. E. Simor, "Clostridium difficile," vol. 171, no. 1, pp. 51–58, 2004.

[124] Z. Prytherch, C. Job, H. Marshall, V. Oreffo, M. Foster, and K. BéruBé, "Tissue-Specific stem cell differentiation in an in vitro airway model.," *Macromol. Biosci.*, vol. 11, no. 11, pp. 1467–77, Nov. 2011.

[125] G. M. Roomans, "TISSUE ENGINEERING AND THE USE OF STEM / PROGENITOR CELLS FOR AIRWAY EPITHELIUM REPAIR," vol. 19, pp. 284–299, 2010.

[126] R. Brandtzaeg, "Immunocompetent cells of the upper airway : functions in normal and diseased mucosa Secretory epithelium," vol. 252, 1995.

❖ REFERENCES

[127] C. Blanpain and E. Fuchs, “p63: revving up epithelial stem-cell potential.,” *Nat. Cell Biol.*, vol. 9, no. 7, pp. 731–3, Jul. 2007.

[128] M. Leushacke and N. Barker, “Ex vivo culture of the intestinal epithelium: strategies and applications.,” *Gut*, vol. 63, no. 8, pp. 1345–54, Aug. 2014.

[129] T. Sato and H. Clevers, “Growing self-organizing mini-guts from a single intestinal stem cell: mechanism and applications.,” *Science*, vol. 340, no. 6137, pp. 1190–4, Jun. 2013.

Acknowledgements

Firstly I need to thank my supervisor Marco Soriani for giving me the possibility to carry out my PhD studies, in his group in Novartis Siena. I'm grateful to Alfredo Pezzicoli and Silvia Rossi Paccani to have guided me as mentors during the last 3 years and to have strongly contributed to my scientific development. Thanks to Silvia Maccari and Anna Rita Taddei, for their wonderful work and the patience they demonstrated towards me and my samples. Part of the thesis work was made possible thanks to Prof. Philippe Sansonetti and to Giulia Nigro, who kindly hosted me in Institut Pasteur laboratories; many thanks to them and to Magdalena to have offered me a growth experience.

My biggest thanks actually go to 2 groups of 'fresh' people. I want to thank 'The Three Musketeers', Buket, Lucia and Maria, because I could not expect better pretty benchmates as well confident of me. At the same time, I don't know how to thank my lasting PhD Student crew, Chiara, Cristina, Edmondo, Luigi, Maddalena, Marco, Sandra, Valentina, the whole sunny side of my Senese days.

I would like to thank all the actual and previous members I met in the IVCB group, especially the people who helped me at the beginning of this travel (Benedetta, Fulvia, Valentina, Vanessa), in the end (Alessandra, Christina, Martina) and who instead was available to provide me scientific help. I thank also Elisa and Marta for their nice company during the thesis writing period. Thanks to all Novartis friends (in particular Giulia, Simone, Luca, Francesca) and also who shared a lunch or opinions with me. A big hug to whom supported me (Corigliano group) via sms and chat.

Finally, the special thanks are for my parents Franco e Maria, my brother Pier Luigi and my aunts Maria Pina and Mirella, "*to have been with me, always*".

I wish my best to all the people contributed as a person or as scientist to make me to reach this goal.

"If a man will begin with certainties, he shall end in doubts; but if he will be content to begin with doubts, he shall end in certainties."

"*Se un uomo parte con delle certezze finirà con dei dubbi; ma se si accontenta di iniziare con qualche dubbio, arriverà alla fine a qualche certezza."*

- Francis Bacon